High Resolution Transcriptional Profiling and Characterization of Cellular Inclusions in *Arabidopsis thaliana* Roots Grown in Low Sulfur Conditions

by

Terry L Jackson

University Program in Genetics and Genomics
Duke University

Approved:

_____
Philip Benfey, Supervisor

_____
Jen-Tsan Ashley Chi

_____
Paul Magwene

_____
David Sherwood

_____
Tai-Ping Sun

Dissertation submitted in partial fulfillment of
the requirements for the degree of Doctor of Philosophy in the University Program in Genetics and Genomics in the Graduate School
of Duke University

2013

ABSTRACT

High Resolution Transcriptional Profiling and Characterization of Cellular Inclusions in *Arabidopsis thaliana* Roots Grown in Low Sulfur Conditions

by

Terry L Jackson

University Program in Genetics and Genomics
Duke University

Approved:

_____
Philip Benfey, Supervisor

_____
Jen-Tsan Ashley Chi

_____
Paul Magwene

_____
David Sherwood

_____
Tai-Ping Sun

An abstract of a dissertation submitted in partial
fulfillment of the requirements for the degree
of Doctor of Philosophy in the Department of
University Program in Genetics and Genomics in the Graduate School
of Duke University

2013

Copyright by
Terry Lynell Jackson
2013

Abstract

Environmental stress affects plant development and productivity. Sulfur deficiency is a key nutrient deficiency that adversely affects crop yield. The model plant Arabidopsis thaliana has played an informative role in deciphering the mechanisms involved in sulfur assimilation, as well as, the response to limited conditions. Using Arabidopsis thaliana as a model to investigate gene expression in the root, microarray data sets have been generated. These data sets consist of whole root sections for 6 time points across 72 hours, and enriched populations of 5 radial cell-types and 4 sections of 3 developmental zones of the root at 3 hrs on sulfur limited conditions. With these data it was determined which cellular tissues and developmental zones were affected most by sulfur limited conditions. Furthermore, a novel phenotype was characterized that occurs in roots after growth on low sulfur conditions. Cellular inclusions build up within the cytoplasm of mature cortical root cells. These inclusions have been termed "sulfur pox" and their composition remains to be determined.

Dedication

To my parents Maj. James T. Jackson Jr. and Paula J. Mims:
Your trust and faith has allowed me to
reclaim and fulfill a once forgotten dream.
To my family and friends:
Without your patience I would have never
found my way through all of the storms in my life.
To my mentors:
We all need someone unexpected to enter
our lives and be our magnificent benefactors.
I will always be forever grateful.
You always believed in me and made a way for me to succeed. Thank you.
To the many men who society shunned:
You were cast away but I will always remember
you intentionally instilled the best of you in me
and trusted me to fulfill a mission of good work and good deeds.
You kept me safe in a land of peril,
helped me recognize and realize my strengths,
and encouraged me to remember my dreams.
I have carried the burden for many years and this is my gift to you.
WE ARE ALL SCIENTISTS BY NATURE.

Contents

Abstract iv

List of Tables ix

List of Figures x

Acknowledgements xiii

Chapter 1. Introduction 1

Overview of the thesis 1

Introduction to the system 1

High Resolution Data Acquisition 4

Transcriptional Networks and Environmental Stress 5

The Phenome Project 7

Sulfur Assimilation in Arabidopsis 11

Sulfur Transport and Regulation in Arabidopsis 12

Omics Studies of the Sulfur Pathway in Arabidopsis 14

Importance of Sulfur to Human Health 16

Sulfur Deficiency 17

Response to Sulfur Limiting Conditions 18

Chapter 2. High Resolution Transcriptional Profiling of Arabidopsis Roots Grown in Low Sulfur Conditions 20

Whole Root Time Course Data Analysis 22

Radial Data Set Analysis 42

Developmental Zone Data Set Analysis 55

Global Analysis of Arabidopsis Roots Grown on Low Sulfur Conditions 67

Methods 71

Growth Conditions and Analysis 71

Data Set Sample Preparation 72

Whole Root Time Course 72

Radial Cell-Types 73

Developmental Zones 73

Fluorescence Activated Cell Sorting 74

RNA Extraction and Microarray Hybridization Preparation 74

Microarray Data Analysis 74

Gene Ontology Assessment 75

Chapter 3. Characterization of Sulfur Pox: Root Cellular Inclusions formed in Low Sulfur Conditions 76

Sulfur Pox are a Novel Cellular Inclusion Body and a Unique Phenotype among 28 Abiotic Stresses 78

Sulfur Pox Microarray Data Sets 85

5 and 10 Day Sulfur Pox Microarray Data Analysis 87

Sulfur Pox Time Course Microarray Data Analysis 93

Non-targeted Metabolomic Analysis of Sulfur Pox Whole Root Sections 95

Sulfur Starvation Compromises Energy Acquisition and Primary Defense Strategies 102

Flavonoids and the Phenypropanoid Pathway 104

Characterization of Primary Flavonoids 105

Localization and Transport of Flavonoids 106
Flavonoid Research in the Arabidopsis Root System 108
The Relationship between Sulfur, Flavonoids, and Light Sensing 109
Phytochromes and Photomorphogenesis 110
Results from Flavonoid and Light Sensing Mutant Experiments 113
Methods 120
Growth Conditions and Analysis 120
Microarray Data Set Sample Preparation 121
Microarray Data Analysis 122
Quantification of –S POX 122
T-DNA Insertion Lines 122
Point mutation Lines 123
Fluorescent Staining 123
Chapter 4. Discussion, Future Directions, Conclusion 124
Discussion 124
Future Directions 125
Conclusion 125
Bibliography 127
Biography 137

List of Tables

Table 1: Nutrient list for Phenome Project. 9

Table 2: Phenome screen questionnaire. 10

Table 3: Gene ontology of low sulfur data sets. 31

Table 4: Overview of whole root time course data set differentially expressed genes. 42

Table 5: Annotations of genes differentially expressed in all cell-types. 50

Table 6: Overview of Radial cell-types differentially expressed genes. 55

Table 7: Annotations of genes differentially expressed in all developmental zones. 63

Table 8: Sulfur Pox zone specific genes. 93

Table 9: List of the Metabolites that increased in abundance in –S root samples. 101

List of Figures

Figure 1: Developmental organization of Arabidopsis roots. 3

Figure 2: Techniques for microarray analysis of isolated root cell populations. 5

Figure 3: Schematic of Sulfur Assimilation in Arabidopsis. 12

Figure 4: Response to sulfur limitation over time in Arabidopsis. 18

Figure 5: Confocal imaging of 5 cell-types used for cell sorting. 21

Figure 6: Microdissections of root developmetal zones. 22

Figure 7: Heatmap of whole root time course. 24

Figure 8: Venn diagram of low sulfur data sets. 25

Figure 9: Heatmap of shared genes from low sulfur data sets. 28

Figure 10: Graphs comparing expression data from low sulfur data sets. 36

Figure 11: Whole root time course data set overall totals. 37

Figure 12: Whole root time course data set heatmaps of gene ontology. 39

Figure 13: Whole root time course data set transcription factor overall totals. 40

Figure 14: Whole root time point specific totals. 41

Figure 15: Whole root time point specific transcription factor totals. 42

Figure 16: Radial cell-type data set overall totals. 44

Figure 17: Radial cell-type data set heatmaps of gene ontology. 47

Figure 18: Radial cell-type data set transcription factor overall totals. 48

Figure 19: Schematic of differential gene response in radial cell-types. 49

Figure 20: Radial cell-type specific totals. 51

Figure 21: Radial cell-type specific transcription factor totals. 51

Figure 22: Radial cell-type specific gene ontology. 54

Figure 23: Developmental zone data set overall totals. 56

Figure 24: Developmental zone data set heatmaps of gene ontology. 58

Figure 25: Developmental zone data set transcription factor overall totals. 59

Figure 26: Schematic of differential gene response in developmetal zones. 60

Figure 27: Developmental zone specific totals. 60

Figure 28: Developmental zone specific gene ontology. 62

Figure 29: Developmental zone specific totals. 63

Figure 30: Gene ontology heatmaps of global analysis. 70

Figure 31: Imaging of cellular inclusions termed "sulfur pox". 78

Figure 32: Sulfur pox develop in roots after 5 days in roots grown directly on low sulfur media. 79

Figure 33: Time course of sulfur pox production in root transferred from enriched media to low sulfur media. 80

Figure 34: Images of differentiated cells types where sulfur pox have been observed. 81

Figure 35: Confocal microscopy of GFP-labeled organelles and sulfur pox localization. 82

Figure 36: Image of sulfur pox resting in basal cavity of root cells. 83

Figure 37: Confocal images of fluorescence staining for vesicles, lipids, and protiens in relation to sulfur pox composition. 85

Figure 38: Graph of seeds tested for sulfur pox. 86

Figure 39: Illustration of root sections containing sulfur pox and length of root excised for microarray experiments. 87

Figure 40: Flow chart of 5 and 10 day sulfur pox microarray data analysis. 89

Figure 41: Heatmap of significant differential gene expression from 5 day and 10 day old roots sections germinated directly on –S media. 92

Figure 42: Heatmap of Sulfur Pox time course differential gene expression. 94

Figure 43: Metabolites of –S root samples that increased. 100

Figure 44: Simplified scheme for phenylpropanoid and flavonoid biosynthesis. 106

Figure 45: Images of phenylpropanoid pathway regulator mutants. 114

Figure 46: Images of transparent testa mutants germinated directly on low sulfur media. 115

Figure 47: Images of transparent testa mutants transferred from enriched media to low sulfur media. 115

Figure 48: Confocal imaging of DPBA stain for presence of flavonoids. 116

Figure 49: Quantification of –S Pox in phenylpropanoid mutants. 118

Figure 50: Images of sulfur pox in phytochrome mutants grown on low sulfur media in the dark. 119

Acknowledgements

Thank you to my advisor, Philip Benfey, who believed in me when no one else felt I was able to perform at this level. He has been a role model for me in every way. He provided me the perfect environment to succeed and all of the tools to make the most of this opportunity.

I also want to thank my committee members for guiding me throughout this process. I put much thought into the professors I wanted to confer this degree upon me and it was the best decision I made on my own.

To the Benfey lab and all of the undergraduates whom I have had the honor to work with and mentor; I could not have done this without you. In your company is the only time I spent on campus when I felt like I was at home. Thank you all for the comfort.

Chapter 1. Introduction

Overview of the thesis

This thesis presents work whose goal was to characterize gene expression of the Arabidopsis *thaliana* root at the resolution of individual cell-types and developmental zones when grown under low sulfur conditions. The thesis also describes the discovery of novel cellular inclusions found in the root when subjected to a low sulfur growth environment. The thesis is partitioned into the following parts: introduction to the system and background information (Chapter 1), the analysis of high resolution transcriptional profiling of cell type and developmental zone data sets (Chapter 2), the characterization of novel cellular inclusions found in root sections (Chapter 3), and discussion, future directions, and conclusions of this research (Chapter 4).

The data sets in Chapter 2 have been published and are publicly available in the manuscript entitled, "Cell Identity Regulators Link Developmental and Stress Responses in the Arabidopsis Root.", which was published in *Developmental Cell*, October 2011. Chapter 3 will be the basis of my first author publication and it is currently in preparation.

Introduction to the system

Plants are sessile by nature and have adapted mechanisms to confront stress from both abiotic and biotic sources. Plants contend with these stressful situations via transcriptional and posttranscriptional regulation, as well as, proteomic and metabolic

changes. This leads to growth alterations in above-ground organs (stem, leaves, and flowers) and in the root system which can be seen macroscopically. In addition to this, plants may be able to mount a defense against pathogens, herbivores, and oxidative damage, and have developed means of detoxifying harmful compounds that would otherwise threaten their survival. (Potters et al. 2007, Hirayama and Shinozaki 2010).

Arabidopsis *thaliana* is well-suited to study the effects of external stimuli on root development. Its roots are organized into cell files in which their lineage can be traced back to a set of initials, or stem cells, located at the root tip. The four outer cell layers have radial symmetry. The initial cells surround a set of non-proliferating cells, the quiescent center (QC). These initial cells produce individual cell files (Figure 1a). The innermost tissue is the vasculature tissue, which with the pericycle is called the stele, where water and nutrients are transported between the root and the shoot of the plant. Adjacent to these cells is the endodermis, a specialized cell type responsible for selective solute uptake. This cell-type arises from the same initial cells as the cortex layer. The endodermis and cortex comprise the ground tissue of the root (Nakajima *et al*., 2001). The epidermal layer interacts with the external environment and is composed of root hair and non-hair cells. This cell layer shares the same initial as the lateral root cap which peels away as the root grows. The root cap, or columella, protects the meristematic region and responds to gravity altering the direction of growth (Dolan *et al*., 1993). These 5 cell populations represent the basic cell types of the root. There are

also three developmental phases of the root which represent temporal information based on distance of displacement of older cells by younger cells and cell morphological features (Figure 1b).

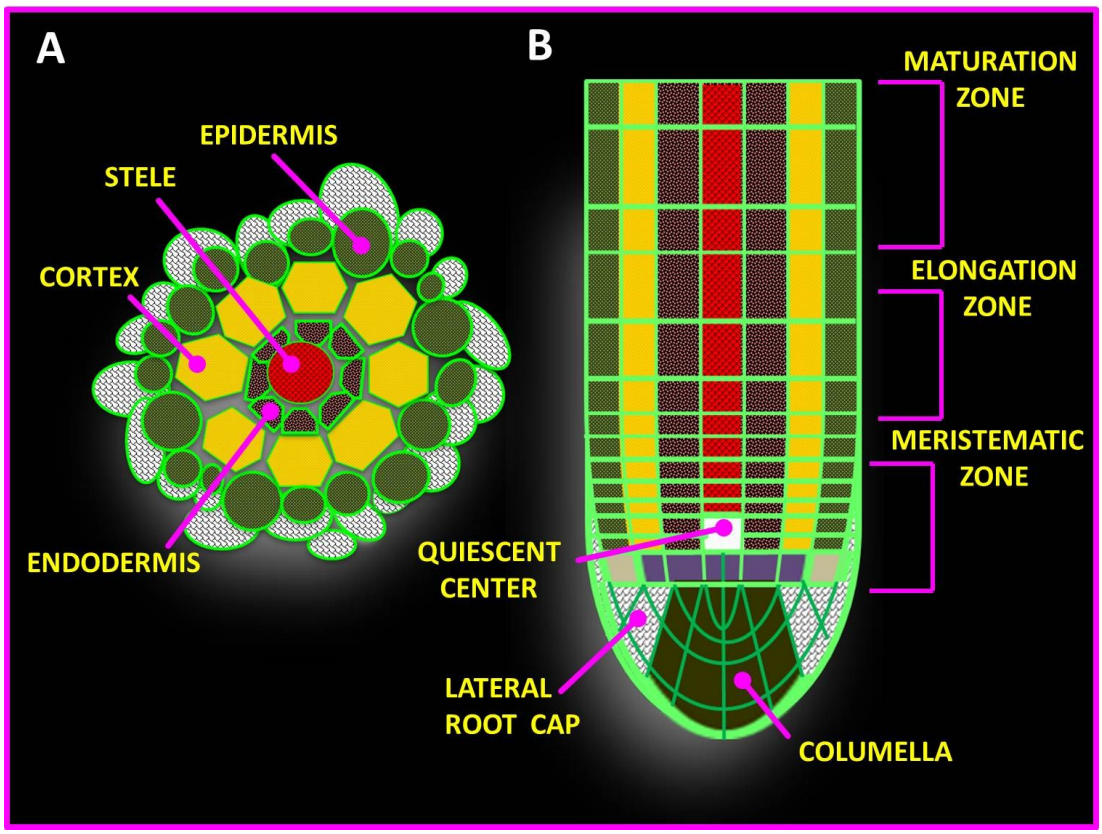

Figure 1: Developmental organization of Arabidopsis roots.

Thus, within the root there is a continuous temporal gradient from newly synthesized to differentiated cells. The meristematic region houses the QC, the initial cells, and their progeny which divide rapidly. The elongation zone, adjacent to the meristematic zone, is where cells begin to expand and increase their size and volume. The maturation zone contains older cells, found in the upper section of the root, which

have acquired their final cell state. Taken together the simplifying aspects of root organization reduce a four dimensional spatiotemporal problem into a more tractable two dimensional problem, which can be readily addressed (Benfey and Scheres, 2000).

High Resolution Data Acquisition

Fluorescence-Activated Cell Sorting (FACS), invented in the late 1960s, was created to perform experiments on live cells that were separated from mixed cell-type cultures based on fluorescence labeling. The fluorescent marker, Green Fluorescent Protein (GFP) was isolated from the jelly fish *Aequoria Victoria* and is commonly used in FACS experiments (Herzenberg *et al*., 2002). Capitalizing on these techniques, root tissue types have been tagged with GFP and marker lines specific to each spatial layer were generated and roots were protoplasted to prepare the cells for FACS (Figure 2) (Birnbaum *et al*., 2005).

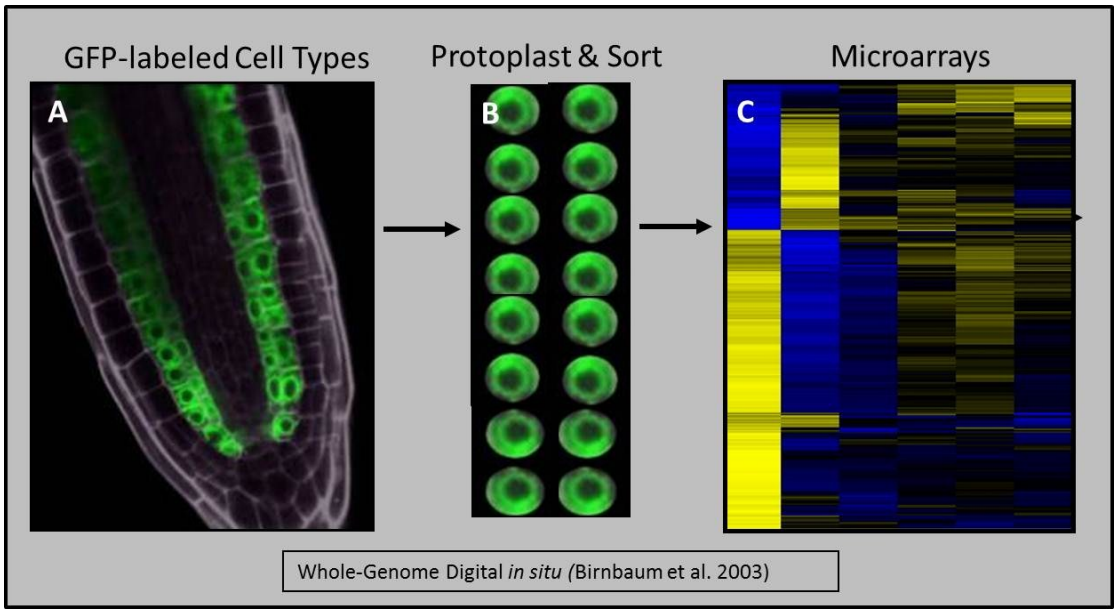

Figure 2: Techniques for microarray analysis of isolated root cell populations.

This technique coupled with microdissection of the developmental zones enables high resolution profiling of roots. This strategy allowed for the isolation of 19 populations of 15 different radial cell types and 12 longitudinal sections to produce a high resolution expression map of the root (Brady *et al.,* 2007). Similarly, genes downstream of the SHORT-ROOT (SHR) and SCARECROW (SCR) genes were identified using these methods (Sozzani *et al.,* 2010).

Transcriptional Networks and Environmental Stress

The genomic era has led to many fully sequenced species which develop and interact with the environment in different ways. The ability of these organisms to cope with their ever-changing environments relies on the complex interaction that occurs within transcriptional and signaling networks. Thus, the environment plays an active

role in stimulating changes in transcriptional states. Under adaptive conditions, when an organism is adjusting to new environmental factors, the network is dynamic and an analysis of these changes can provide a large amount of information about the network (Van den Bulcke *et al*., 2006). Microarray analysis provides the opportunity to amass large data sets from which stress responsive genes can be extracted; and transcriptional regulators can be tested to determine their downstream targets and position in the stress response network (Chen and Zho 2004). For example, a glucocorticoid-receptor-mediated microarray experiment uncovered 8 transcription factors (TF) activated by NONEXPRESSER OF PATHOGENESIS-RELATED GENES 1 (NPR1), the transcription cofactor induced by salicylic acid to activate systematic acquired resistance (SAR) in Arabidopsis as a result of pathogen invasion. Five of these WRKY TFs were then confirmed to disrupt NPR1 function and regulate the SAR transcriptional network. Identification of these nodes validates the use of genomic tools to understand environmental stress response at the functional level (Wang *et al*., 2006). Researchers have used publicly available microarray data sets of whole root and enriched cell type specific and developmental zone expression profiles to compare multiple stresses to each other to determine if a universal stress response exists. One group gathered data from biotic, abiotic and chemical stress regimens from microarrays containing roughly 22,700 probes. Approximately 8,500 were determined to be involved in a common stress response, while nearly 200 of these genes identified to be associated with an extensive

number of stresses. Furthermore, there was an additional association with stresses being specific to certain root cell identities (Ma and Bohnert, 2007). In Arabidopsis, FATTY ACID DESATURASE 2 (FAD2), along with cis-elements in the promoter was shown to be involved in both abiotic stress response and phytohormone response (Yuan *et al.*, 2012). The oxidized lipids 12-oxo-phytodienoic acid (OPDA) and A_1-phytoprostanes (PPA_1) were connected to detoxification mechanisms and stress response. Expression profiles from cultures treated for 4 hrs revealed a set of genes that have a similar response to xenobiotics. Comparisons to biotic stress data showed the PPA_1 response shared an up-regulation of genes with the response to Pseudomonas *syringae.* This led to the connection of these two oxidized lipids being regulated by TGA transcription factors which were identified using the TGA triple mutant *tga2-5-6* (Mueller et al 2008).

Like pathogen invasion, abiotic stress also invokes a stress response in plants. The roots of plants are sophisticated organs that have complex transcriptional networks that must respond to toxic conditions and nutrient deficits, which are not fully understood at cell-specific resolution. (Gifford *et al.*, 2008) Additionally, many studies point to transcriptional stress responses without a comprehensive analysis of the phenotypic changes that occur under these conditions.

The Phenome Project

The goals of the Phenome Project were to i) classify the broad phenotypic effects occurring under multiple environmental stimuli and ii) generate high resolution

transcriptional profiles of a core set of stresses affecting Arabidopsis roots. Twenty-eight abiotic stresses were tested by removing individual nutrients as well as adding toxic compounds. Growth media included high salt, high pH, cadmium toxicity, and drought simulation (Table 1). Seedlings were scored four times over 11 days, while confocal microscopy was performed twice during this time. The effect of each abiotic stress was scored on a three point scale, where zero designated no effect, one was a moderate effect, and two was a severe effect on that phenotype. Forty-one phenotypes were ultimately documented (Table 2). Preliminary results of the phenotype associated with sulfur deficiency, as well as its relevance to agriculture led me to decide to investigate it in relation to regulatory networks in Arabidopsis roots.

This study, in addition to others, highlights how FACS coupled with microarray analyses can be utilized to study how environmental stimuli affect different cell-types and developmental zones. Furthermore, the Benfey lab continues to utilize this method of transcriptional profiling for research involving cell fate specification, root development, and building transcriptional networks.

Table 1: Nutrient list for Phenome Project.

Type of nutrient	Nutrient	MS constituent
Primary	N	Ammonium nitrate (NH4NO3)
		potassium nitrate (KNO3)
	P	Potassium phosphate monobasic (KPO4 H20)
	K	Potassium iodide (KI)
		potassium nitrate (KNO3)
		Potassium phosphate monobasic (KPO4 H20)
Secondary	Ca	Calcium chloride anhydrous (CaCl2)
	Mg	Magnesium sulfate (MgSO4)
	S	Cupric sulfate (CuSO4)
		Ferrous sulfate (FeSO4)
		Magnesium sulfate (MgSO4)
		Manganese sulfate H20 (MnSo4)
		Zinc sulfate 7H20 (ZnSO4)
Micro-nutrients	Fe	Ferrous sulfate (FeSO4)
	Mn	Manganese sulfate H20 (MnSo4)
	Zn	Zinc sulfate 7H20 (ZnSO4)
	Cu	Cupric sulfate (CuSO4)
	B	Boric acid (H3BO3)
	Mo	Molybdic acid (sodium salt) 2H20 (Na2MoO4)
	Cl	Calcium chloride anhydrous (CaCl2)
		Cobalt chloride (CoCl2)
Others	Co	Cobalt chloride (CoCl2)
	I	Potassium iodide (KI)
In addition: Cadmium, salinity, drought, Mn toxicity, pH and sucrose tested		

Sodium Chloride stress (+NaCl) and iron deficiency (–Fe) were used to determine cell-type specific and developmental-zone specific responses to different types of environmental stimuli. In this study, transcriptional profiling was performed for a whole root time course, 6 cell-types and 4 longitudinal zones. The +NaCl and –Fe data sets confirmed the hypothesis that an increase in differentially expressed genes occurs with increased cellular resolution via cell-type population enrichment. They differed in the length of time it takes for maximum differential gene expression to peak in the time

course experiments (1hr for +NaCl, 12hrs for -Fe). The cortex layer and the elongation zone had the most differential expression in the +NaCl data set versus the stele and the maturation zone for the –Fe data set. This shows that the cell-type response is dependent on the stress. Mutants in epidermal patterning were used with salt stress to determine how developmental pathways regulate the salt stress response and 4 sets of genes were found whose differential expression was controlled by correct patterning of this cell-type (Dinniney et al. 2008).

Table 2: Phenome screen questionnaire.

Cellular organization of root tip (confocal)	Root hair development	Shoot development
Is the QC disorganized?	Is the root twisted?	Is the shoot chlorotic
Is the size of the elongation zone increased?	Are the hairs longer than normal?	Is there excessive anthocyanin?
Is the size of the elongation zone decreased?	Are the hairs shorter than normal?	Are the leaves darker green?
Is the size of the meristematic zone increased?	Are the hairs ecessively and consistently branched?	Is germination reduced?
Is the size of the meristematic zone decreased?	Are the hairs swollen?	Is true leaf emergence slowed?
Is the radial organization of the root affected?	Is hiair placement altered?	Is the size of the shoot decreased?
Is there precocious 2nd cortex formation?	Is hair development suppressed?	Is the size of the shoot increased?
Is the root cap affected?	Are there wavy hairs?	Are leaves less hyponastically curved?
Lateral root development	Are there ectopic hair cells?	Is there less anthocyanin in the hypocotyl?
Is lateral root initiation suppressed?	**Root growth and shape**	Is there less anthocyanin in the shoot?
Is lateral root initiation activated?	Is root growth inhibited?	Is there more anthocyanin in the hypocotyl?
Is lateral root outgrowth suppressed?	Is growth accelerated?	Is there more anthocyanin in the shoot?
Is lateral root outgrowth activated?	Does the root tip bend upon transfer?	Is the shoot darker green?
	Is there excessive waving?	Is true leaf emergence slowed?
	Is there radial swelling?	Is hypocotyl elongation decreased?
	Is there radial shrinkage?	Are leaves more hyponastically curved?
	Are the roots very straight?	Is the shoot more compact?
		Are the plants dying?
		Are there necrotic lesions?
		Is trichome development suppressed?

The cell-type specific and developmental zone data sets of these two stimuli were then compared with two additional stresses, low pH and low sulfur. This analysis reinforced the concept that transcriptional stress responses are cell-type specific and somewhat unique to each stress, and that roots respond differently spatially and temporally to different stresses. The report also confirmed previous findings that there is a subset of genes involved in a common stress response which came from analyzing

whole root data from 14 stresses and finding that half of these share common genes regulated by induction of stress (Iyer-Pascuzzi et al. 2011). However, there was no universal response, common across all stresses.

Sulfur Assimilation in Arabidopsis

Plastids are the organelle that performs sulfate reduction after acquisition of sulfate from the soil. Key points in the assimilation process are activation of sulfate to form adenosine 5′-phosphosulfate (APS) by ATP sulfurylase (ATPS), and its subsequent reduction by APS reductase (APR) into sulfite which is then further reduced into sulfide by sulfite reductase (SiR) (Bick and Leustek, 1998). An alternative exists for APS at this step where it can undergo phosphorylation and proceed in the sulfation process as 3′-phosphoadenosine 5′-phosphosulfate (PAPS) (Mugford et al., 2009). Otherwise, cysteine is produced by the integration of sulfide with O-acetylserine (OAS) (Bogdanova and Hell, 1997) (Figure 3).

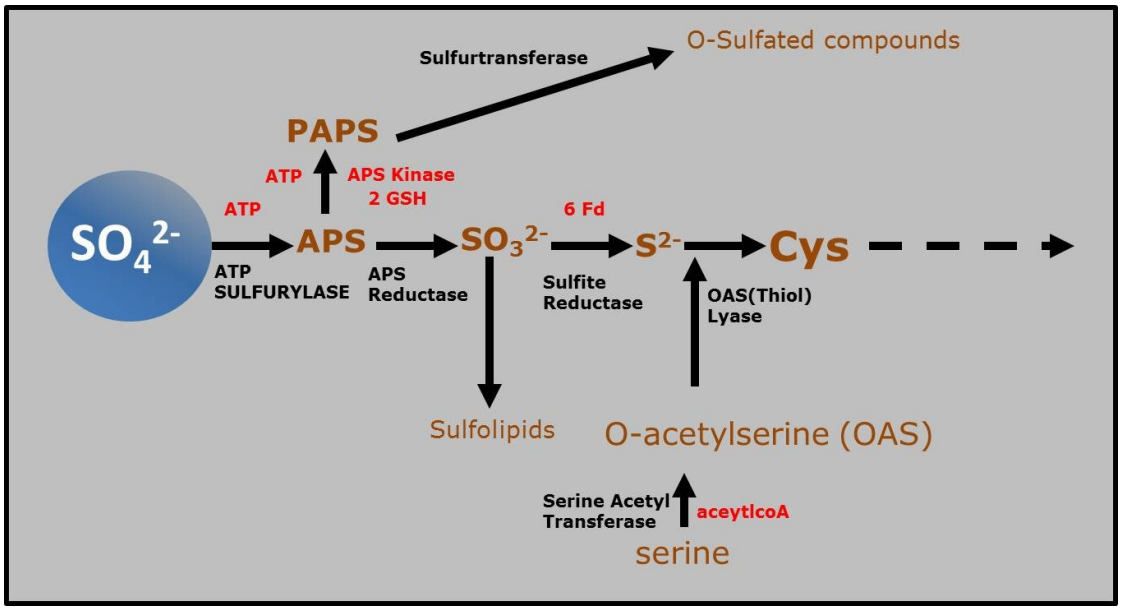

Figure 3: Schematic of Sulfur Assimilation in Arabidopsis.

Cysteine is a sulfur-containing amino acid and plays a vital role in protein regulation. It is incorporated into glutathione which acts as a redox buffer, a signal for sulfur assimilation, and acts as a storage form of reduced sulfur (Leustek *et al*., 2000). It is also a substrate for the production of methionine which is synthesized through multiple steps culminating in the methylation of homocysteine by methionine synthase (Hell and Wirtz, 2011). Additionally, sulfur is incorporated into Coenzyme A which catalyzes many reactions such as the cascade reaction leading into the TCA cycle (Hesse *et al*., 2007).

Sulfur Transport and Regulation in Arabidopsis

Sulfur is generally taken up by plants as sulfate by the root system; this transport must be coordinated throughout the entire plant. Twelve transporters have been

identified and grouped by phylogenetic relationships (Hawkesford, 2000; Buchner *et al*., 2004). Group 1 has three transporters. SULTR1,1 and SULTR1,2 are high affinity transporters that co-localize to the root hairs, epidermis and cortex layers of the root (Shibagaki *et al*., 2002; Yoshimoto et al. 2002). These transporters are regulated by the internal sulfur levels within the plant at both the mRNA level and posttranscriptional level (Yoshimoto et al., 2007). Furthermore, for transcriptional regulation of SULTR1,1 to take place, upstream phosphorylation/dephosphorylation of the protein must occur (Maruyama-Nakashita *et al*., 2004). SULTR1;3 is also a high affinity sulfur transporter. In RT-PCR experiments its mRNA was detected in both shoots and roots and localization of the translational fusion with GFP in transgenic plants was visualized in the phloem, which transports sulfate from shoots to roots, in the cotyledons, as well as in roots and the hypocotyl (Yoshimoto *et al*., 2003). In Group 2, SULTR2;2 is a low affinity transporter. Its promoter was fused to GFP and expression was also detected in the phloem. The localization of SULTR2;1, also a low-affinity transporter, was elucidated using the promoter fusion with β-glucuronidase. Expression was localized in the root xylem parenchyma and pericycle cells and in the xylem parenchyma and phloem of leaves (Takahashi *et al*., 2000). In Group 3, SULTR3;1 was recently localized using a GFP fusion to the coding region. The transporter localized to chloroplasts (Min-Jie Cao *et al*., 2012). SULTR3;5 was determined to co-localize with SULTR2,1 in the phloem of roots, and is a low-affinity transporter (Kataoka and Hayashi, 2004). Two transporters,

SULTR4;1 and SULTR4;2 are responsible for sulfate transport in and out of the vacuole where sulfate reserves are stored (Katoaka and Hayashi, 2004).

In addition to the regulatory mechanisms already described regarding transporters, there are other means of regulation of sulfur in Arabidopsis. SLIM1, a member of the *ETHYLENE-INSENSITIVE3-LIKE3* (*EIL3*) family, is a transcription factor identified in a mutant screen using the promoter of SULTR1;2, a low affinity sulfur transporter which is induced under sulfur limitation. *slim1* seedlings are deficient in sulfur uptake, thus, SLIM1 appears to be a transcriptional regulator of sulfur uptake in Arabidopsis (Maruyama-Nakashita 2006). SLIM1 also induces the MiRNA-395 locus which is localized to both shoots and roots in Arabidopsis and has as one of its targets SULTR2;1, the low-affinity sulfate transporter (Kawashima et al 2009, Takahashi 2000, Katoaka 2004).

Omics Studies of the Sulfur Pathway in Arabidopsis

The body of experimental results regarding sulfur assimilation and response to sulfur deprived conditions has led to an understanding of the system as a whole. Regulation of gene expression within plants is a complex coordinated activity that is necessary to control processes such as development, plant defense, and stress responses (Singh *et al*., 1998) Transcriptional regulation is mediated by TF binding to the regulatory elements of genes and activating or repressing the activity of that gene. Macroarray and microarray studies have generated a large number of genes regulated in

the sulfur pathway. A transcriptome and metabolic study of 6 to 13 days old plants exposed to sulfur deprivation shows activation of genes involved in sulfur transport, flavonoid biosynthesis, R2R3 MYB transcription factors, nitrilase (which catalyzes the degradation of glucosinolates), glutathione S-transferases, and genes induced by auxin and jasmonic acid (Nikiforova 2003). This study also reports a decline in total sulfur, glutathione and cysteine and an increase in serine, O-acetylserine (OAS) and tryptophan. In three-week old Arabidopsis seedlings that were subjected to sulfur deficient conditions for 48hrs and treated with OAS in leaves and shoots, profiling revealed regulation of genes responsive to the OAS stimulus. These included sulfur transporters, genes involved in pathogen resistance, abiotic stress response, photosynthesis, protein degradation, jasmonic acid responsive genes among others (Hirai 2003). Further, it was determined that supplementation of OAS significantly increased root OAS, GSH, and cysteine content. Additionally, in the same year, research was published on macroarray experiments performed on Columbia-0 (COL-0) and the sel-10 T-DNA insertional mutant in the Wassilewskija (Ws) accession line for 12 to 13 days under varying conditions, including transfer experiments from high to low and low to high sulfate for 24 hrs (Maruyama-Nakashita et al. 2003). The sel-10 mutant is defective in SULTR1;2 function, thus; genes responding to its absence in tandem with the response to the various treatments could be assessed. Roots showed an up-regulation of sulfate transporters SULTR1;1 and SULTR2;1, as well as, APR2 which is

involved in the assimilation process. Additionally, glucosinolate synthesis genes were up-regulated in roots along with a putative isoflavone reductase-like gene which also was found in the aforementioned study by Nikiforova. Furthermore, in the root, glucosinolate degradation genes showed significant down-regulation while genes involved in oxidative stress and jasmonate production were up-regulated in leaves. The sel-10 mutants also exhibited a significant reduction of sulfate and GSH in leaves and roots and of methionine in leaves. Additional studies applying the integration of high throughput transcriptional data and metabolomic analysis have begun to illustrate the complex connections between genes, metabolites, hormones, and interactions between sulfur and other nutrients (Nikiforova et al. 2004, Saito 2004, Hirai et al. 2005, Amtmann and Armengaud 2009, Hoefgen and Nikiforova 2008).

Importance of Sulfur to Human Health

Humans and other mammals are unable to synthesize the sulfur containing amino acid, methionine, and therefore, must obtain this and other sulfur-containing compounds from food resources. Sulfur deficiency has been implicated as a risk factor in human disease and verified as necessary for high quality crop yields. Elevated cysteine to sulfate ratios have been detected in patients suffering from Alzheimer's, Parkinson's, motor neuron, and cardiovascular disease (Heafield et al 1990; Ingenbleek 2009). The acquisition of sulfur from plants is unable to satisfy the nutritional need in humans (Hung et al. 2002). Thus, disease prevalence is high in areas and individuals that practice

a vegetarian lifestyle (Ingengleek and McKully 2012).

Sulfur Deficiency

Sulfur is an essential plant macronutrient. Restrictions of industrial emissions of sulfur into the atmosphere have resulted in a scarcity of sulfur availability in agronomically important soil (Saito 2004). Therefore, understanding how plants absorb sulfur is important from an agronomic perspective. Due to the essential role of sulfur; a deficiency creates a cascade of events that impair processes of plant development (Hesse 2007) There is a decrease in lipid and chlorophyll production, as well as an overall reduction in plant growth (Nikiforova *et al*., 2005). Disease resistance is inhibited due to decreased production of glutathione, glucosinolates, and sulfurous gases (Bloem *et al*., 2004).

Numerous genomic, metabolomic, and proteomic studies have identified many of the genes and biological functions regulated by sulfur (Hirai and Saito 2004). In crop production, sulfur deficiency has been of growing concern over the past few decades. Soil samples in India reveal a deficiency in sulfur between 73% and 95%. It is also a major problem in Europe and the United States (Haneklaus et al 2007, Kost et al 2008). In many of these areas there are three possible causes of this deficiency: i) the reduction of sulfur containing gases from industrial emissions, ii) soil leaching and iii) the reduction of sulfur containing fertilizers (McGrath and Zhao, 1992) Therefore, there have been an increasing number of studies to identify and understand the sulfur assimilation pathway

in plants and the effects of short and long term sulfur deficiency.

Response to Sulfur Limiting Conditions

The phenotypic and morphological changes that exemplify the pleiotropic cascade of events in response to sulfur limiting conditions have been well established and documented (Figure 4). As sulfur limitation proceeds, developmental processes become increasingly impaired (Hesse 2007). The effect of sulfur has been shown to occur in phases at the transcriptional and metabolic level. An early response corresponds to the initial induction of the stress. A secondary response occurs after prolonged exposure to sulfur deficiency. (Nikiforova, 2008) The interval between these responses coincides with modification of transcriptional activity (Amtmann and Armengaud 2009).

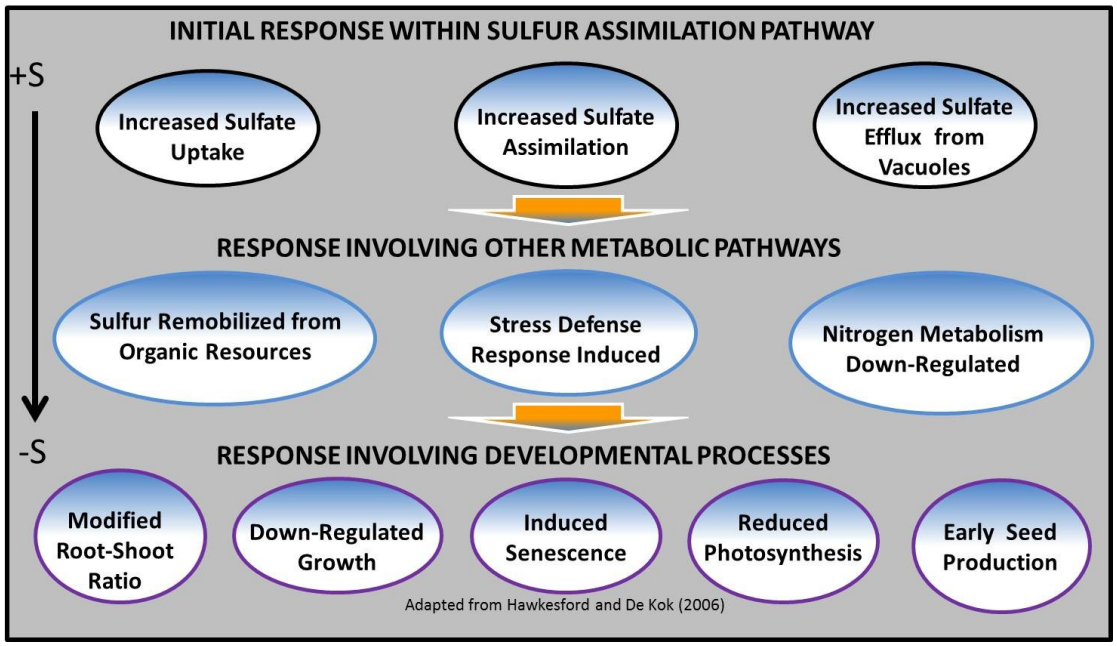

Figure 4: Response to sulfur limitation over time in Arabidopsis.

Sulfur deficient plants also undergo a complex reorganization of metabolites in an effort to return to a sufficient level of homeostasis (Nikiforova 2005). Upon germination, plants deprived of sulfur have a slower stress response compared to those that are transferred from sufficient to insufficient conditions, which exhibit only a small fraction of significant changes in metabolite concentrations. (Nikiforova, 2003, 2005). There is a decrease in lipid and chlorophyll production, and an overall reduction in plant growth, and lateral root growth (Kutz et al. 2002, Nikiforova *et al*., 2005). Disease resistance is also inhibited due to decreased production of glutathione, glucosinolates, and sulfurous gases (Bloem *et al*., 2005). Chlorosis of leaves, stunted growth, and lateral root initiation all become evident after long term sulfur deprivation.

Chapter 2. High Resolution Transcriptional Profiling of Arabidopsis Roots Grown in Low Sulfur Conditions

Introduction of the Experimental Approach

The data presented here evaluates gene expression in response to low sulfur (–S) at cell-type and developmental zone specific resolution. The rationale of this approach resides in the spatial organization of the root into radial cell files that proliferate from the root apex, elongate, and mature into differentiated cell types, which also provides temporal data.

Preliminary data was gathered through a time course (TC) experiment on whole roots to capture the initial changes in gene expression and maximize the number of significant differentially expressed genes. The time course was performed at 0, 3, 12, 24, 48, and 72 hours (hrs). These time points were chosen because microarray profiles of whole roots under –S conditions have been performed by multiple investigators. An "Atgen Express" data set, which was employed as a comparison, used 0, 2, 4, 8, 12, and, 24 hr time points (http://arabidopsis.org/servlets/TairObject?type=expression_set &id=1007967006). Microarray results have been published that focus on 6, 10, and 13 days of constitutive and induced –S conditions (Nikiforova *et al*., 2002). Another investigator grew plants for 3 weeks before transfer to –S conditions for 48 hrs (Maruyama-Nakashita *et al*., 2003). It is of interest to be able to compare this data set to similar data sets and to build on this body of information. In addition, the 72 hr time point had yet to be studied in roots for -S response and thus could provide new insights

into the response.

The results of the time course revealed that the 3 hr time point provided the largest set of differentially expressed genes and was used for the radial and developmental zone data sets. Also comparisons with the AtGen Express data verified that our experimental conditions were activating sulfur-responsive genes.

Cell sorting of GFP marker lines for each cell type was used to enrich populations of the radial cell-types. The radial data set consists of 5 cell types: columella, epidermis, cortex, endodermis, and stele. These cell types were sorted using GFP-markers lines: PET111, WER, CORTEX315, SCR, and WOL, respectively (Figure 5).

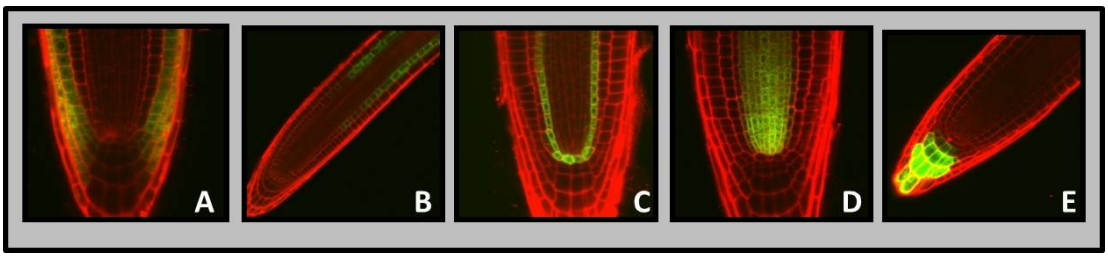

Figure 5: Confocal imaging of 5 cell-types used for cell sorting.

The developmental zone data set was produced by microdissecting 4 sections from the root meristematic, elongation, and maturation zones (Figure 6). The sections were taken by cutting the roots with a micro razor while viewing under a dissecting microscope.

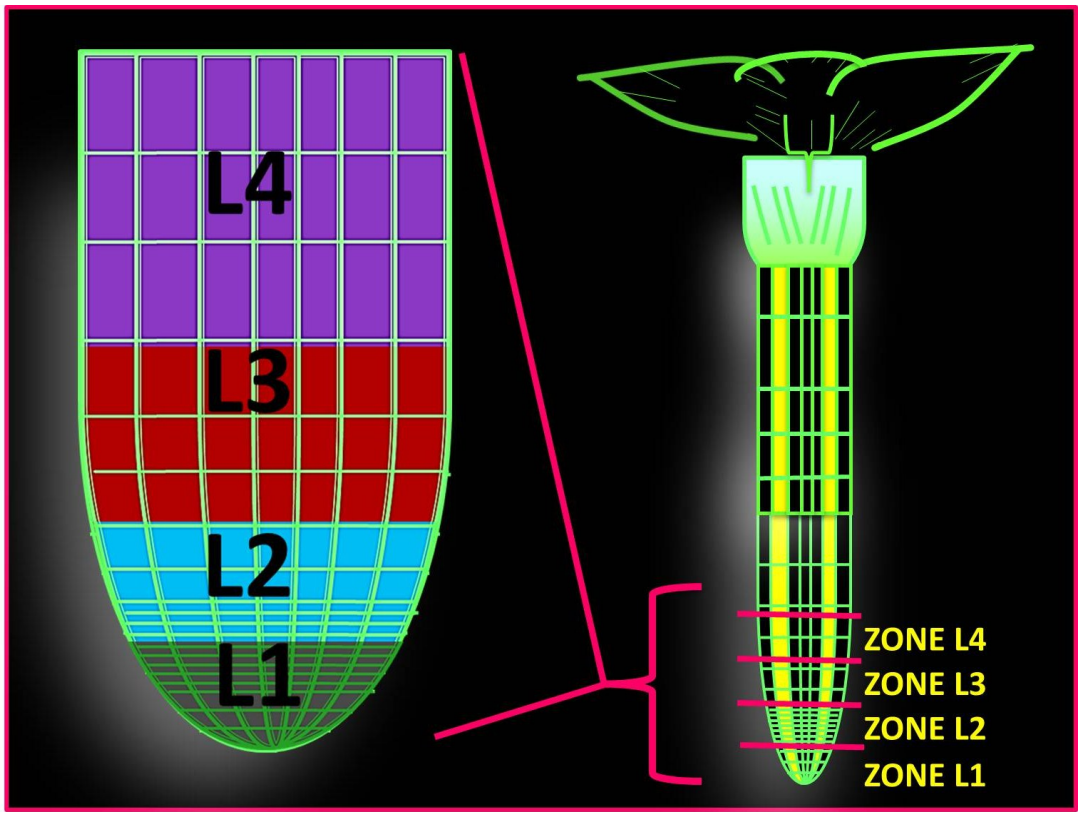

Figure 6: Micro-dissections of root developmental zones.

Whole Root Time Course Data Analysis

To determine a time point to conduct cell-type and developmental zone expression profiles a time course was performed on 5 day old whole roots at 0, 3, 12, 24, 48, and 72hrs of growth under –S conditions. Pair-wise comparisons using a mixed model ANOVA and threshold cut-offs of a q-value of 10^{-4} and 1.5-fold difference as compared to the 0 time point were performed. We used these criteria to identify differentially expressed genes from all of our data sets.

The whole root time course analysis produced a total of 823 genes that met statistical criteria to be considered significantly differentially expressed. The next step

was to interpret the expression patterns of these genes over time. To this end, a dendrogram was produced to visualize the transcriptional changes (Figure 7). This heatmap is color coded orange for genes that are activated while blue represents repression of gene expression. Black represents the median value across the expression data. The heatmap also shows the relationship between genes with distantly related patterns having a greater number of branches and being farther apart. The cluster pattern produced here indicates that there are dramatic changes in gene expression at the early time points. We also see the first evidence of a secondary and delayed wave of expression occurring after a few days of sustained sulfur limiting conditions.

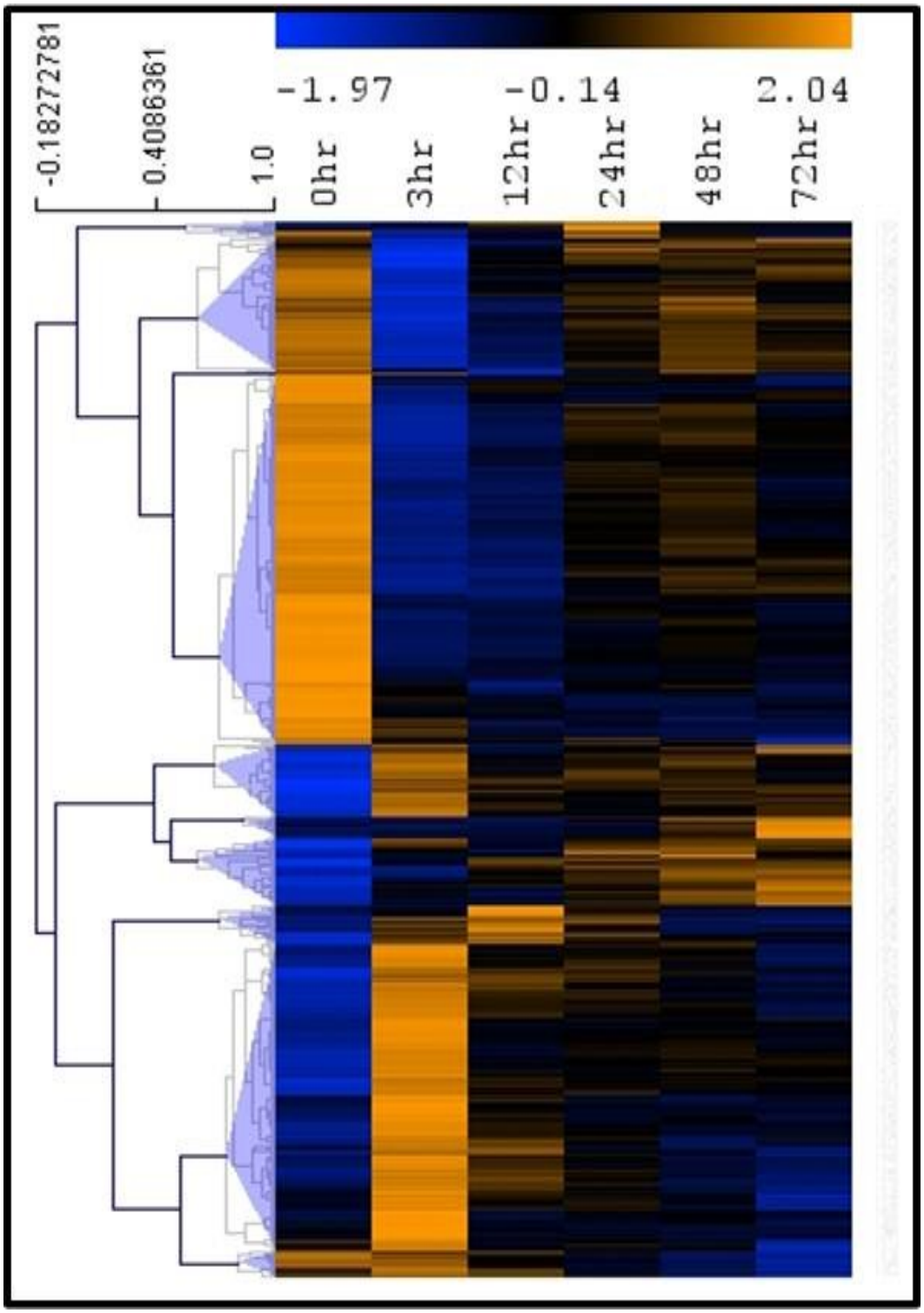

Figure 7: Heatmap of whole root time course.

Of these 823 statistically significant differentially expressed genes, there were 439 unique genes in the data set. In other words, many of these genes appear in the data set more than once. These genes were then compared to the AtGen Express Data of similar expression analyses of roots grown in –S conditions. The AtGen Express time course used 0, 2, 4, 8, 12, and 24hr time points and identified 766 unique genes that were differentially expressed. From the comparison of the TC data with the AtGen Express, 148, or 13.8% of the genes are shared by both data sets (Figure 8). This low number of intersecting genes is possibly due to the initial normalization of the data sets together. Furthermore, differences in the time points assayed and experimental conditions may have had an effect on the results.

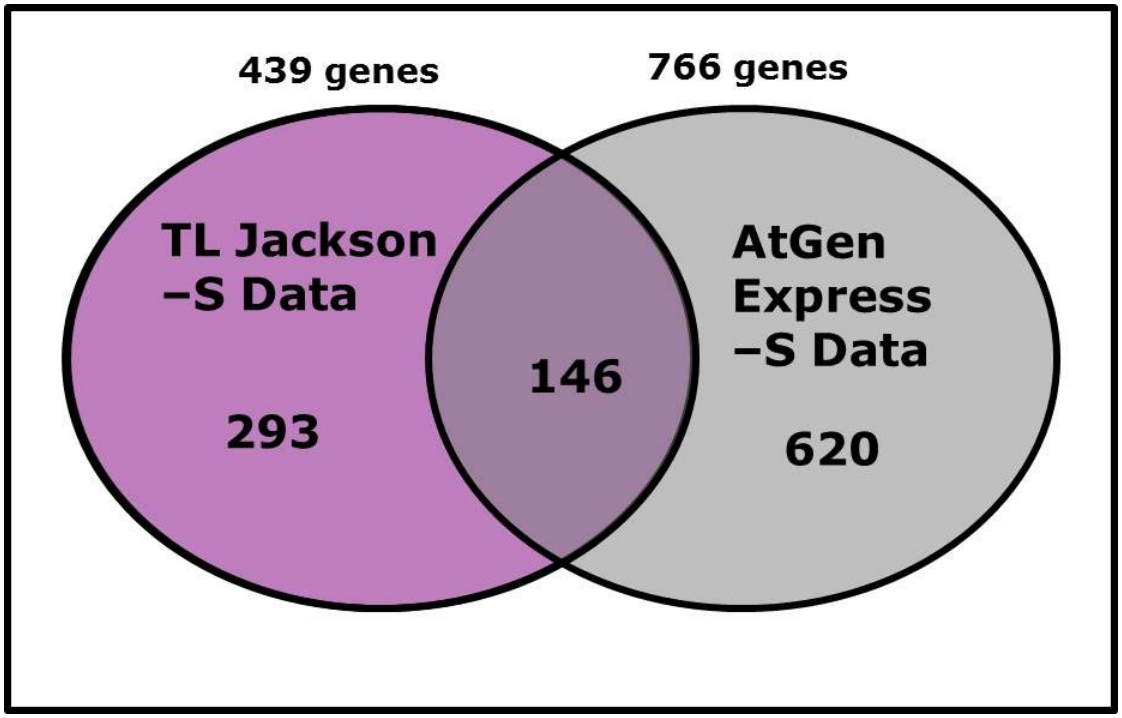

Figure 8: Venn diagram of low sulfur data sets.

Despite the low overlap in significantly affected genes, the genes that are common between the two data sets were informative. It was necessary to compare similar time points to each other. Each data set utilized 6 time points, yet the Atgen Express time points were all within 24hr as previously mentioned. The time course performed here also utilizes 48hr and 72hr samples. Therefore, these latter time points were eliminated from further analysis as were the 2 hr and 8 hr results from AtGen Express. The primary difference in the data sets was now a 1hr difference between 3hrs and 4hrs which we decided to include in the remaining analysis. First, heatmaps were generated to create expression profiles of the data in order to determine if there were any obvious patterns. Heatmaps were created either using an automated clustering algorithm or without clustering. In the latter case, the genes were arranged in gene identification order (Figure 9). First, we clustered both data sets using Pearson correlation followed by hierarchical clustering. The MeV program generates a clustered heatmap but also stores the data as it was originally inputted and supplies a dendrogram of it. Once the clustered heatmap is produced, the user can manipulate the number of nodes to further organize, dissect, and analyze the data. Here the nodes are the lavender triangular shapes that peak at a branch and the base joins the heatmap to cover the regions of data selected to contain closely related information.

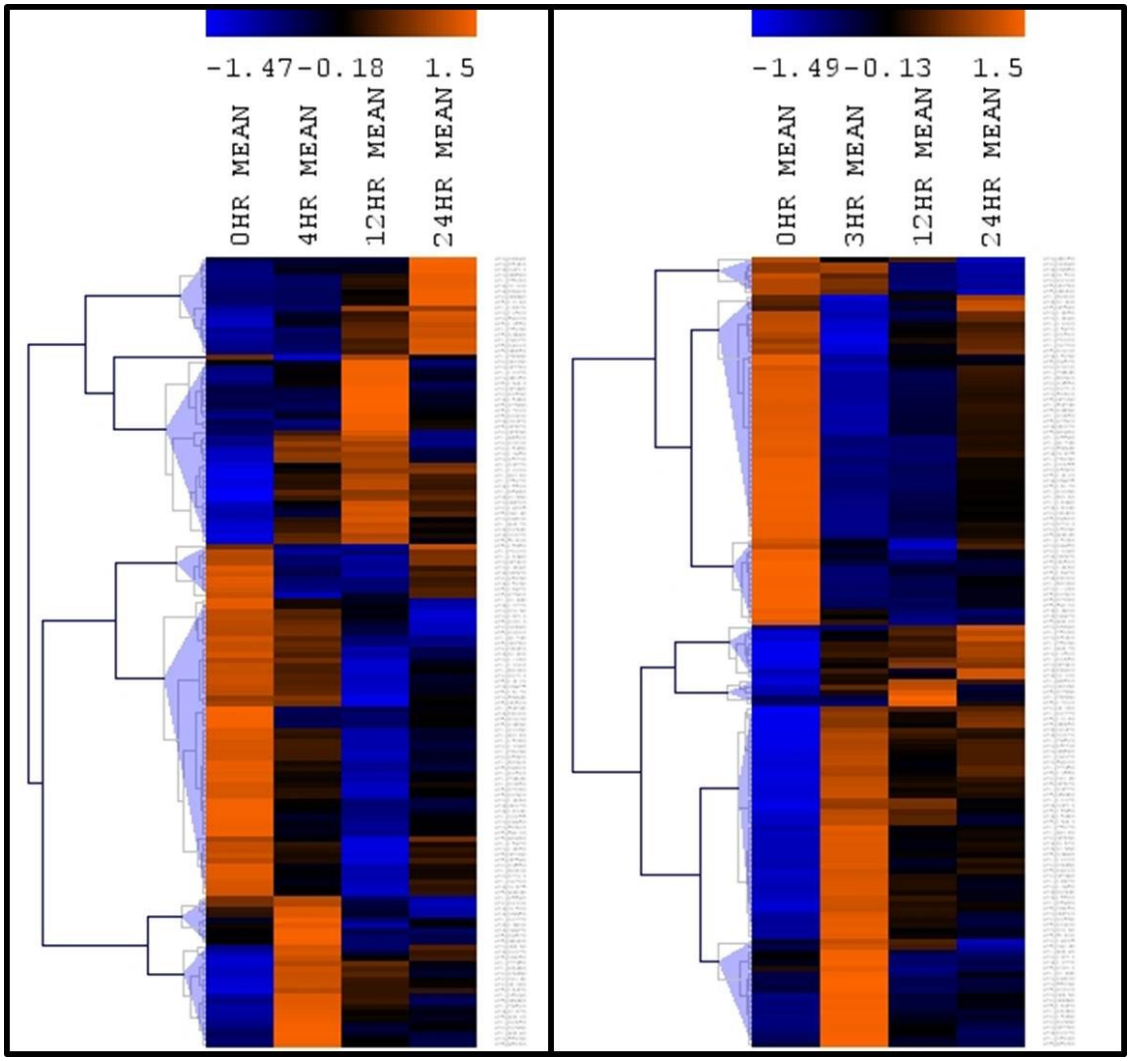
-1.47
-0.18
1.5
0HR MEAN
4HR MEAN
12HR MEAN
24HR MEAN
-1.49
-0.13
1.5
0HR MEAN
3HR MEAN
12HR MEAN
24HR MEAN

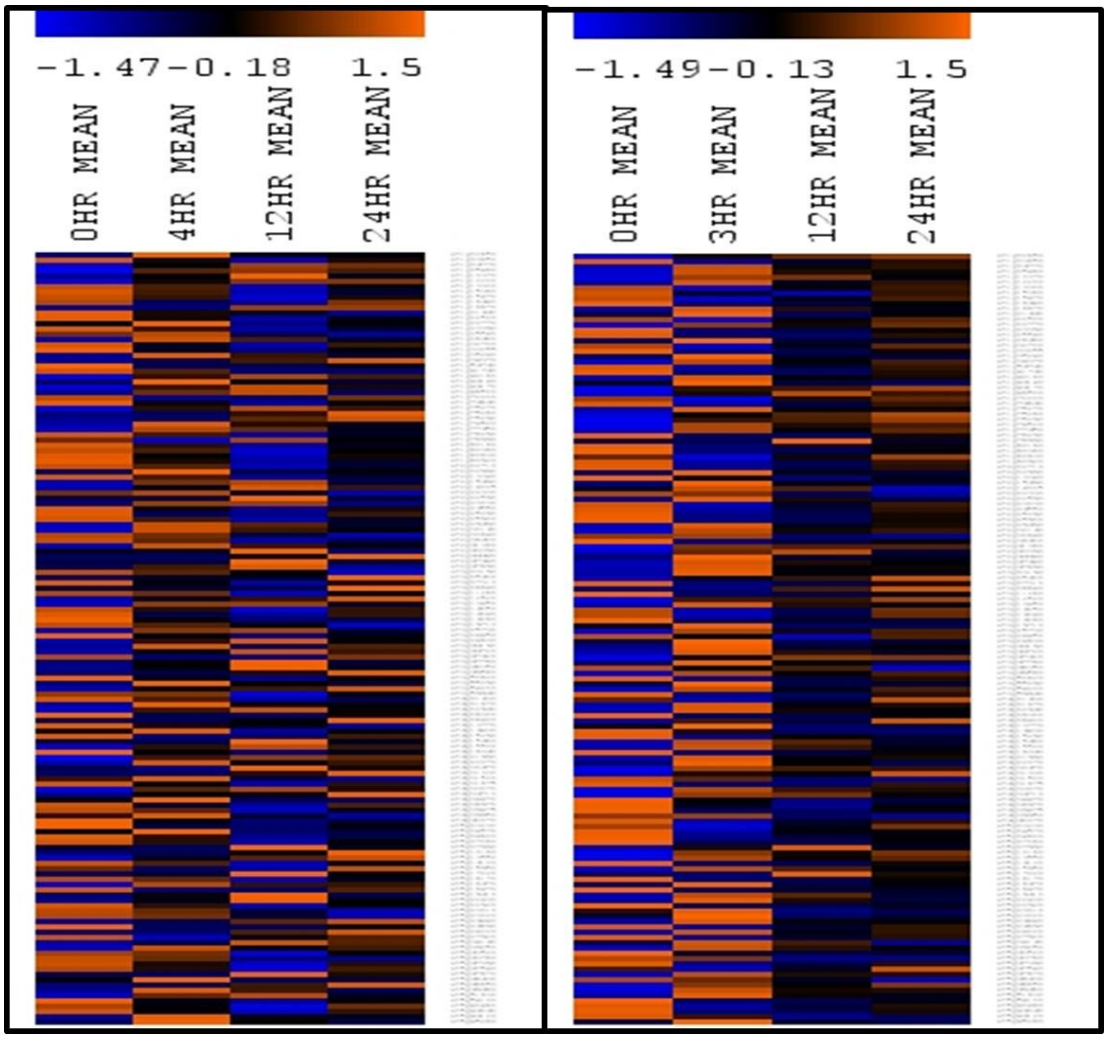

Figure 9: Heatmap of shared genes from low sulfur data sets.

In Figure 9, the heatmaps to the right are the AtGen Express expression profiles and those on the left are from my research. The top panel was created using the automated clustering and lower panel was without clustering. The data from these results are interpreted as being more similar than different. In Figure 9a, where clustering was utilized, the arrangement of the patterns for each time point are not identical but this can be attributed to the clustering which is evident not only from the

pattern of the heatmaps but also from the branching. The AtGen Express heatmap appears to have a greater amount of variation and discontinuity compared to the profile I generated. An alternative interpretation, which I favor, is that the plants in each experiment responded very differently during the first 12 hours of sulfur limiting conditions. After four hours of deprivation, for the AtGen Express experiment, the effect on transcription is mild and a large number of genes have yet to respond to the stress conditions. The major response is not apparent until the 12hr time point. On the other hand, the response was immediate and drastic within 3hrs in my data set. 90 percent of the genes reacted to the change in the environmental conditions 9hr prior to the AtGen Express data which peaked at 12 hours. By this time, the roots have begun to adapt to the conditions in my experiment and expression is beginning to return to pre-stress levels. Remarkably, after this very different initial reaction to the deficient conditions, by the 24 hour time point gene expression in both experiments is very similar. My interpretation is based on personal observations in the laboratory of the health, hardiness, and longevity of seedlings grown on low sulfur media. Phenotypic variation is commonly observed.

After reaching this conclusion, it was of interest to inspect the data without the clustering to see if there was a delayed pattern that was visible since the gene arrangement of both data sets would be identical. The zero hour time point was exceptional and it is easy to tell that the banding is practically the same in both profiles.

Thus, the root systems were developing the same under normal conditions. It must be remembered that black is not the lower limit of this analysis but it is the median of the expression data rendering it neutral or at most trending in one direction or the other. At 12 hours after exposure it appears that my data set is just as active as it was at 3 hours in this representation, and it is, but it is no longer obvious that all active processes are now repressed and previously down-regulated genes have been extensively induced. The advantage of this arrangement is the ability to follow the transition of genes across the time course on both heatmaps. These genes form bands of the colors represent if they are activated, repressed, or relatively neutral. The banding patterns they create show that specific genes are behaving in the same way. The response of my experiments have been so severe that the banding pattern at three hours consists of bands from the 3 hour and 12hr time point in the AtGen Express heatmap. At 12 hours, when their gene response peaks, it is also clear that my data set is rebounding from the initial shock. The remnants of genes that are still recovering can be seen and matched to the gene expression in that data set. Therefore it seems the only difference is that one experimental procedure produced an early response that quickly altered its transcriptional state and remained relatively at low level of transcriptional activity for over twelve hours versus responding gradually and after multiple hours of sustained stress. Similar genes were involved in both cases and by 24 hours the situation was the same in both experiments.

The banding patterns revealed through the expression analysis were very

revealing and informative but little was known about the function of the genes that these data sets had in common. It was unknown what role, if any, these genes played in sulfur deficiency. The set of gene identification numbers for the 146 genes shared with the AtGen Express data set were processed to determine the gene ontology annotations for enriched processes Table 3).

Table 3: Gene ontology of low sulfur data sets.

Gene Ontology Description	neg *log* p_value
sulfate assimilation	-4.15900422
glutathione transferase activity	-4.934451054
tryptophan catabolism	-4.313386466
sulfate transport	-5.967833493
alanine-glyoxylate transaminase activity	-5.875472577
toxin catabolism	-5.037284081
indoleacetic acid biosynthesis	-5.480518857
camalexin biosynthesis	-5.875472577
sulfate transporter activity	-5.667937708
glucosinolate biosynthesis	-6.334286875

The gene ontology results further validate that the experimental procedures effectively promotes sulfur deficiency and induces sulfur responsive genes. As a final measure to ensure the genes from the comparative analysis behaved in the same manner, genes that are down-regulated in the AtGen data set were also down-regulated

in mine. We determined which genes in the data set were associated with many of the GO categories in Table 3, in addition to a few other genes that fell just short of qualifying for statistical enrichment. Once these genes were determined we returned to the expression data to plot the results Figure (10).

The collection of graphs that make up Figure 10 provide that last piece of data needed to move forward with the rest of this project. These graphs represent 6 groups of genes identified from GO annotations. They are Sulfur Transport and Assimilation, Phenylpropanoid Derivatives, Glucosinolate Biosynthesis, Stimulus Response, Alanine: glyoxylate aminotransferase 3 Activity, and Photosystem Subunits. For each of these groups two graphs are listed. The graph on the left is of mean expression values from the AtGen Express data and on the right the same type of results from the work performed here. These graphs very clearly show similar trends in gene expression and provide substantial evidence in support of my earlier interpretation of the clustered and unclustered heatmaps. It is noticeable in genes from each graph except the one for Glucosinolate Biosynthesis.

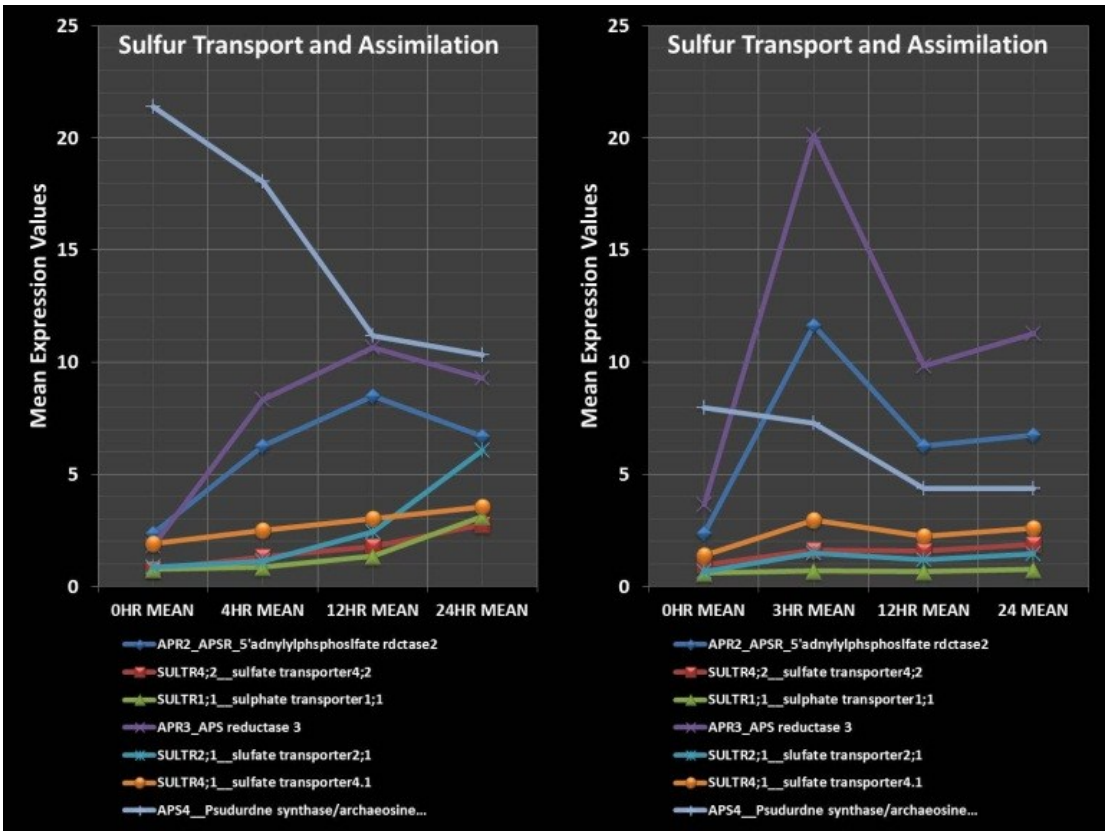
Sulfur Transport and Assimilation
Mean Expression Values
25
20
15
10
5
0
0HR MEAN
4HR MEAN
12HR MEAN
24HR MEAN
APR2_APSR_5'adnylylphsphoslfate rdctase2
SULTR4;2__sulfate transporter4;2
SULTR1;1__sulphate transporter1;1
APR3_APS reductase 3
SULTR2;1__slufate transporter2;1
SULTR4;1__sulfate transporter4.1
APS4__Psudurdne synthase/archaeosine...
Sulfur Transport and Assimilation
Mean Expression Values
25
20
15
10
5
0
0HR MEAN
3HR MEAN
12HR MEAN
24 MEAN
APR2_APSR_5'adnylylphsphoslfate rdctase2
SULTR4;2__sulfate transporter4;2
SULTR1;1__sulphate transporter1;1
APR3_APS reductase 3
SULTR2;1__slufate transporter2;1
SULTR4;1__sulfate transporter4.1
APS4__Psudurdne synthase/archaeosine...

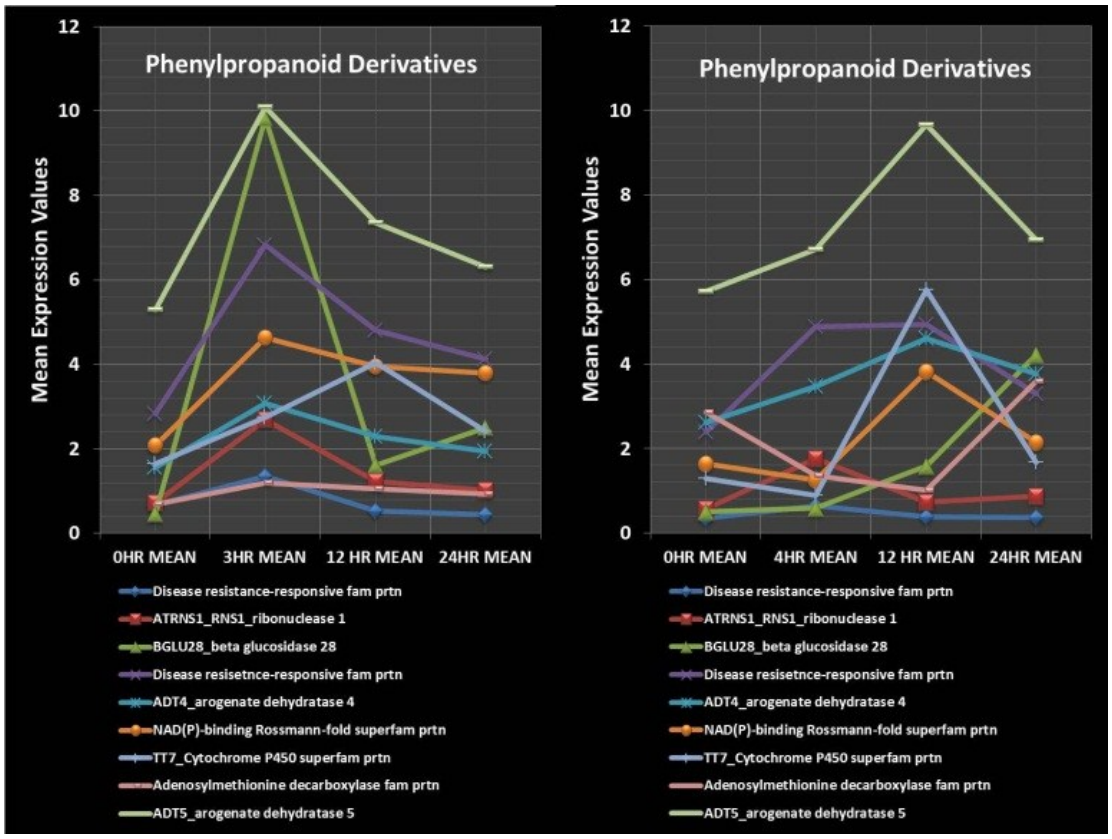
Phenylpropanoid Derivatives
Mean Expression Values
12
10
8
6
4
2
0
0HR MEAN
3HR MEAN
12 HR MEAN
24HR MEAN
Disease resistance-responsive fam prtn
ATRNS1_RNS1_ribonuclease 1
BGLU28_beta glucosidase 28
Disease resisetnce-responsive fam prtn
ADT4_arogenate dehydratase 4
NAD(P)-binding Rossmann-fold superfam prtn
TT7_Cytochrome P450 superfam prtn
Adenosylmethionine decarboxylase fam prtn
ADT5_arogenate dehydratase 5
Phenylpropanoid Derivatives
Mean Expression Values
12
10
8
6
4
2
0
0HR MEAN
4HR MEAN
12 HR MEAN
24HR MEAN
Disease resistance-responsive fam prtn
ATRNS1_RNS1_ribonuclease 1
BGLU28_beta glucosidase 28
Disease resisetnce-responsive fam prtn
ADT4_arogenate dehydratase 4
NAD(P)-binding Rossmann-fold superfam prtn
TT7_Cytochrome P450 superfam prtn
Adenosylmethionine decarboxylase fam prtn
ADT5_arogenate dehydratase 5

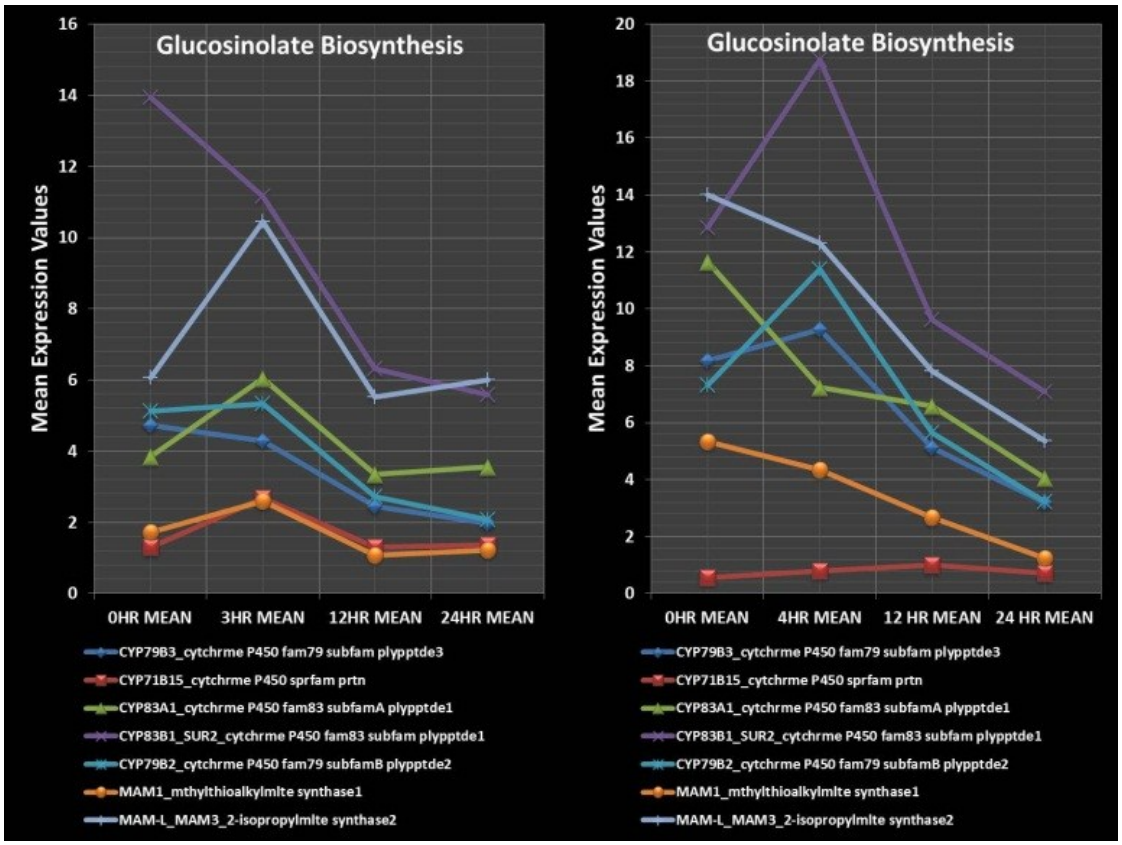
Glucosinolate Biosynthesis
Mean Expression Values
0HR MEAN
3HR MEAN
12HR MEAN
24HR MEAN
CYP79B3_cytchrme P450 fam79 subfam plypptde3
CYP71B15_cytchrme P450 sprfam prtn
CYP83A1_cytchrme P450 fam83 subfamA plypptde1
CYP83B1_SUR2_cytchrme P450 fam83 subfam plypptde1
CYP79B2_cytchrme P450 fam79 subfamB plypptde2
MAM1_mthylthioalkylmlte synthase1
MAM-L_MAM3_2-isopropylmlte synthase2
Glucosinolate Biosynthesis
Mean Expression Values
0HR MEAN
4HR MEAN
12 HR MEAN
24 HR MEAN
CYP79B3_cytchrme P450 fam79 subfam plypptde3
CYP71B15_cytchrme P450 sprfam prtn
CYP83A1_cytchrme P450 fam83 subfamA plypptde1
CYP83B1_SUR2_cytchrme P450 fam83 subfam plypptde1
CYP79B2_cytchrme P450 fam79 subfamB plypptde2
MAM1_mthylthioalkylmlte synthase1
MAM-L_MAM3_2-isopropylmlte synthase2

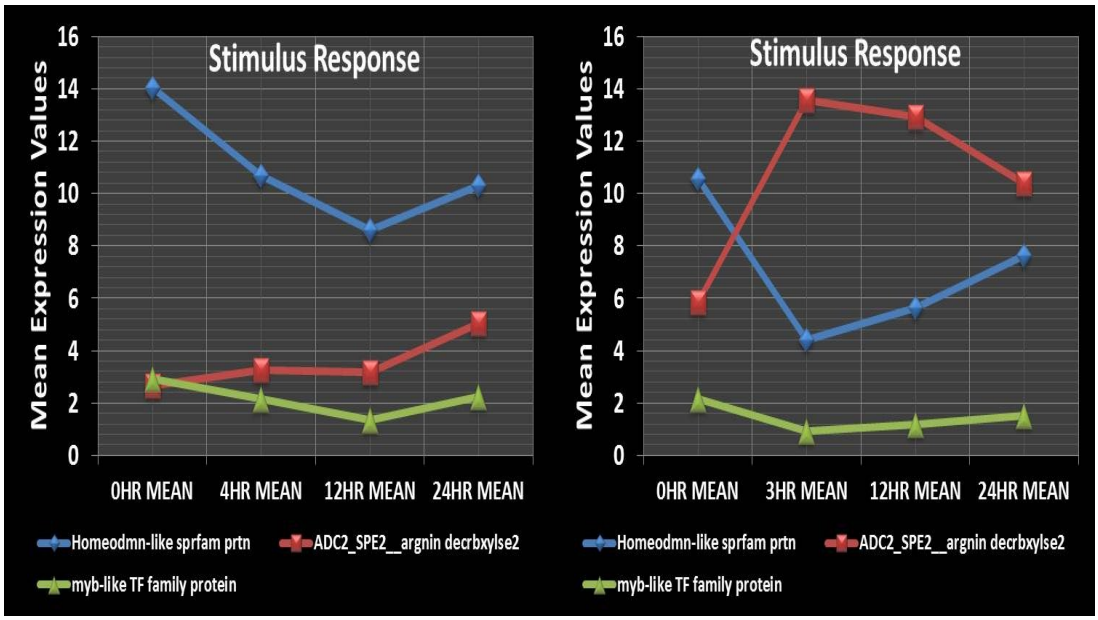
Stimulus Response
Mean Expression Values
0HR MEAN
4HR MEAN
12HR MEAN
24HR MEAN
Homeodmn-like sprfam prtn
ADC2_SPE2__argnin decrbxylse2
myb-like TF family protein
Stimulus Response
Mean Expression Values
0HR MEAN
3HR MEAN
12HR MEAN
24HR MEAN
Homeodmn-like sprfam prtn
ADC2_SPE2__argnin decrbxylse2
myb-like TF family protein

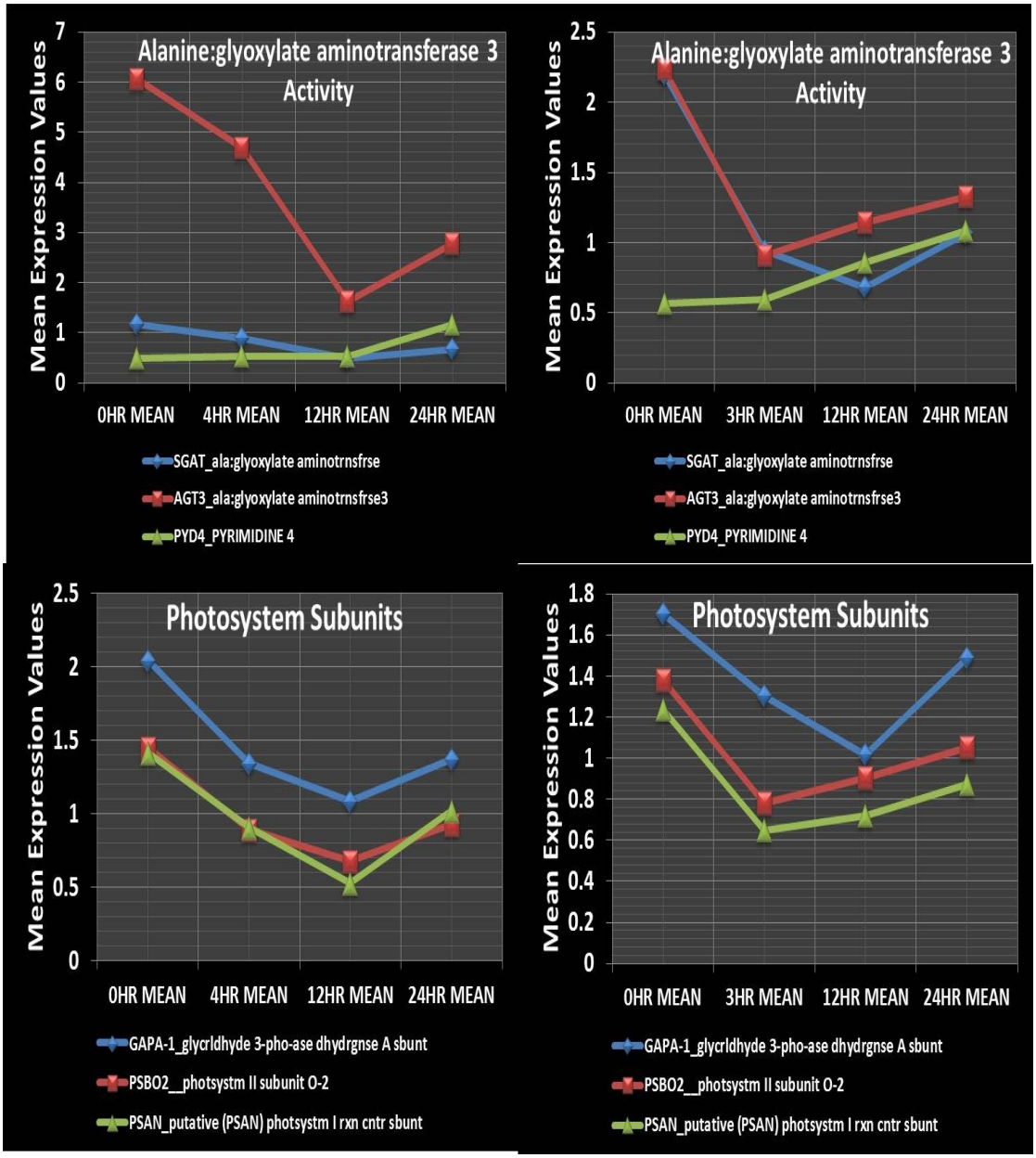

Figure 10: Graphs comparing expression data from low sulfur data sets.

Following verification of the experimental procedures it was necessary to further analyze the results of the whole root time course experiment. There were a number of key questions I wanted to answer from the analysis of this microarray data set. My

intent was to ask these same questions across the data sets being generated. First I looked at the data set as a whole and determined the total number of differentially regulated genes. In this case it is the total number from all of the time points which we have already established as being 823 genes. Next, I listed the number of genes for each time point. Then I determined if the genes in each time point were up-regulated or down-regulated (Figure 11). Here, we see that the response from the removal of sulfur for the environment was severe in the early hours of the experiment but there is a marked decline and a period of low activity within 24 hours. The data suggest the beginning of a second wave of transcriptional activity by the end of the time course. This bimodal response has been mentioned in the introduction.

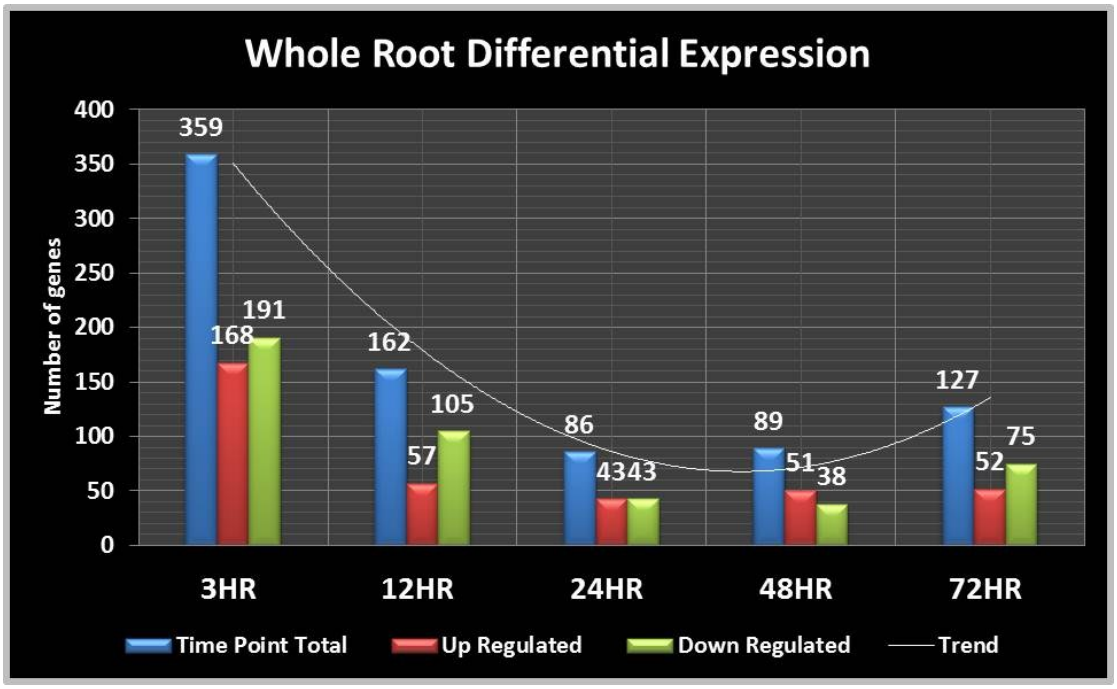

Figure 11: Whole root time course data set overall totals.

Heatmaps of the GO categories enriched across these data were created from the data compiled in Figure 11 (Figure 12). An interesting point in Figure 11a is that the enrichment of sulfur assimilation and transport is no longer significant. This may be due to a larger data set being used where other processes affected by sulfur limitation are pronounced across a greater number of genes. It is of importance to mention that sulfur related GO categories were enriched but the significance decreased slightly compared to the smaller data set used earlier which disqualified it from being significant when all genes were combined. Still it appears abundantly in the list of up-regulated go categories in figure 12b. The combined lists in Figure 12a suggest very little is occurring between 3 and 72 hours, which is why it is important to uncouple the genes and divide them into activated and repressed genes as well to further elucidate the activities that are being lost to noise.

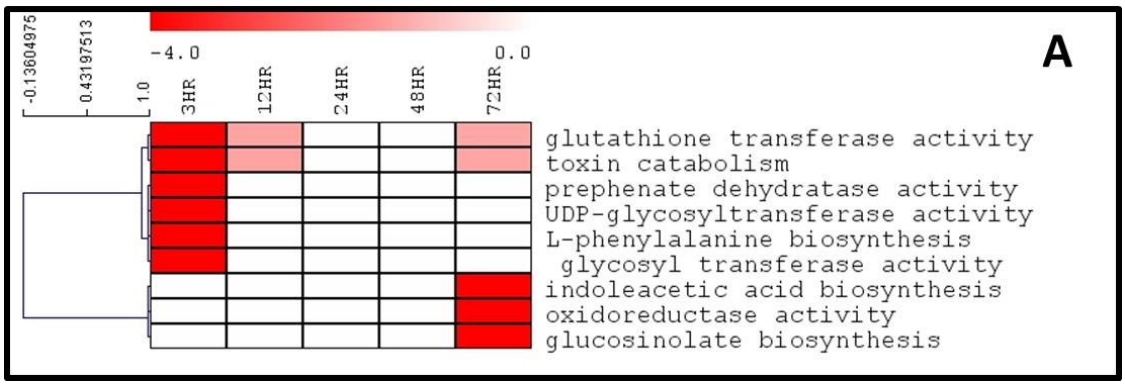

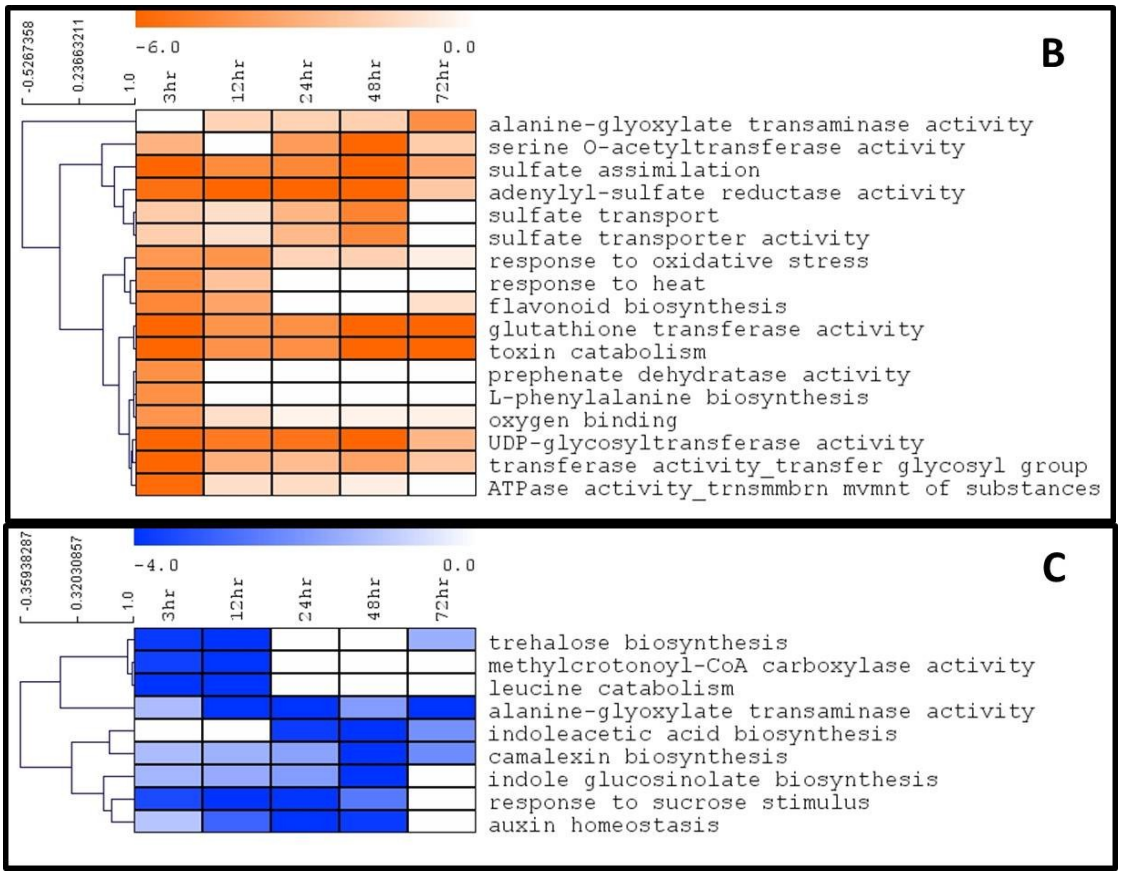

Figure 12: Whole root time course data set heatmaps of gene ontology.

I also determined the number of transcription factors, in the same manner (Figure 13) with the goal of identifying novel developmental regulators in order to assemble and understand transcriptional networks. The numbers of transcription factors expressed across the time course were similar to the expression pattern of all of the genes in the experiment. We did not find the SLIM1 regulator of sulfur transport in the data set. This is most likely due to the timing of the experiment as it was probably activated earlier than 3 hrs.

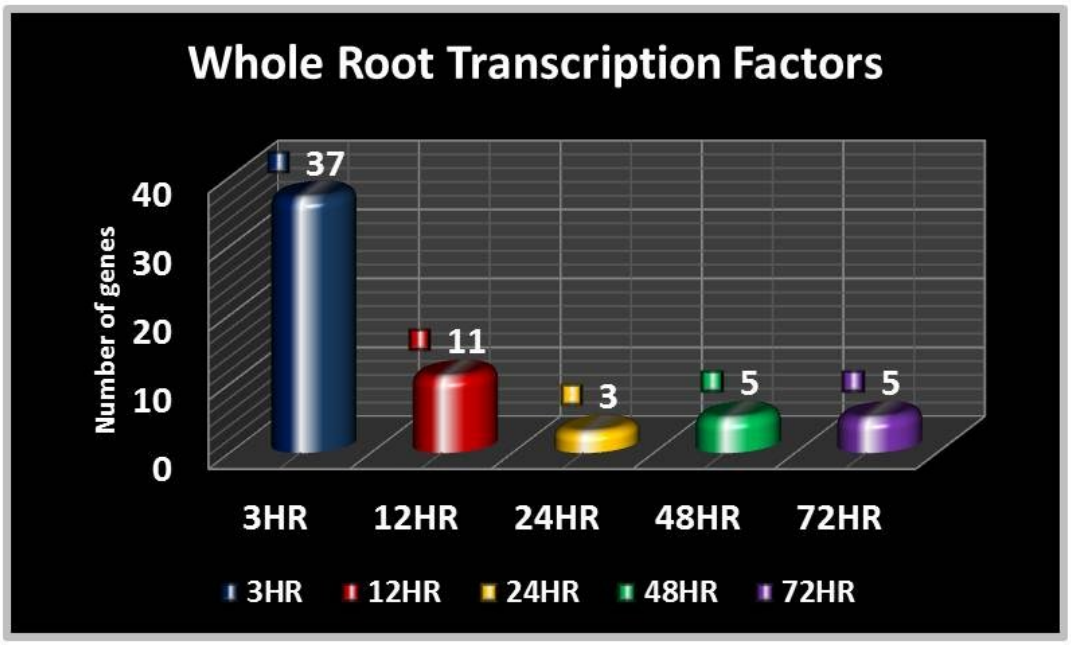

Figure 13: Whole root time course data set transcription factor overall totals.

Following the analysis of the overall number of genes differentially expressed I wanted to determine the genes that were specific to each time point. To do so, I compiled lists describing the number of genes that were specific to a data point and manner in which they were regulated under –S conditions (Figure 14). There were 265 genes that were unique to a particular time point. Of these 266 genes 81% were found at 3hrs, 7% at 12hrs, 2% at 24hrs and 48hrs, and 8% at 72hrs.

Then I determined how this related to transcription factors. The TC data set had a total of 61 TFs differentially regulated with 25 being specific to the 3hr time point and 1 at 48hrs. Of the 61 TFs, 16 were uncharacterized and have T-DNA insertion lines available. I summarize the results in each section before continuing to the next part of the analysis

(Table 4).

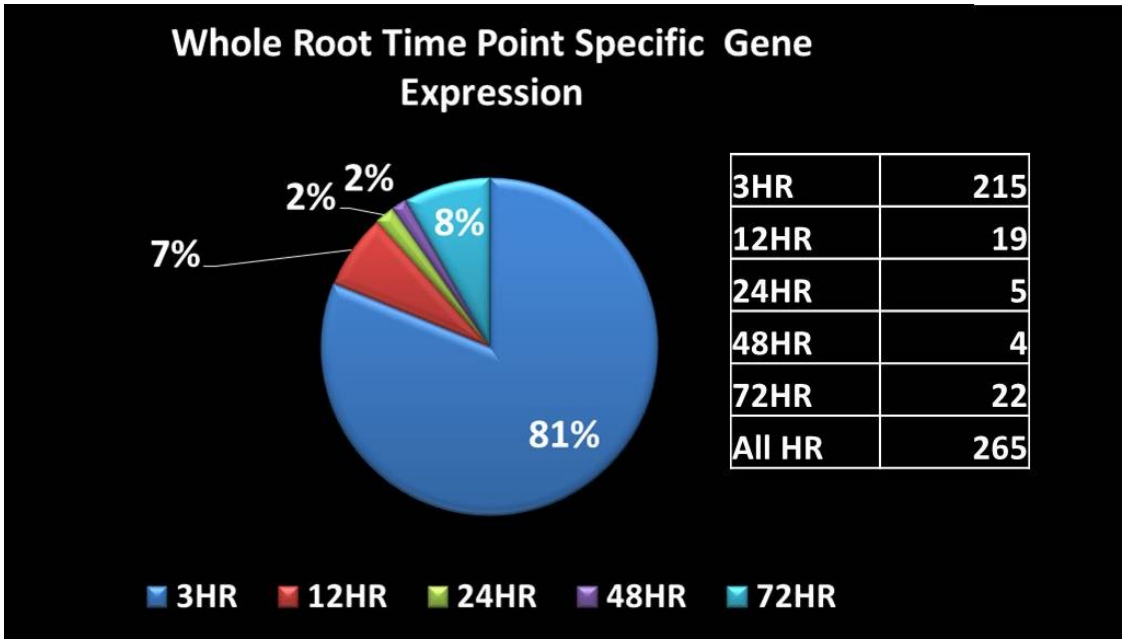

Figure 14: Whole root time point specific totals.

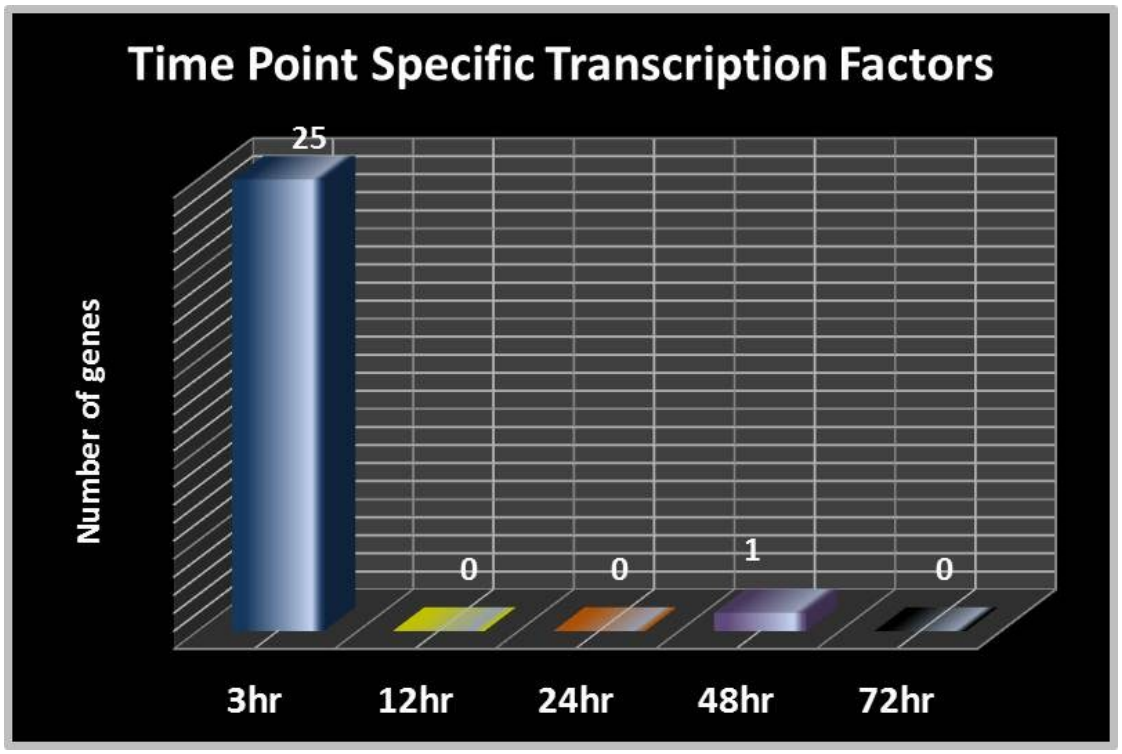

Figure 15: Whole root time point specific transcription factor totals.

Table 4: Overview of whole root time course data set differentially expressed genes.

Time Point	Time Point Total	Up Regulated	Down Regulated	Time Point Specific	Transcription Factors
3HR	359	168	191	215	37
12HR	162	57	105	19	11
24HR	86	43	43	5	3
48HR	89	51	38	4	5
72HR	127	52	75	22	5
All HR	823	371	452	265	61

With these results the 3hr time point was chosen to conduct the radial cell-type and developmental zone specific analyses.

Radial Data Set Analysis

Fluorescence activated cell sorting of GFP-labeled marker lines allows for cell-

type specific resolution of gene expression in the root of Arabidopsis. For this analysis 5 marker lines were used to sort columella, epidermal, cortex, endodermal, and stele cells independently. Our hypothesis was that enriched populations of cell-types will reduce the level of noise associated with mixed populations and; thus, reveal differentially expressed genes important for response to this abiotic stress. This approach has already been proven in the lab to generate much larger data sets compared to whole root experiments.

We do, in fact see a large difference in the overall number of significant genes in the cell-types with thousands of genes being represented (Figure 16). The epidermis was the most responsive radial zone cell-type followed by the cortex. The columella had approximately 150 fewer differentially regulated genes than the cortex. The endodermis and stele had far fewer, a greater than 50% reduction in the number of significant genes. The minor increase of the down-regulation of genes seen in the whole root data set is

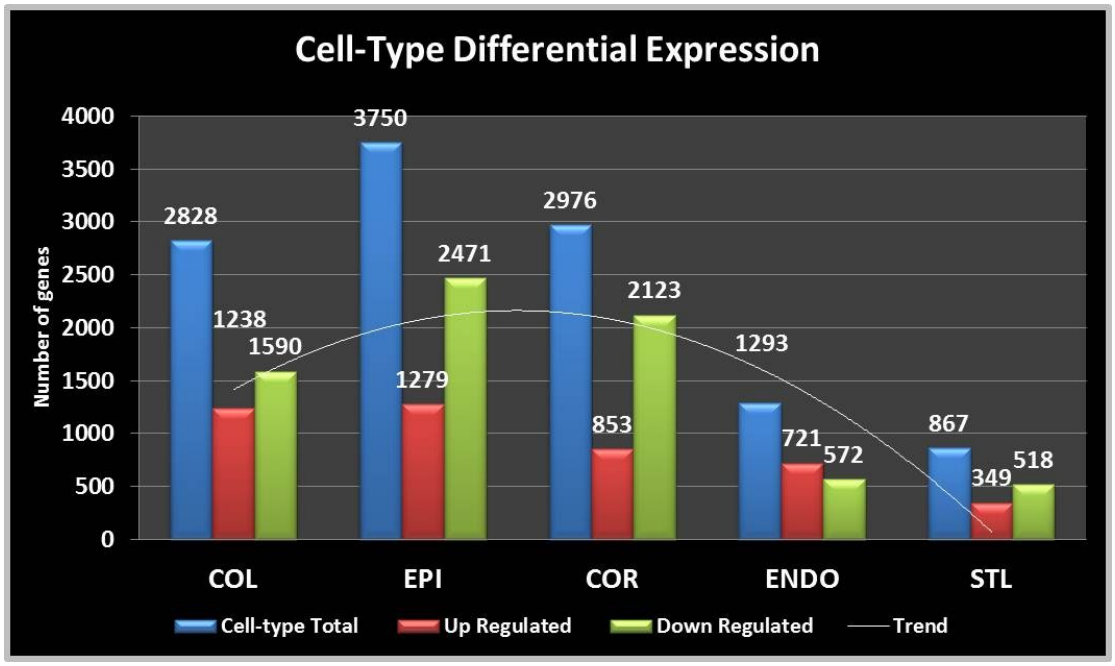

Figure 16: Radial cell-type data set overall totals.

magnified in the radial zone data set.

GO Category enrichment of these cell-types begins to reveal the effect on cellular processes and how the root manages dealing with the stress situation (Figure 17). Translational processes are heavily affected in the epidermis and cortex. Besides this association and a few other incidents, the response of each cell-type is mainly unique. As the epidermis by far down-regulates many processes the remaining cell types actively regulates the up and down-regulation of processes. Sulfate is being actively redistributed in many cell-types and assimilation is active as well.

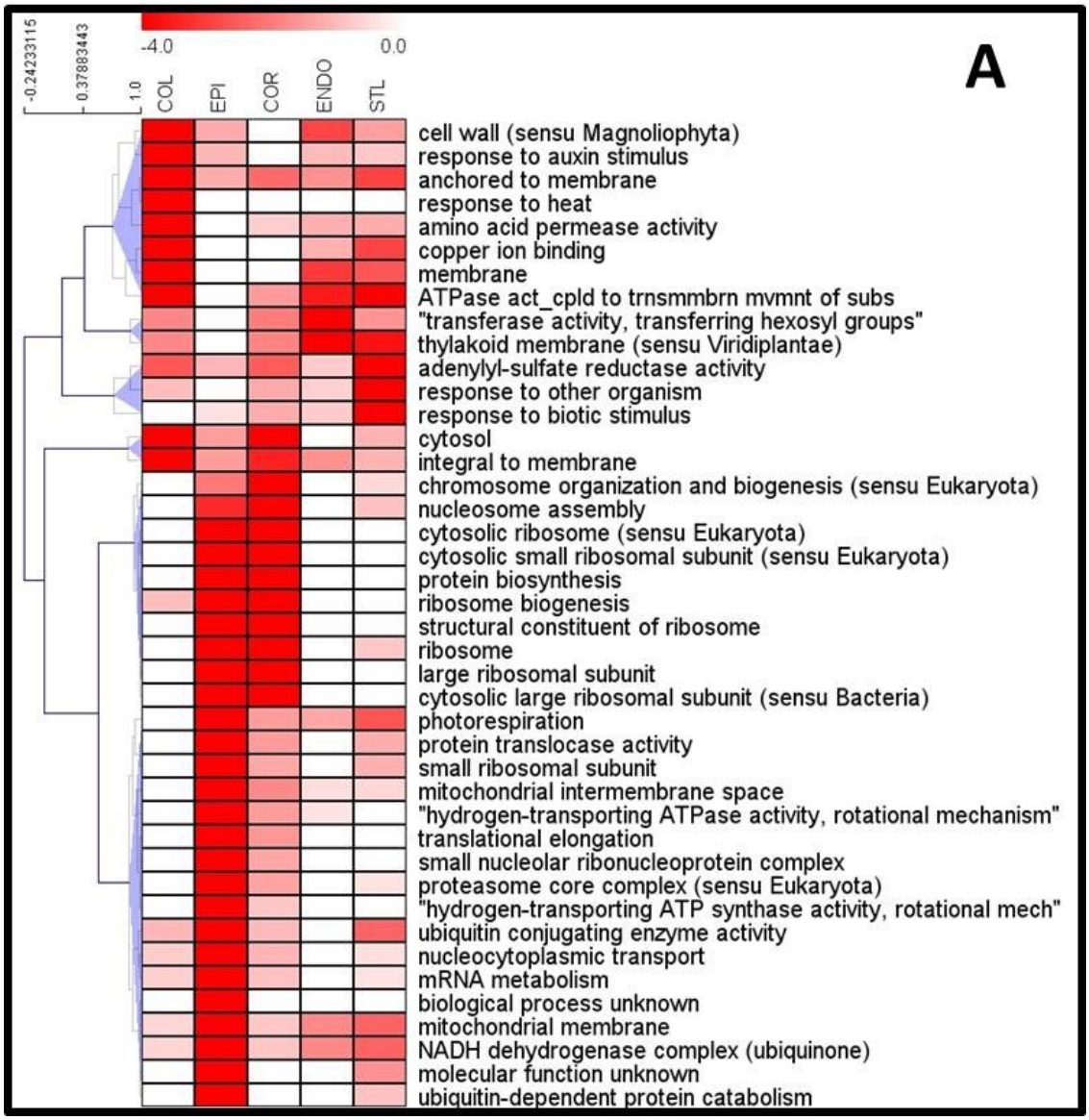
A
-4.0
0.0
-0.24233115
0.37883443
1.0
COL
EPI
COR
ENDO
STL
cell wall (sensu Magnoliophyta)
response to auxin stimulus
anchored to membrane
response to heat
amino acid permease activity
copper ion binding
membrane
ATPase act_cpld to trnsmmbrn mvmnt of subs
"transferase activity, transferring hexosyl groups"
thylakoid membrane (sensu Viridiplantae)
adenylyl-sulfate reductase activity
response to other organism
response to biotic stimulus
cytosol
integral to membrane
chromosome organization and biogenesis (sensu Eukaryota)
nucleosome assembly
cytosolic ribosome (sensu Eukaryota)
cytosolic small ribosomal subunit (sensu Eukaryota)
protein biosynthesis
ribosome biogenesis
structural constituent of ribosome
ribosome
large ribosomal subunit
cytosolic large ribosomal subunit (sensu Bacteria)
photorespiration
protein translocase activity
small ribosomal subunit
mitochondrial intermembrane space
"hydrogen-transporting ATPase activity, rotational mechanism"
translational elongation
small nucleolar ribonucleoprotein complex
proteasome core complex (sensu Eukaryota)
"hydrogen-transporting ATP synthase activity, rotational mech"
ubiquitin conjugating enzyme activity
nucleocytoplasmic transport
mRNA metabolism
biological process unknown
mitochondrial membrane
NADH dehydrogenase complex (ubiquinone)
molecular function unknown
ubiquitin-dependent protein catabolism

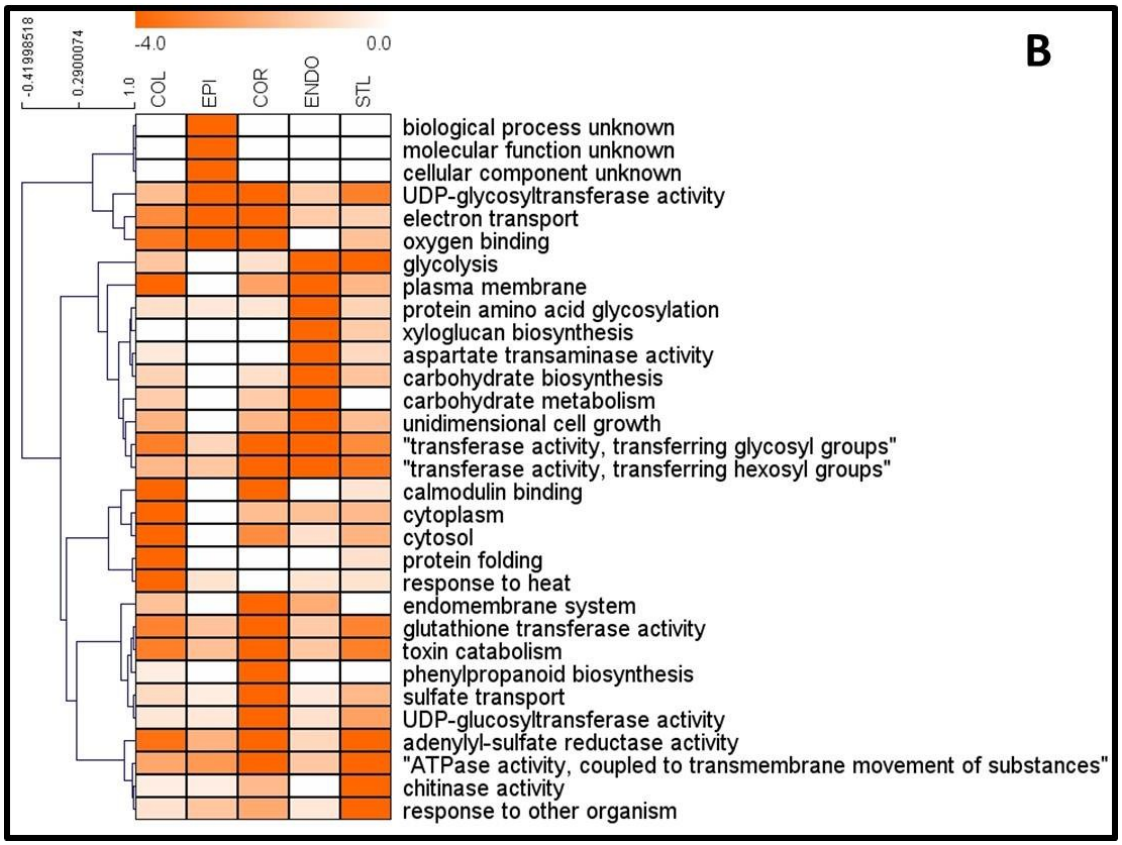
B
-4.0
0.0
-0.41998518
0.2900074
1.0
COL
EPI
COR
ENDO
STL
biological process unknown
molecular function unknown
cellular component unknown
UDP-glycosyltransferase activity
electron transport
oxygen binding
glycolysis
plasma membrane
protein amino acid glycosylation
xyloglucan biosynthesis
aspartate transaminase activity
carbohydrate biosynthesis
carbohydrate metabolism
unidimensional cell growth
"transferase activity, transferring glycosyl groups"
"transferase activity, transferring hexosyl groups"
calmodulin binding
cytoplasm
cytosol
protein folding
response to heat
endomembrane system
glutathione transferase activity
toxin catabolism
phenylpropanoid biosynthesis
sulfate transport
UDP-glucosyltransferase activity
adenylyl-sulfate reductase activity
"ATPase activity, coupled to transmembrane movement of substances"
chitinase activity
response to other organism

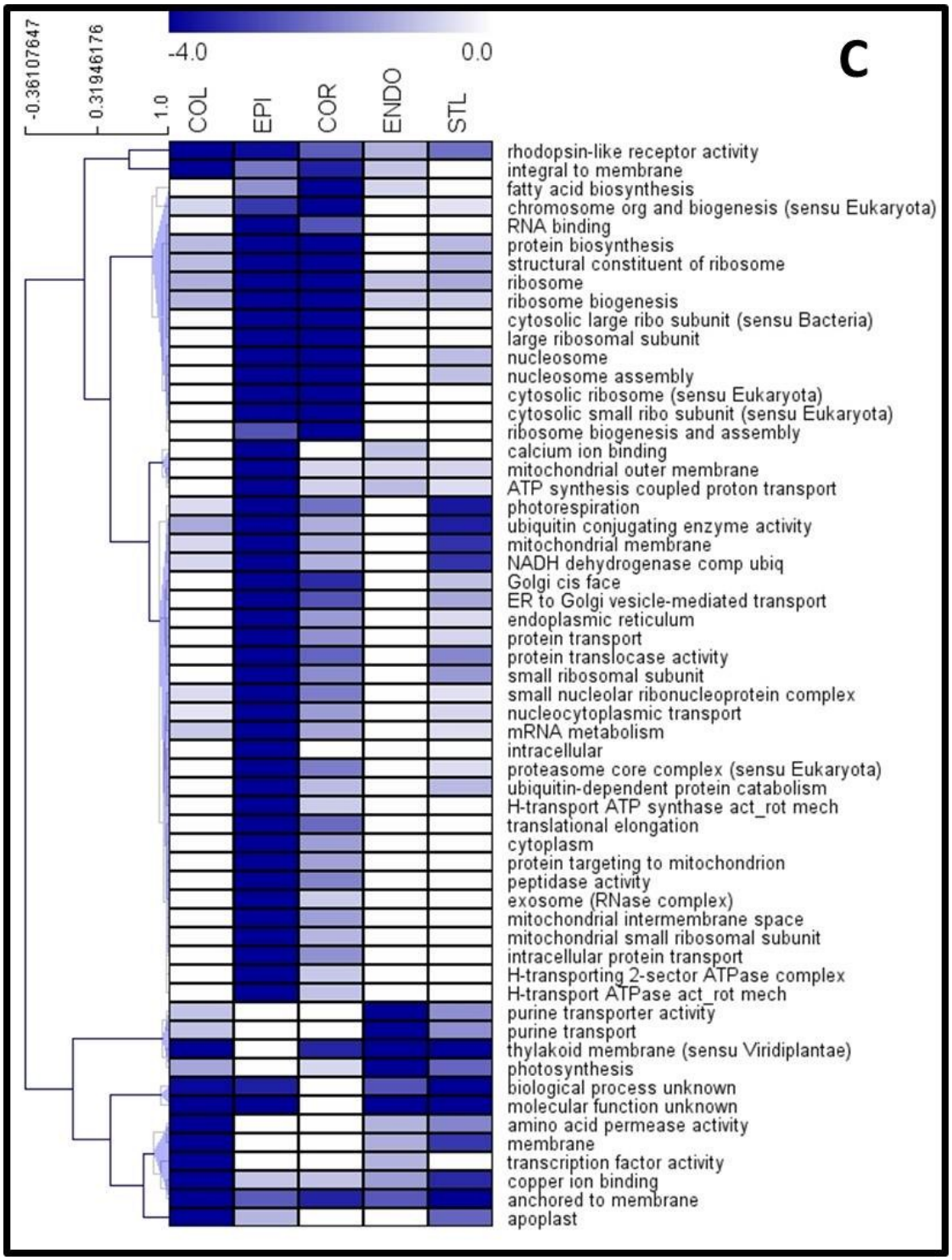

Figure 17: Radial cell-type data set heatmaps of gene ontology.

The columella has the greatest number of transcription factors affected followed by the epidermis and decreasing with each internal cell-type in relation to the external environment (Figure 18).

The analysis of these five cell-types reveals the hierarchy of tissue response in the root (Figure 19). The transcriptional response to –S conditions is greatest in the outer layers and decreases with each successive cell-type further into the root.

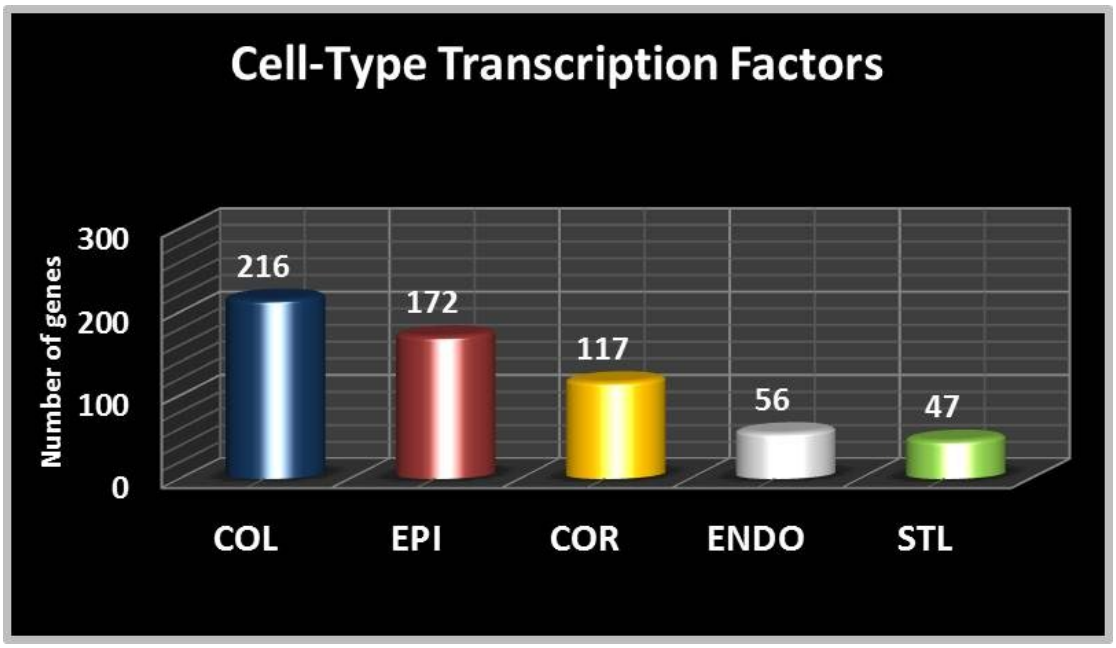

Figure 18: Radial cell-type data set transcription factor overall totals.

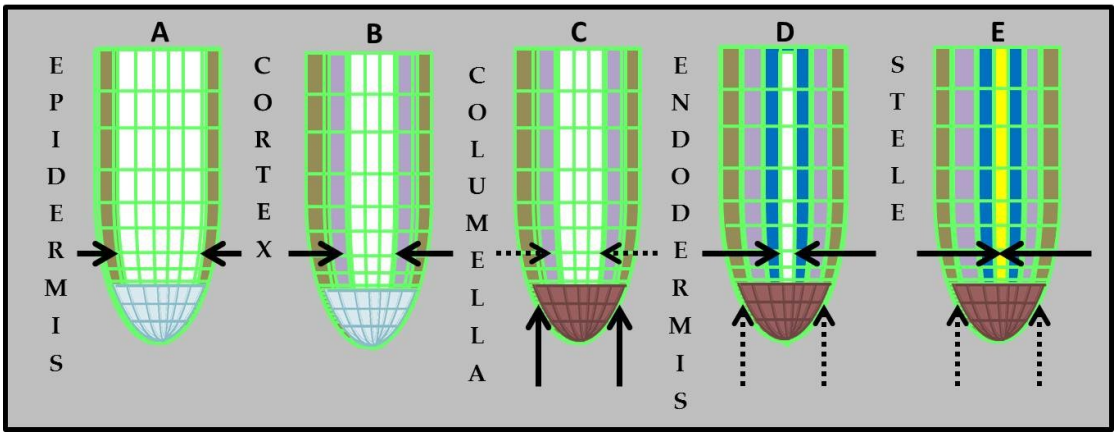

Figure 19: Schematic of differential gene response in radial cell-types.

There were 23 genes differentially expressed in all of the cell types including sulfate transporter 4.1 (SULTR4;1), 5'adenylylphosphosulfate reductase 2 (APR2), ATP sulfurylase 3 (APS1), glutaredoxin, 3 TFs, and 7 unknown or unnamed proteins (Table 5). These shared genes are consistent with the known sulfur deficient stress response in Arabidopsis. These categories reveal the activation of sulfur assimilation genes, response to oxidative stress and transcriptional regulation.

Table 5: Annotations of genes differentially expressed in all cell-types.

GENE ID #	ANNOTATION
At2g34660	ABCC2_MRP2_multidrug resistance-associated protein 2
At3g10500	anac053_NAC053_NAC domain containing protein 53
At1g62180	APR2_5'adenylylphosphosulfate reductase 2
At3g22890	APS1_ATP sulfurylase 1
At5g57920	AtENODL10_ENODL10_early nodulin-like protein 10
At1g10170	ATNFXL1_NFXL1_NF-X-like 1
At2g24500	FZF_Zinc finger protein 622
At1g77370	Glutaredoxin family protein
At5g07860	HXXXD-type acyl-transferase family protein
At5g47110	LIL3:2_Chlorophyll A-B binding family protein
At5g41560	molecular_function unknown
At4g32260	PDE334_ATPase, F0 complex, subunit B/B', bacterial/chloroplast
At2g43500	Plant regulator RWP-RK family protein
At1g12810	proline-rich family protein
At3g22680	RDM1__RNA-DIRECTED DNA METHYLATION 1
At5g13550	SULTR4;1__sulfate transporter 4.1
At1g05560	UGT75B1_UDP-glucosyltransferase 75B1
At3g11340	UGT76B1_UDP-Glycosyltransferase superfamily protein
At5g14690	unknown protein
At3g32930	unknown protein
At3g12870	unknown protein
At3g02640	unknown protein
At2g31090	unknown protein

Cell sorting of these cell-types recovered a total of 5767 sulfur deprivation-responsive genes that are cell-type specific (Figure 20). The epidermis had the largest percentage of these genes, 38 %, followed by 27% for the columella, 24% for the cortex, 9% by the endodermis, and only 2% were found in the stele.

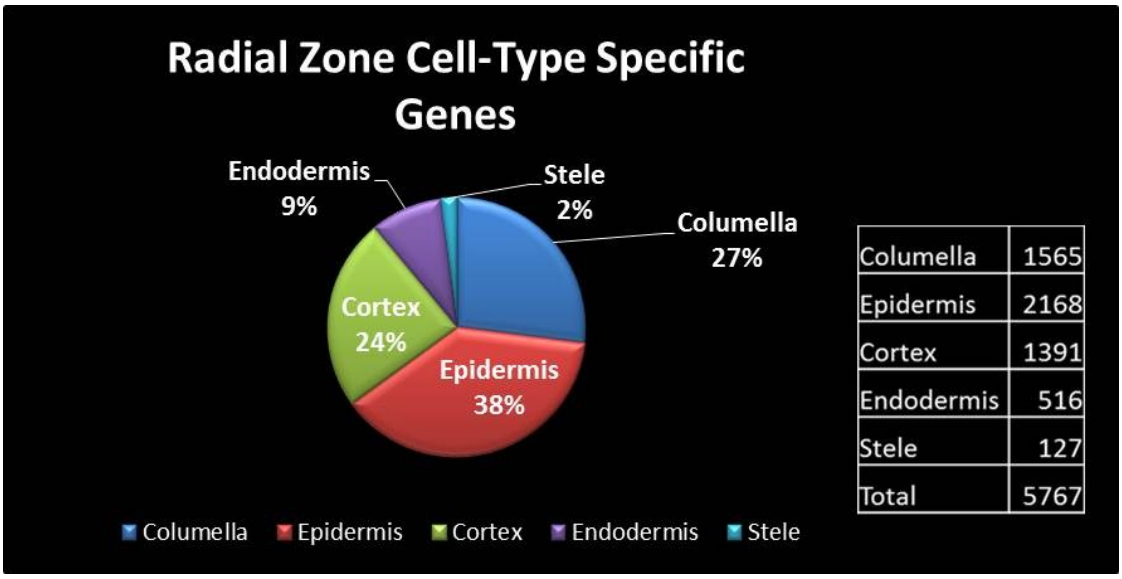

Figure 20: Radial cell-type specific totals.

The total number of significant TFs was 329. Of these 329 TFs, 45% were from the columella, 30% epidermis, 16% cortex, 6% endodermis, and 3% were in the stele (Figure 21).

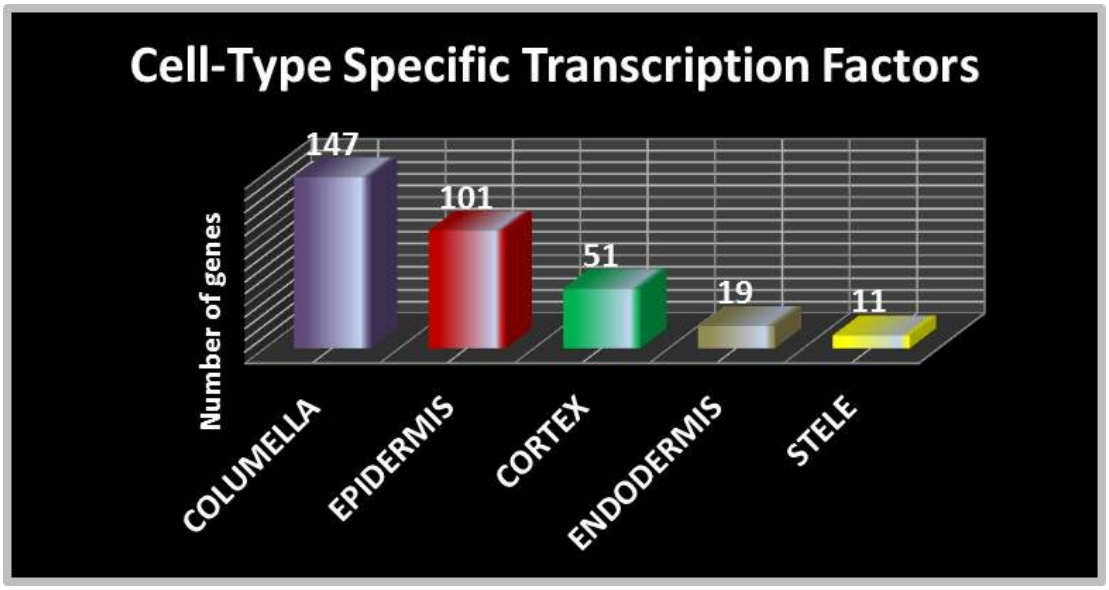

Figure 21: Radial cell-type specific transcription factor totals.

We then looked at the GO Categories represented by these cell-type specific genes to determine the types of genes that are over-represented in each cell layer (Figure 22). Overall, only two processes have specific genes grouped into the same category (Figure 22a). The columella and epidermis both have 5

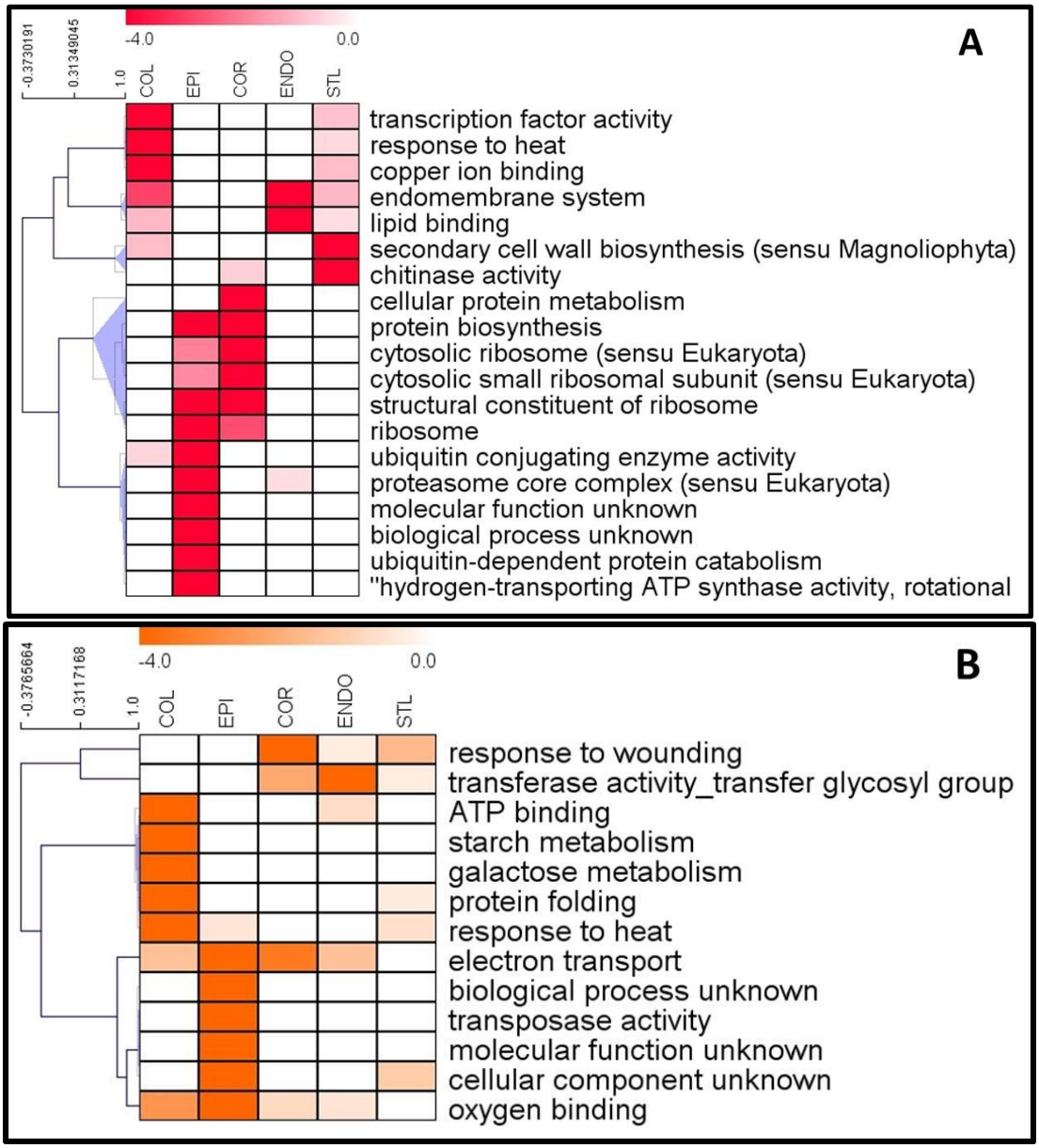
A
-0.3730191
0.31349045
1.0
-4.0
0.0
COL
EPI
COR
ENDO
STL
transcription factor activity
response to heat
copper ion binding
endomembrane system
lipid binding
secondary cell wall biosynthesis (sensu Magnoliophyta)
chitinase activity
cellular protein metabolism
protein biosynthesis
cytosolic ribosome (sensu Eukaryota)
cytosolic small ribosomal subunit (sensu Eukaryota)
structural constituent of ribosome
ribosome
ubiquitin conjugating enzyme activity
proteasome core complex (sensu Eukaryota)
molecular function unknown
biological process unknown
ubiquitin-dependent protein catabolism
"hydrogen-transporting ATP synthase activity, rotational
B
-0.3765664
0.3117168
1.0
-4.0
0.0
COL
EPI
COR
ENDO
STL
response to wounding
transferase activity_transfer glycosyl group
ATP binding
starch metabolism
galactose metabolism
protein folding
response to heat
electron transport
biological process unknown
transposase activity
molecular function unknown
cellular component unknown
oxygen binding

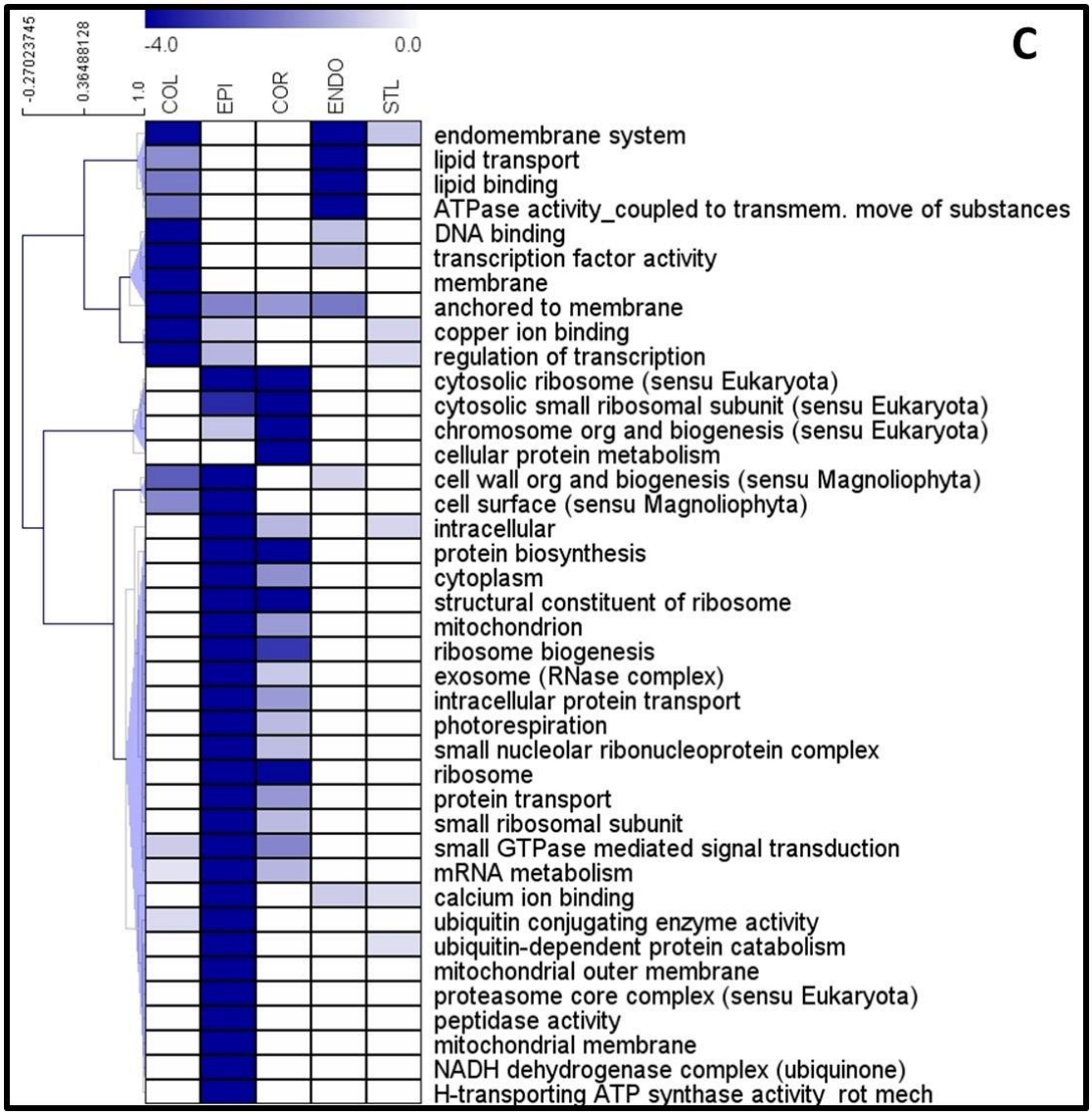

Figure 22: Radial cell-type specific gene ontology.

categories of up-regulated specificity, and the other only have one or two that are significant (Figure 22b). As for down-regulated GO categories, again the epidermis dominates and dwarfs the other cell-types with a wide range of biological processes affected.

In conclusion, the cell sorting process of cell-types produces a larger data set of significant differentially expressed genes compared to whole root methods. Every category analyzed in this section holds true to the power of this procedure (Table 6).

Table 6: Overview of Radial cell-types differentially expressed genes.

Cell-type	Cell-type Total	Up Regulated	Down Regulated	Cell-type specific	Transcription Factors
COL	2828	1238	1590	1565	216
EPI	3750	1279	2471	2168	172
COR	2976	853	2123	1391	117
ENDO	1293	721	572	516	56
STL	867	349	518	127	47
ALL	11714	4440	7274	5767	608

Developmental Zone Data Set Analysis

Microdissecting the developmental stages of the root allows for high resolution gene expression profiling. This data set shows a consistent pattern of a larger number of genes being down-regulated at 3hr versus up-regulated. The L4 section contains the largest set of zone specific genes and TFs. In all there were 4973 zone specific responsive genes. Figure 8 shows the results of this data set. The results from all Phenome stresses studied thus far; +NaCl, -Fe, Low pH, and –S, have a varied developmental zone outcome of sections that yield the highest number of differentially expressed genes. This again demonstrates how different stresses affect the root in a different manner.

The total number of significantly expressed genes of the developmental zones was greater than the cell-type data set. 12,718 genes are the total of the overall data set. The maturation zone (L4) the largest number of genes expressed significantly, followed by the elongation zone, the apical meristem, and finally the basal meristem. There are

also a larger number of down-regulated genes for each zone compared to up-regulated (Figure 23).

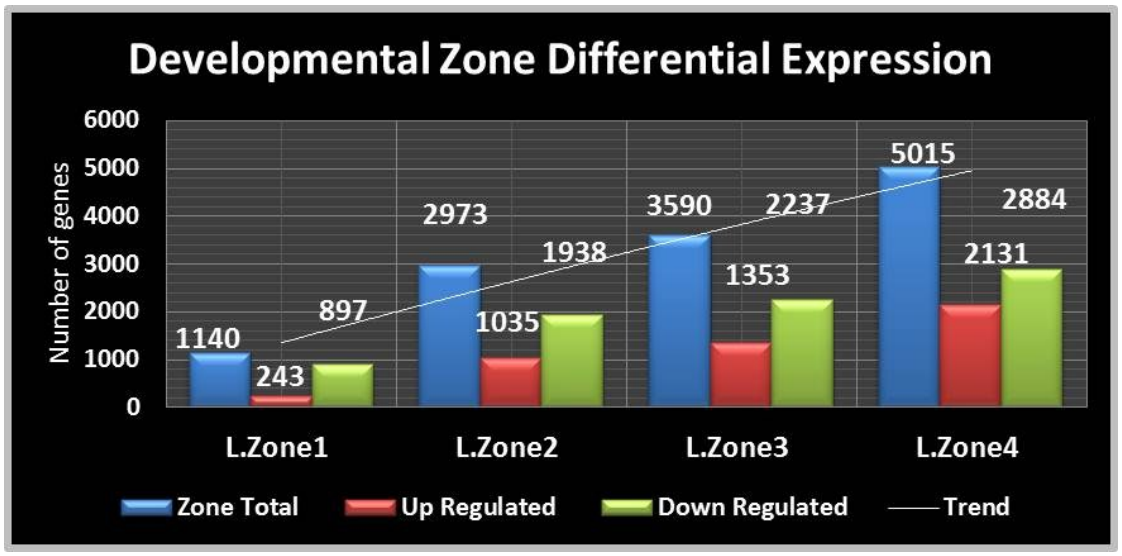

Figure 23: Developmental zone data set overall totals.

The analysis of the GO categories for the overall gene set of the developmental zones again shows that translational processes are highly affected. We also notice the apical meristem and maturation zone have several categories affected biological activity and the basal meristem has very little (Figure 24a). The maturation zone up-regulates translational activity and nuclear organization (Figure 2b) but down-regulates activities involved in oxidative stress. Down-regulated processes are evenly

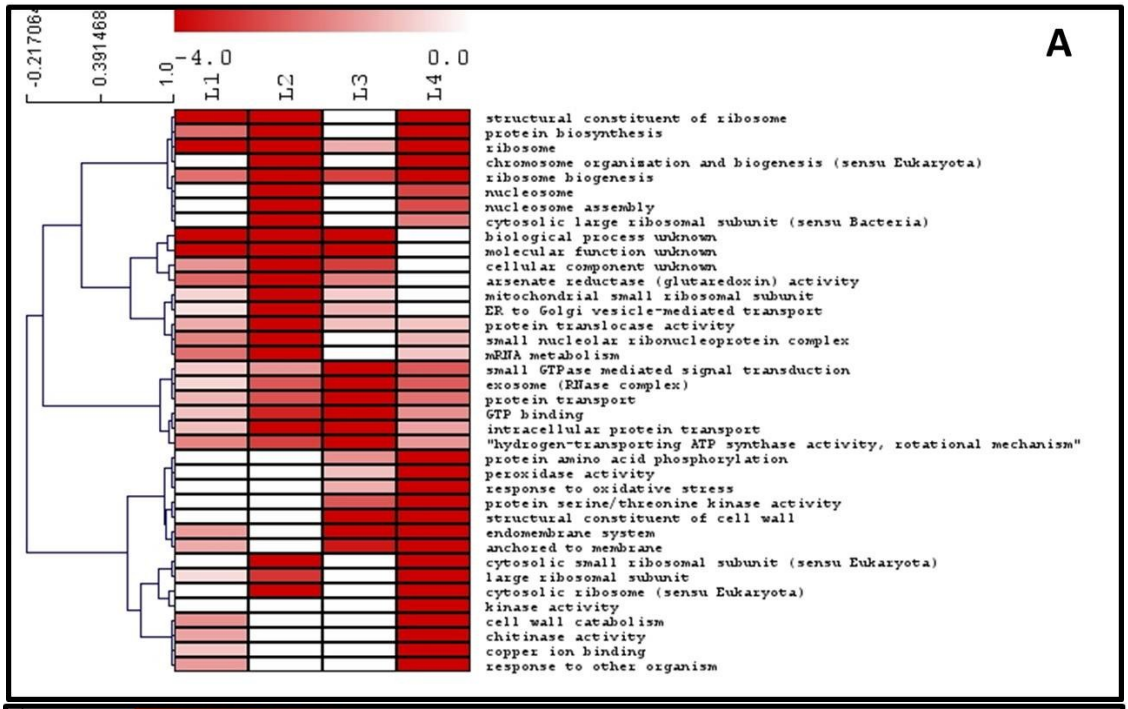
A
-0.21706
0.391468
1.0
-4.0
0.0
L1
L2
L3
L4
structural constituent of ribosome
protein biosynthesis
ribosome
chromosome organization and biogenesis (sensu Eukaryota)
ribosome biogenesis
nucleosome
nucleosome assembly
cytosolic large ribosomal subunit (sensu Bacteria)
biological process unknown
molecular function unknown
cellular component unknown
arsenate reductase (glutaredoxin) activity
mitochondrial small ribosomal subunit
ER to Golgi vesicle-mediated transport
protein translocase activity
small nucleolar ribonucleoprotein complex
mRNA metabolism
small GTPase mediated signal transduction
exosome (RNase complex)
protein transport
GTP binding
intracellular protein transport
"hydrogen-transporting ATP synthase activity, rotational mechanism"
protein amino acid phosphorylation
peroxidase activity
response to oxidative stress
protein serine/threonine kinase activity
structural constituent of cell wall
endomembrane system
anchored to membrane
cytosolic small ribosomal subunit (sensu Eukaryota)
large ribosomal subunit
cytosolic ribosome (sensu Eukaryota)
kinase activity
cell wall catabolism
chitinase activity
copper ion binding
response to other organism

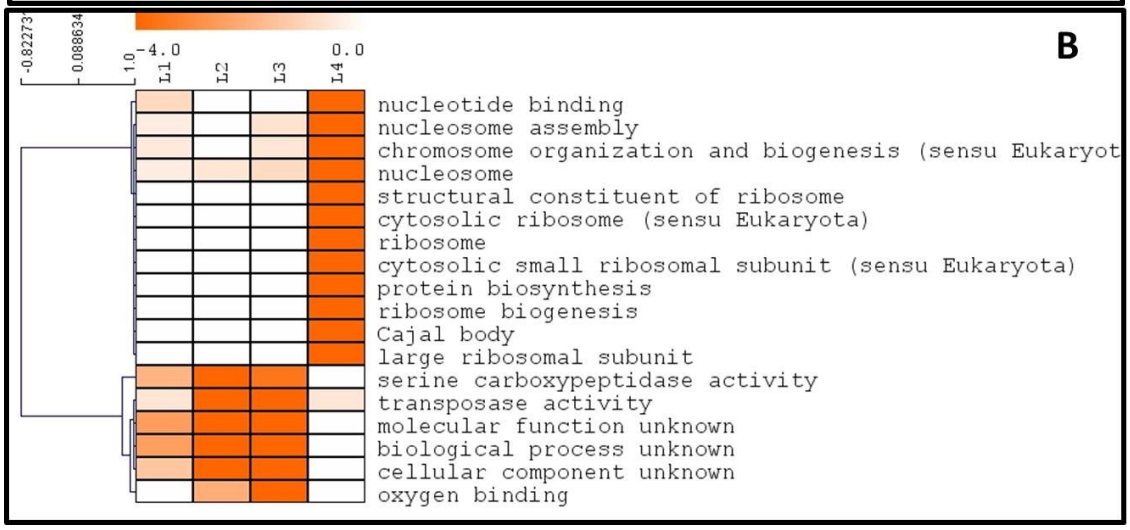
B
-0.82273
0.088634
1.0
-4.0
0.0
L1
L2
L3
L4
nucleotide binding
nucleosome assembly
chromosome organization and biogenesis (sensu Eukaryot
nucleosome
structural constituent of ribosome
cytosolic ribosome (sensu Eukaryota)
ribosome
cytosolic small ribosomal subunit (sensu Eukaryota)
protein biosynthesis
ribosome biogenesis
Cajal body
large ribosomal subunit
serine carboxypeptidase activity
transposase activity
molecular function unknown
biological process unknown
cellular component unknown
oxygen binding

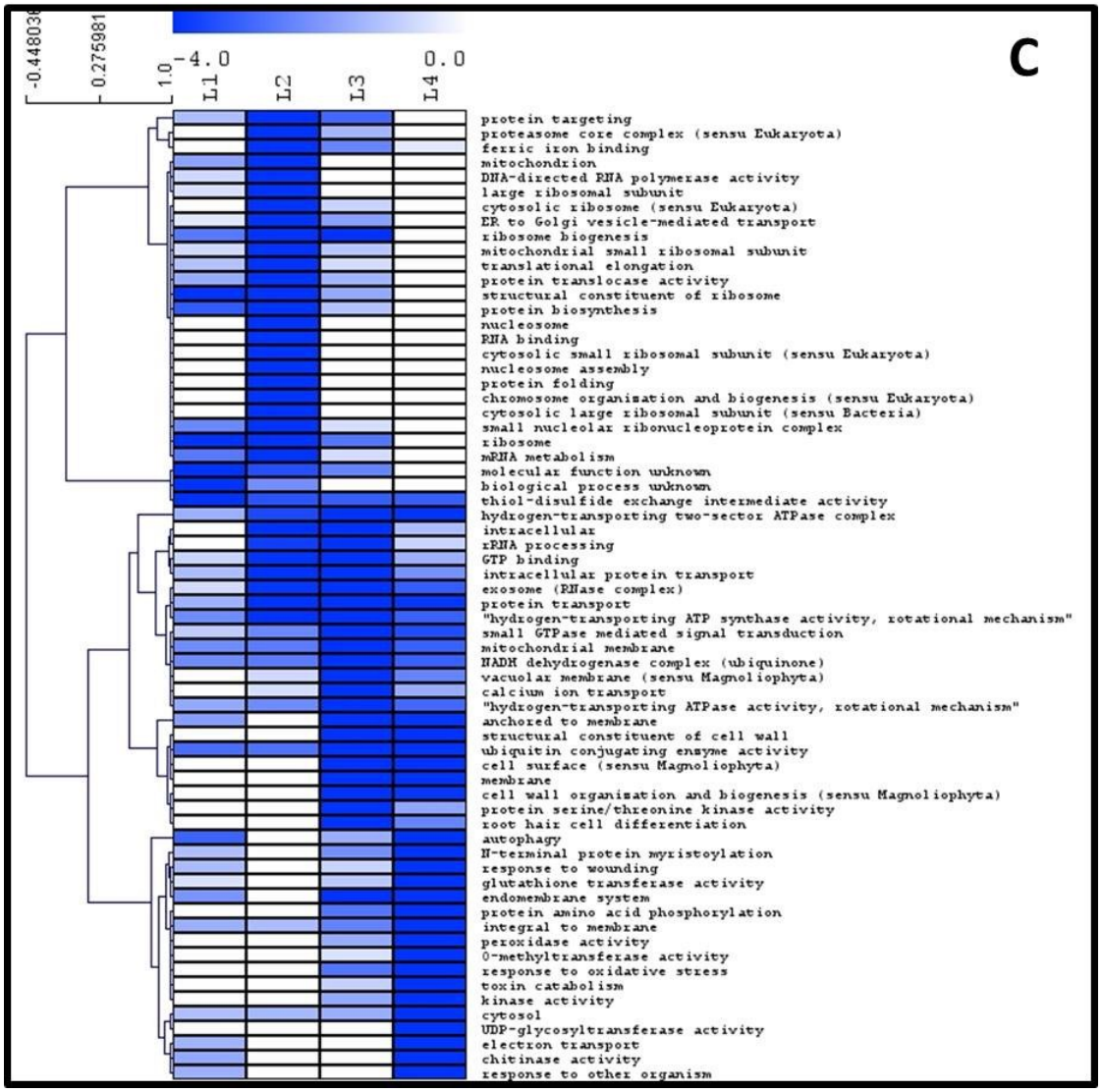

Figure 24: Developmental zone data set heatmaps of gene ontology.

distributed in all developmental zones except the apical meristem which shows very little enriched activity Figure 24c).

There are a total of 577 transcription factors differentially expressed overall for the developmental zone analysis. The maturation zone has 239 genes which is the largest number of TFs among the four sections. This is followed by 182 of the elongation zone,

118 for the basal meristem, and 38 for the apical portion of the meristematic region (Figure 25).

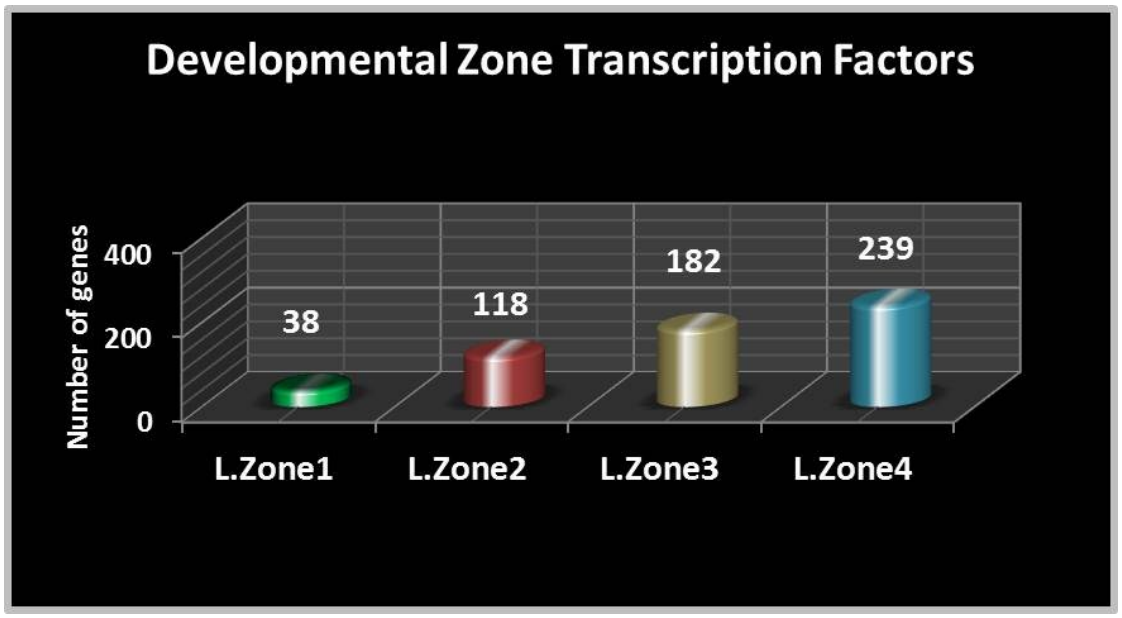

Figure 25: Developmental zone data set transcription factor overall totals.

These data reveal the maturation zone is more susceptible to low sulfur stress and the effect on differential expression decreases steadily in the direction of the root tip (Figure 26). Taken together, with the radial data results it becomes clear that differential gene expression moves from older cells of the outer layers to the youngest cells and in the inner layers.

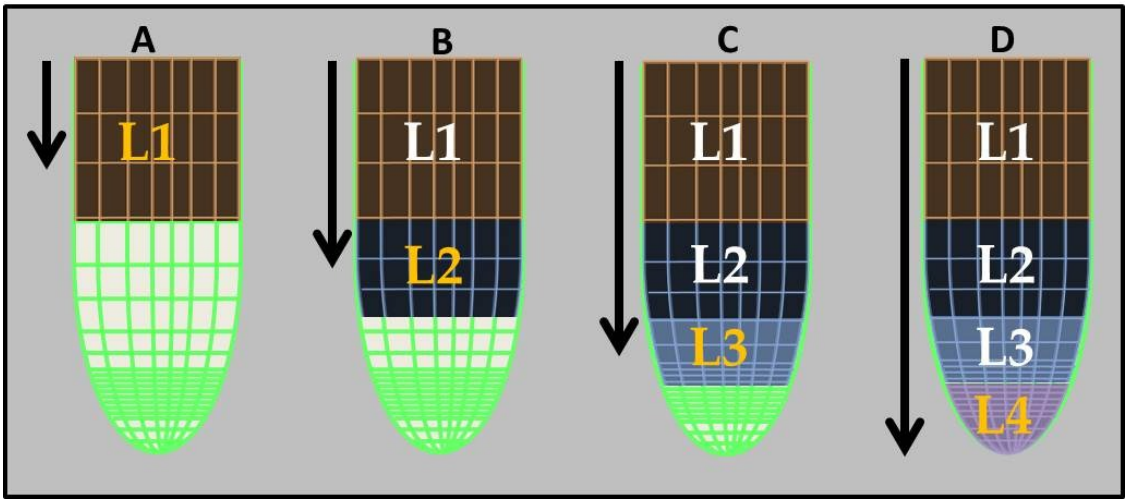

Figure 26: Schematic of differential gene response in developmetal zones.

Fifty-six percent of developmental zone specific genes are from the maturation zone, the elongation zone and basal meristem are nearly the same with 19% and 20%, respectively. The apical meristem sustains only 5% of these zone specific genes (Figure 27).

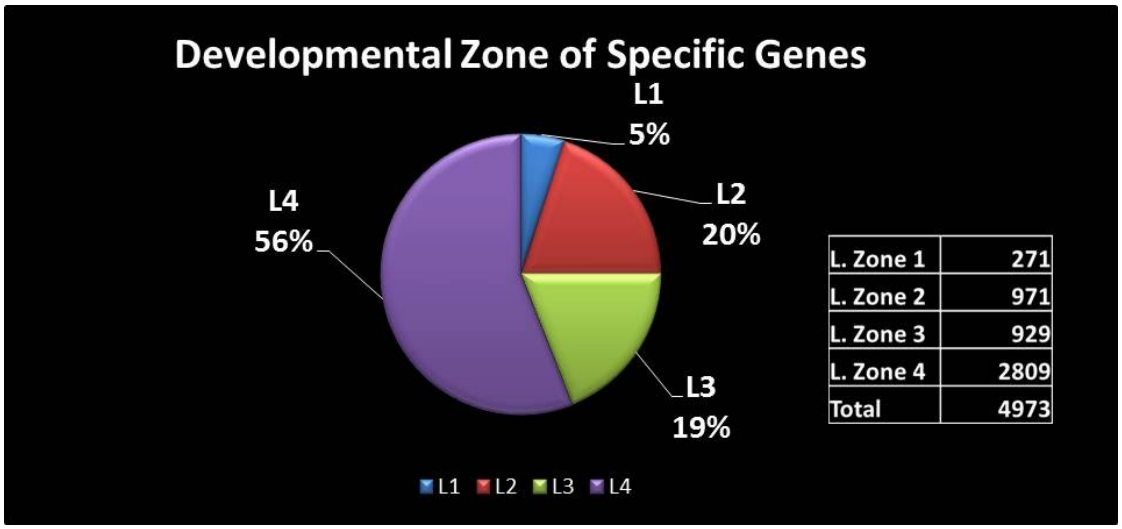

Figure 27: Developmental zone specific totals.

The GO categories for these developmental zone specific genes are similar to the

results from the analysis of all of the genes expressed in all of the zones (Figure 28). The maturation zone clearly is affected overall as well as for processes up-regulated. The down-regulated categories have processes distributed between the basal meristem, elongation zone, and maturation zone. The minimal effect on the apical meristem could

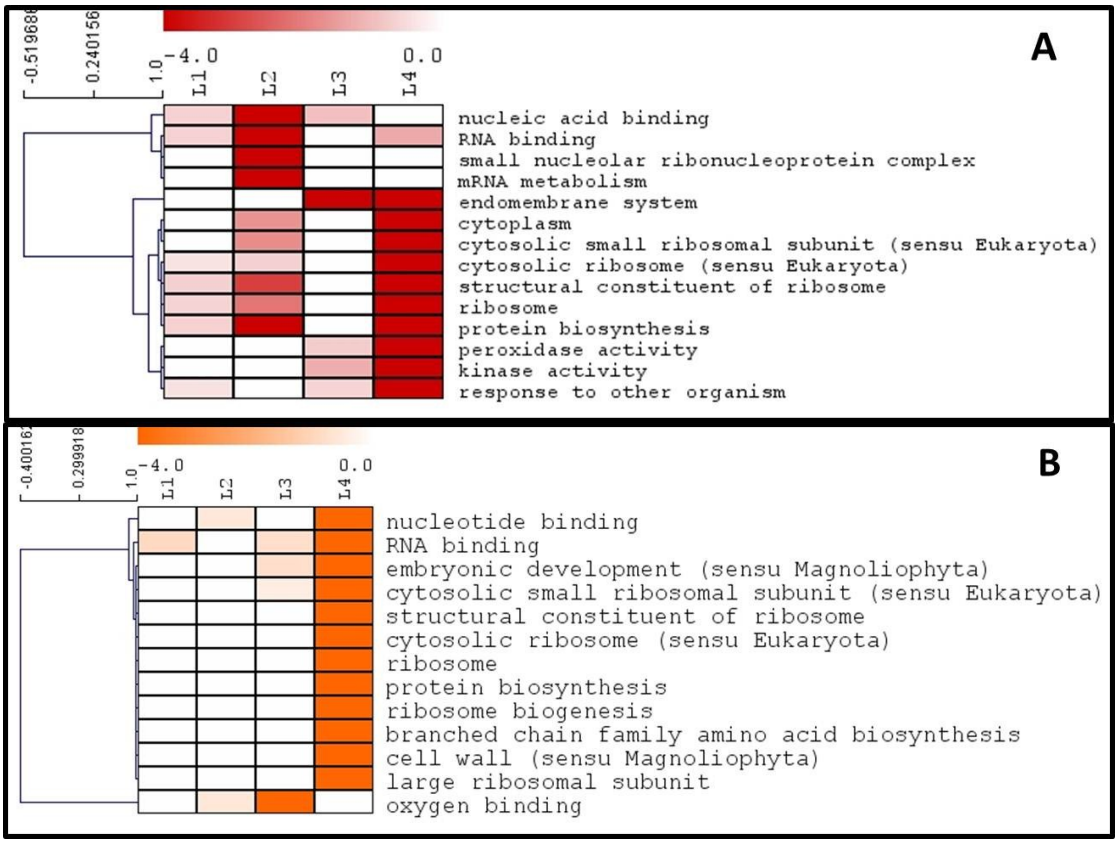

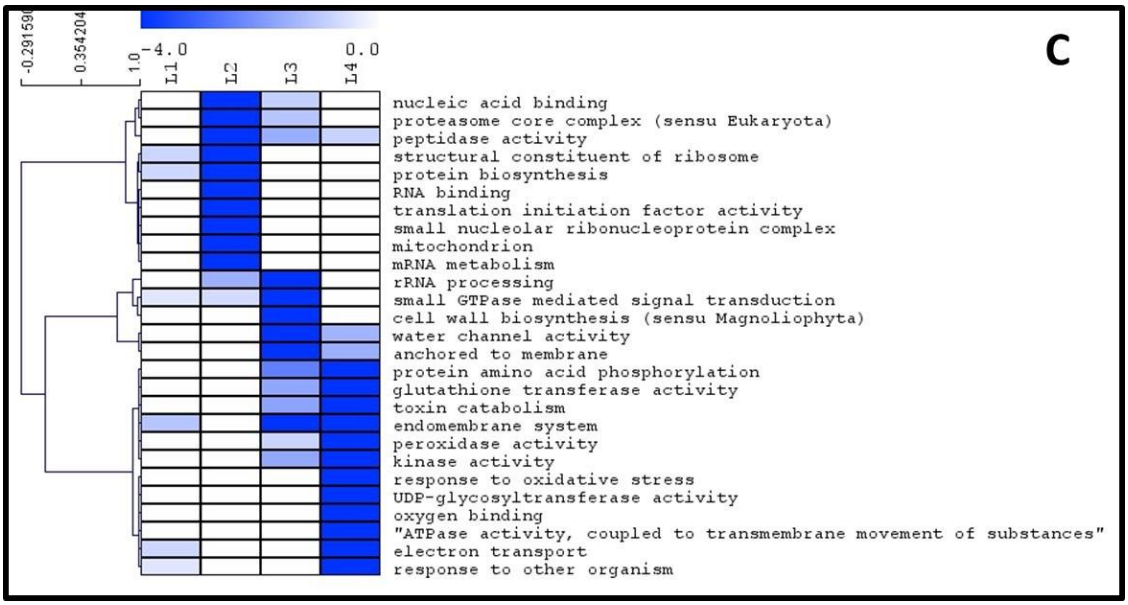

Figure 28: Developmental zone specific gene ontology.

be as a protective effect since the apical meristem contains the quiescent center and the initials. The root exerts energy to maintain homeostasis to produce new cells. The total number of developmental zone specific TFs for all of the sorted lines was 273. Of these 273 TFs, 56% were from L4, 24% L3, 15% L2, and 5% L1 (Figure 29).

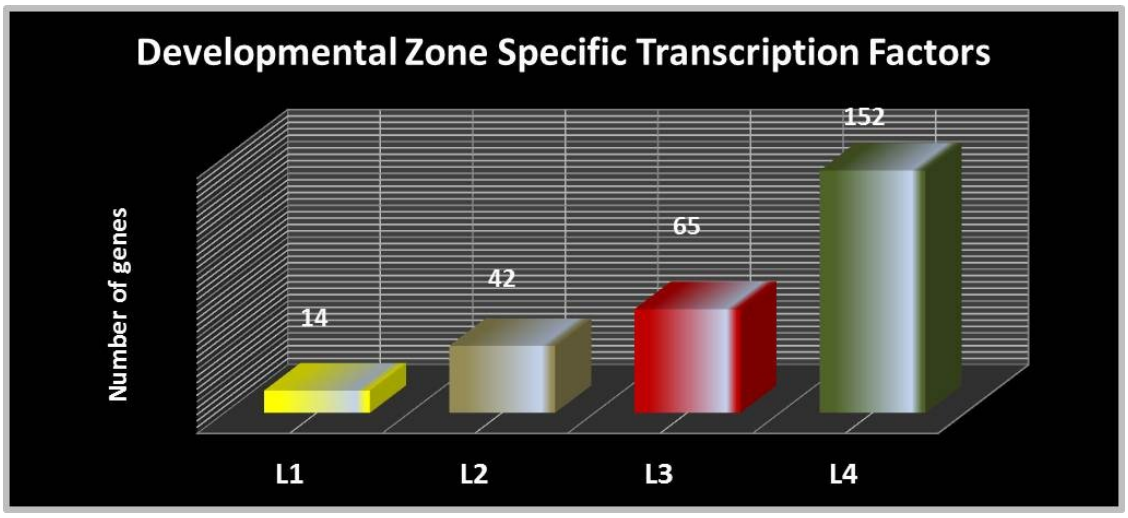

Figure 29: Developmental zone specific totals.

There were 267 genes that were universally expressed across all of the cell types Table 7). Analysis of the Gene Ontology (GO) enrichment associated with these ubiquitously expressed genes revealed biological functions consistent with the sulfur deficient stress response in Arabidopsis. These categories include thiol-disulfide exchange intermediate activity, photorespiration, mitochondrial membrane, NADH dehydrogenase complex (ubiquinone), and a large number of unknown components, processes, and functions. Those without annotations and of unknown functions were removed from the table listing their gene identification numbers and annotation.

Table 7: Annotations of genes differentially expressed in all developmental zones.

AGI	ANNOTATION
At4g02980	ABP_ABP1__endoplasmic reticulum auxin binding protein 1
At1g68300	Adenine nucleotide alpha hydrolases-like superfamily protein
At2g47710	Adenine nucleotide alpha hydrolases-like superfamily protein
At5g65330	AGL78__AGAMOUS-like 78
At3g04570	AHL19__AT-hook motif nuclear-localized protein 19

At3g57870	AHUS5_ATSCE1_EMB1637_SCE1_SCE1A__sumo conjugation enzyme 1
At3g15580	APG8H_ATG8I__Ubiquitin-like superfamily protein
At2g31760	ARI10_ATARI10__RING/U-box superfamily protein
At2g25180	ARR12_RR12__response regulator 12
At3g53060	ASK6_SK6__SKP1-like 6
At3g21840	ASK7_SK7__SKP1-like 7
At3g21850	ASK9_SK9__SKP1-like 9
At4g00860	AT0ZI1_ATOZI1__Protein of unknown function (DUF1138)
At4g27150	AT2S2_SESA2__seed storage albumin 2
At3g51810	AT3_ATEM1_EM1_GEA1__Stress induced protein
At1g66240	ATATX1_ATX1__homolog of anti-oxidant 1
At4g30960	ATCIPK6_CIPK6_SIP3_SNRK3.14__SOS3-interacting protein 3
At2g18250	ATCOAD_COAD__4-phosphopantetheine adenylyltransferase
At2g27490	ATCOAE__dephospho-CoA kinase family
At4g04740	ATCPK23_CPK23__calcium-dependent protein kinase 23
At5g12140	ATCYS1_CYS1__cystatin-1
At3g12490	ATCYS6_ATCYSB_CYSB__cystatin B
At2g38050	ATDET2_DET2_DWF6__3-oxo-5-alpha-steroid 4-dehydrogenase family protein
At4g14430	ATECI2_ECHIB_ECI2_IBR10_PEC12__indole-3-butyric acid response 10
At3g08970	ATERDJ3A_TMS1__DNAJ heat shock N-terminal domain-containing protein
At3g54900	ATGRXCP_CXIP1__CAX interacting protein 1
At5g39950	ATH2_ATTRX2_ATTRXH2_TRX2_TRXH2__thioredoxin 2
At5g42980	ATH3_ATTRX3_ATTRXH3_TRX3_TRXH3__thioredoxin 3
At4g03520	ATHM2__Thioredoxin superfamily protein
At3g17210	ATHS1_HS1__heat stable protein 1
At5g52200	AtI-2_I-2__phosphoprotein phosphatase inhibitors
At3g48890	ATMAPR3_ATMP2_MAPR3_MSBP2__membrane-associated progesterone binding protein 3
At5g52240	AtMAPR5_ATMP1_MSBP1__membrane steroid binding protein 1
At3g52420	ATOEP7_OEP7__outer envelope membrane protein 7
At1g51650	ATP synthase epsilon chain, mitochondrial
At4g26710	ATPase, V0 complex, subunit E
At3g54850	ATPUB14_PUB14__plant U-box 14
At1g18220	ATPUP9_PUP9__purine permease 9
At1g09630	ATRAB-A2A_ATRAB11C_ATRABA2A_RAB-A2A_RAB11c__RAB GTPase 11C
At5g42890	ATSCP2_SCP2__sterol carrier protein 2
At5g59300	ATUBC7_UBC7__ubiquitin carrier protein 7
At3g54300	ATVAMP727_VAMP727_VAMP727__vesicle-associated membrane protein 727
At1g76760	ATY1_TRX-Y1_TY1__thioredoxin Y1
At3g48140	B12D protein
At4g15470	Bax inhibitor-1 family protein

At1g73870	B-box type zinc finger protein with CCT domain
At1g48440	B-cell receptor-associated 31-like
At5g42570	B-cell receptor-associated 31-like
At5g09830	BolA-like family protein
At4g11800	Calcineurin-like metallo-phosphoesterase superfamily protein
At1g64850	Calcium-binding EF hand family protein
At2g44310	Calcium-binding EF-hand family protein
At2g27960	CKS1_CKS1AT__cyclin-dependent kinase-subunit 1
At5g09570	Cox19-like CHCH family protein
At5g25130	CYP71B12__cytochrome P450, family 71, subfamily B, polypeptide 12
At3g10860	Cytochrome b-c1 complex, subunit 8 protein
At5g05370	Cytochrome b-c1 complex, subunit 8 protein
At2g34120	Cytochrome C oxidase polypeptide VIB family protein
At5g08535	D111/G-patch domain-containing protein
At5g25940	early nodulin-related
At3g10780	emp24/gp25L/p24 family/GOLD family protein
At5g12450	FBD-like domain family protein
At2g02660	F-box associated ubiquitination effector family protein
At1g36030	F-box family protein
At3g24760	Galactose oxidase/kelch repeat superfamily protein
At3g61570	GC3_GDAP1__GRIP-related ARF-binding domain-containing protein 1
At1g77370	Glutaredoxin family protein
At3g29075	glycine-rich protein
At4g10330	glycine-rich protein
At2g41490	GPT__UDP-glcnac-adolichol phosphate glcnac-1-p-transferase
At5g63030	GRXC1__Thioredoxin superfamily protein
At1g75600	Histone superfamily protein
At5g62110	Homeodomain-like superfamily protein
At1g76780	HSP20-like chaperones superfamily protein
At2g25500	Inosine triphosphate pyrophosphatase family protein
At5g63990	Inositol monophosphatase family protein
At4g36890	IRX14__Nucleotide-diphospho-sugar transferases superfamily protein
At3g19780	LOCATED IN: endomembrane system
At2g24040	Low temperature and salt responsive protein family
At5g51410	LUC7 N_terminus domain-containing protein
At2g39725	LYR family of Fe/S cluster biogenesis protein
At3g09470	Major facilitator superfamily protein
At3g44100	MD-2-related lipid recognition domain-containing protein
At5g12230	MED19A
At4g13380	MEE56__Heavy metal transport/detoxification superfamily protein

At1g65820	microsomal glutathione s-transferase, putative
At2g22425	Microsomal signal peptidase 12 kDa subunit (SPC12)
At5g63000	Mitochondrial import inner membrane translocase subunit Tim17/Tim22/Tim23 family protein
At1g23260	MMZ1_UEV1A__MMS ZWEI homologue 1
At2g44620	MTACP-1_MTACP1__mitochondrial acyl carrier protein 1
At1g14450	NADH dehydrogenase (ubiquinone)s
At2g02510	NADH dehydrogenase (ubiquinone)s
At3g03100	NADH:ubiquinone oxidoreductase, 17.2kDa subunit
At5g47890	NADH-ubiquinone oxidoreductase B8 subunit, putative
At3g03070	NADH-ubiquinone oxidoreductase-related
At3g62790	NADH-ubiquinone oxidoreductase-related
At1g27970	NTF2B__nuclear transport factor 2B
At3g10090	Nucleic acid-binding, OB-fold-like protein
At1g12400	Nucleotide excision repair, TFIIH, subunit TTDA
At4g35670	Pectin lyase-like superfamily protein
At2g07340	PFD1__PREFOLDIN 1
At4g03930	Plant invertase/pectin methylesterase inhibitor superfamily
At2g24880	Plant self-incompatibility protein S1 family
At3g26870	Plant self-incompatibility protein S1 family
At1g51110	Plastid-lipid associated protein PAP / fibrillin family protein
At4g11830	PLDGAMMA2__phospholipase D gamma 2
At1g33830	P-loop containing nucleoside triphosphate hydrolases superfamily protein
At5g54855	Pollen Ole e 1 allergen and extensin family protein
At3g60540	Preprotein translocase Sec, Sec61-beta subunit protein
At5g38650	Proteasome maturation factor UMP1
At3g06630	protein kinase family protein
At1g18160	Protein kinase superfamily protein
At2g16620	Protein kinase superfamily protein
At5g11410	Protein kinase superfamily protein
At1g71950	Proteinase inhibitor, propeptide
At5g59770	Protein-tyrosine phosphatase-like, PTPLA
At2g43460	Ribosomal L38e protein family
At5g40190	RNA ligase/cyclic nucleotide phosphodiesterase family protein
At2g35635	RUB2_UBQ7__ubiquitin 7
At3g23460	S-adenosyl-L-methionine-dependent methyltransferases superfamily protein
At4g11740	SAY1__Ubiquitin-like superfamily protein
At2g46505	SDH4__succinate dehydrogenase subunit 4
At2g21520	Sec14p-like phosphatidylinositol transfer family protein
At3g48570	secE/sec61-gamma protein transport protein
At2g20840	Secretory carrier membrane protein (SCAMP) family protein

At2g21970	SEP2__stress enhanced protein 2
At2g24340	sequence-specific DNA binding transcription factors
At2g19790	SNARE-like superfamily protein
At3g51660	Tautomerase/MIF superfamily protein
At3g14520	Terpenoid cyclases/Protein prenyltransferases superfamily protein
At1g04290	Thioesterase superfamily protein
At2g20830	transferases;folic acid binding
At5g50870	UBC27__ubiquitin-conjugating enzyme 27
At1g65110	Ubiquitin carboxyl-terminal hydrolase-related protein
At3g23605	Ubiquitin-like superfamily protein
At5g42300	UBL5__ubiquitin-like protein 5
At4g10790	UBX domain-containing protein
At5g45570	Ulp1 protease family protein
At2g23400	Undecaprenyl pyrophosphate synthetase family protein
At5g08290	YLS8__mRNA splicing factor, thioredoxin-like U5 snRNP
At3g52770	ZPR3__protein binding

Global Analysis of Arabidopsis Roots Grown on Low Sulfur Conditions

These data sets present an opportunity to dissect the global sulfur deficient stress response at high spatiotemporal resolution which has not been previously attempted. Within 3hrs of -S a clear transcriptional response occurs in roots. To understand the global expression elicited under these conditions this time point was combined with the radial, and developmental data since these cell-types and developmental zones were analyzed at the 3 hour time point (Figure 30).

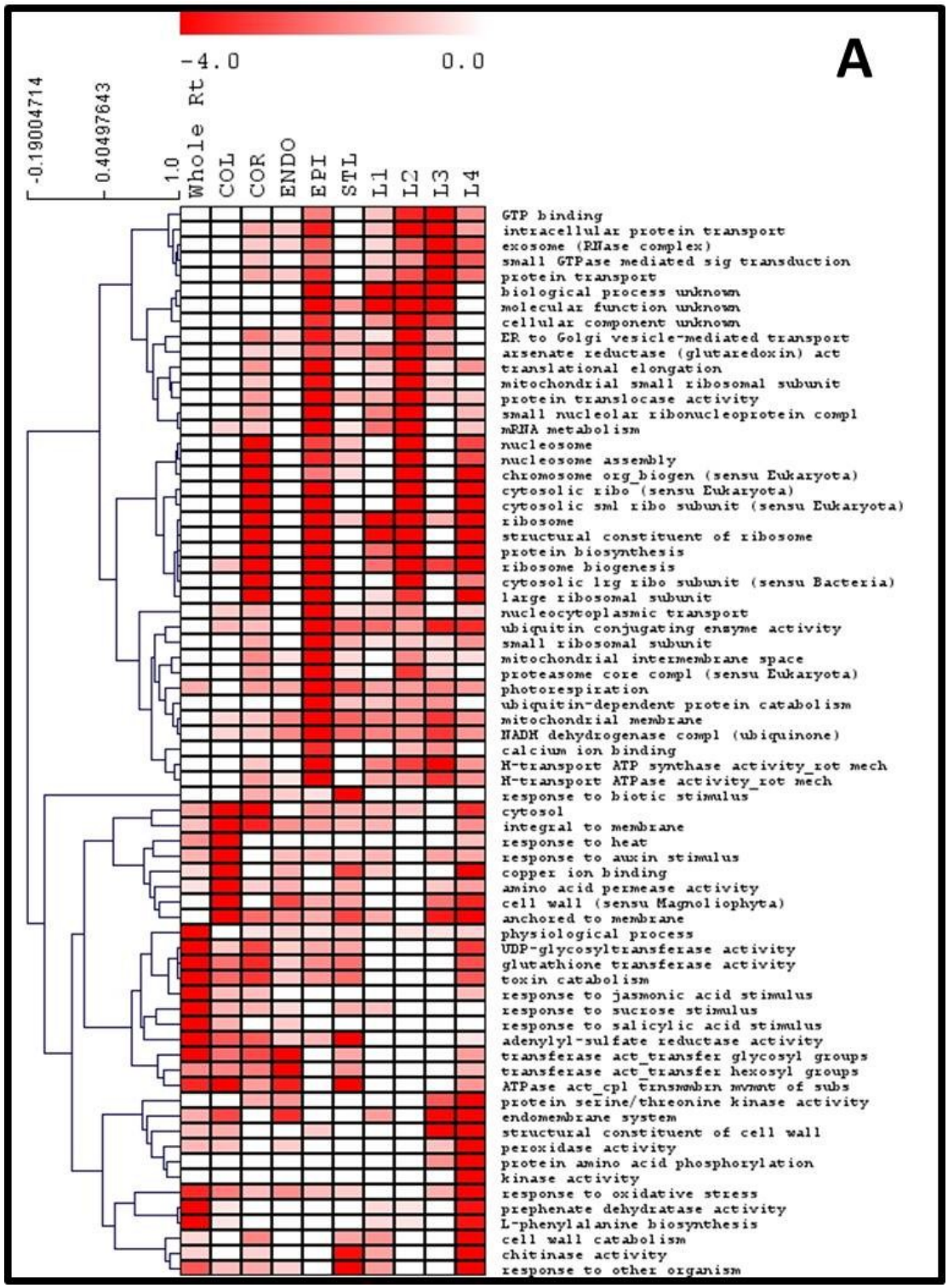
A
-4.0
0.0
-0.19004714
0.40497643
1.0
Whole Rt
COL
COR
ENDO
EPI
STL
L1
L2
L3
L4
GTP binding
intracellular protein transport
exosome (RNase complex)
small GTPase mediated sig transduction
protein transport
biological process unknown
molecular function unknown
cellular component unknown
ER to Golgi vesicle-mediated transport
arsenate reductase (glutaredoxin) act
translational elongation
mitochondrial small ribosomal subunit
protein translocase activity
small nucleolar ribonucleoprotein compl
mRNA metabolism
nucleosome
nucleosome assembly
chromosome org_biogen (sensu Eukaryota)
cytosolic ribo (sensu Eukaryota)
cytosolic sml ribo subunit (sensu Eukaryota)
ribosome
structural constituent of ribosome
protein biosynthesis
ribosome biogenesis
cytosolic lrg ribo subunit (sensu Bacteria)
large ribosomal subunit
nucleocytoplasmic transport
ubiquitin conjugating enzyme activity
small ribosomal subunit
mitochondrial intermembrane space
proteasome core compl (sensu Eukaryota)
photorespiration
ubiquitin-dependent protein catabolism
mitochondrial membrane
NADH dehydrogenase compl (ubiquinone)
calcium ion binding
H-transport ATP synthase activity_rot mech
H-transport ATPase activity_rot mech
response to biotic stimulus
cytosol
integral to membrane
response to heat
response to auxin stimulus
copper ion binding
amino acid permease activity
cell wall (sensu Magnoliophyta)
anchored to membrane
physiological process
UDP-glycosyltransferase activity
glutathione transferase activity
toxin catabolism
response to jasmonic acid stimulus
response to sucrose stimulus
response to salicylic acid stimulus
adenylyl-sulfate reductase activity
transferase act_transfer glycosyl groups
transferase act_transfer hexosyl groups
ATPase act_cpl trnsmmbrn mvmnt of subs
protein serine/threonine kinase activity
endomembrane system
structural constituent of cell wall
peroxidase activity
protein amino acid phosphorylation
kinase activity
response to oxidative stress
prephenate dehydratase activity
L-phenylalanine biosynthesis
cell wall catabolism
chitinase activity
response to other organism

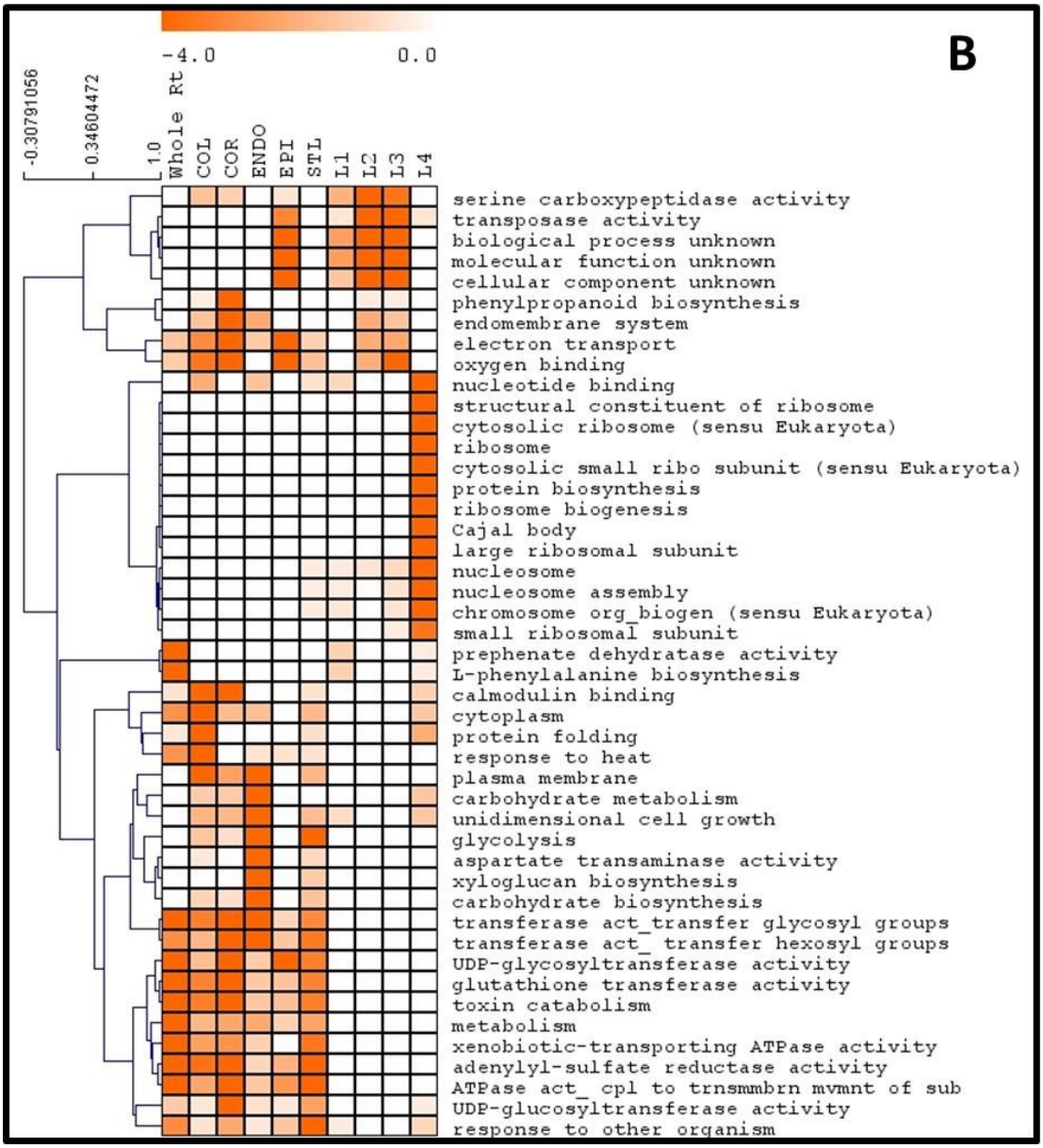
B
-4.0
0.0
-0.30791056
0.34604472
1.0
Whole Rt
COL
COR
ENDO
EPI
STL
L1
L2
L3
L4
serine carboxypeptidase activity
transposase activity
biological process unknown
molecular function unknown
cellular component unknown
phenylpropanoid biosynthesis
endomembrane system
electron transport
oxygen binding
nucleotide binding
structural constituent of ribosome
cytosolic ribosome (sensu Eukaryota)
ribosome
cytosolic small ribo subunit (sensu Eukaryota)
protein biosynthesis
ribosome biogenesis
Cajal body
large ribosomal subunit
nucleosome
nucleosome assembly
chromosome org_biogen (sensu Eukaryota)
small ribosomal subunit
prephenate dehydratase activity
L-phenylalanine biosynthesis
calmodulin binding
cytoplasm
protein folding
response to heat
plasma membrane
carbohydrate metabolism
unidimensional cell growth
glycolysis
aspartate transaminase activity
xyloglucan biosynthesis
carbohydrate biosynthesis
transferase act_transfer glycosyl groups
transferase act_ transfer hexosyl groups
UDP-glycosyltransferase activity
glutathione transferase activity
toxin catabolism
metabolism
xenobiotic-transporting ATPase activity
adenylyl-sulfate reductase activity
ATPase act_ cpl to trnsmmbrn mvmnt of sub
UDP-glucosyltransferase activity
response to other organism

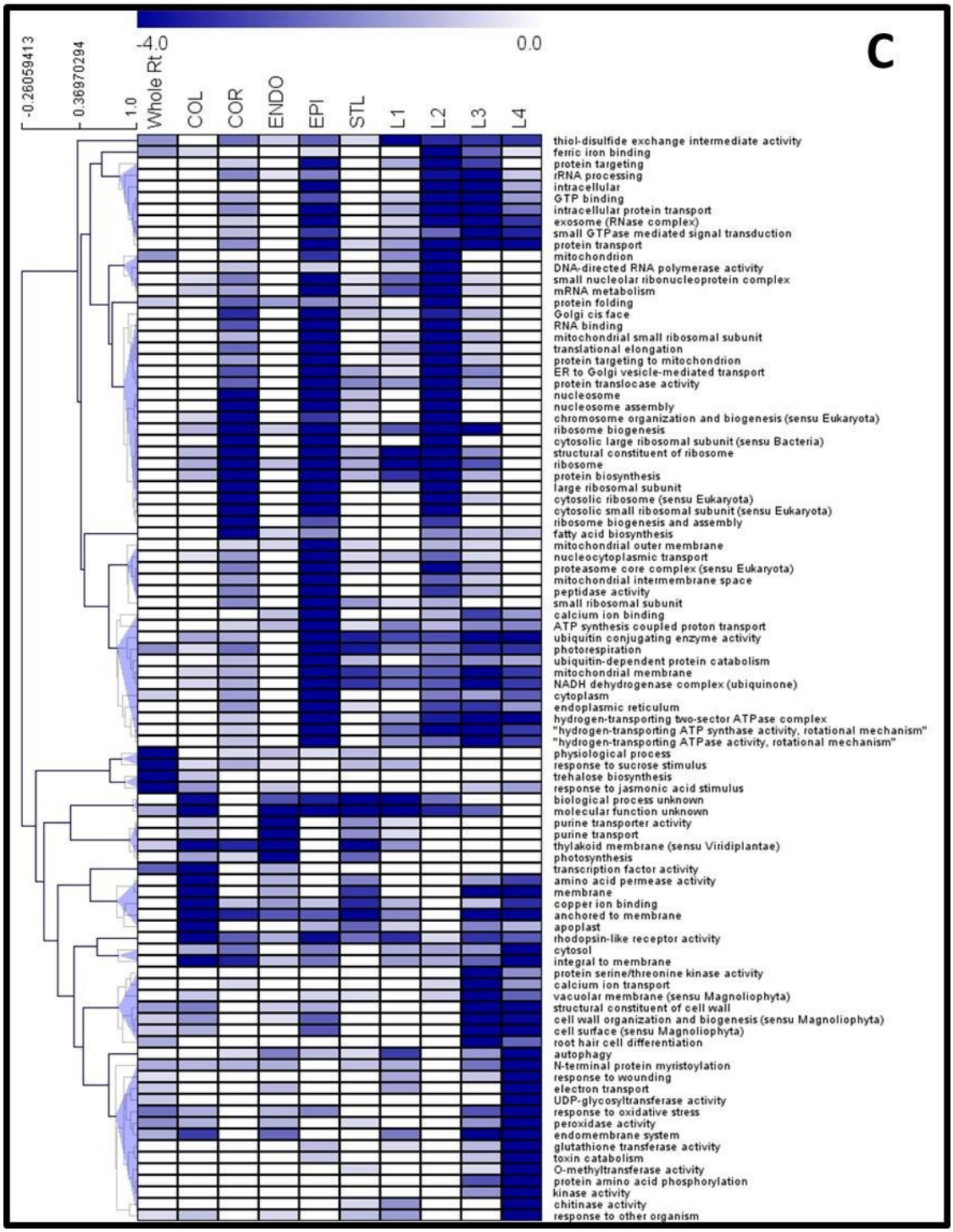

Figure 30: Gene ontology heatmaps of global analysis.

Figure 30 summerizing the main effort of this chapter of my thesis, to create a

high resolution profile of low sulfur stress on the root organ. This was achieved by determining a time point of maximum differential expression of genes and then performing microarray analysis on enriched cell populations from radial cell-types and developmental zones. Sulfur deprivation causes a larger number of genes to down regulate versus those that are up-regulated. Many of the processes down-regulated utilize sulfur in the activities they are involved in such as many translational processes. Meanwhile, it up-regulates processes to transport sulfur reserves, break down toxins, heavy metals, and free radicals that are building up within cells. This analysis reveals that the response is dramatic within 3 hours but it is effective to maintain short-term homeostasis.

Methods

Growth Conditions and Analysis

Arabidopsis plants were grown on 1% sucrose using prepackaged Murashige & Skoog (MS) media (Caisson), complete MS standard media, or media without sulfate. The MS and complete media each contained 1.5mM of sulfate. The only sulfur in the media was from the MES buffer ($C_6H_{13}NO_4S$) which has a molar mass of 195.2g/mol. In the media prepared for these experiments only 0.25g of MES was added to every 500L of media solution. Thus, it was concluded that the amount of sulfur in the media was negligible. The solution was raised to a pH of 5.7 using potassium hydroxide KOH and 1% of Agar was added before autoclaving the media. After autoclaving the media was

cooled and 50mL was poured onto square plates, allowed, to solidify, and stored at 4°C until plating of seeds. Plants grown on the MS media and the self-made media were compared for consistency and also used for transfer experiments onto no sulfur media. COL-0, wild type, seeds were used throughout the experiments, (except an additional set of plates containing pSCR:GFP marker line seeds used to detect lateral root length) and placed in single file rows approximately 10-12 seeds per plate, wrapped with parafilm, and placed into an incubator at 22C with 16hrs of light and 8hrs of dark. Roots were scored 0-2, 0 meaning results were consistent with the control media, 1 was a mild effect, and 2 was a severe effect observed. Root size and growth, lateral root formation, and confocal imaging were parameters used to score the phenotypes.

Visualization of the sulfur pox was performed using bright field microscopy at 10 or 63X magnification. Protoplasting was conducted using the method described (Birnbaum et al., 2003).

Data Set Sample Preparation

Whole Root Time Course

Sample preparation of the TC data set consisted of growing 5day old plants on MS media and then transferring to -S media for 0, 3, 12, 24, 48, and 72 hours. For each time point two biological replicates were prepared from 15-20 roots that were dissected 0.5mm form the hypocotyl/root junction. These roots were placed in RLT lysis buffer

from the RNA easy Micro Kit (Qiagen GmbH) that consisted of 1% BME and sonicated for 10 seconds.

Radial Cell-Types

The radial zone data was plated with the seeds of each reporter line spread in a consistent row of seeds 4-6 seeds thick, two lines per plate and 3 biological replicates were created. Dissected roots were then placed in placed in enzyme solution that will digest the cell wall. After digestion the solution is passed thru two filters to remove debris and centrifuged. These cells are then placed on ice for FACS sorting. The sorted cells are collected in the RLT lysis buffer and placed on dry ice for RNA extraction. The remaining steps are stated above.

Developmental Zones

The longitudinal sections of the developmental zones were plated 10-12 seeds per plate and after 3hrs on –S conditions they were cut into 4 sections using a Micro Feather #715 razor. Sections L1 and L2 cut the apical and basal meristem into 2uM sections. The elongation zone was the L3 sample which was cut ~ 4-5uM thick. The maturation zone section was ~10uM thick. 12-15 roots were dissected in this manner with 2 biological replicates prepared. All sections were immediately placed in RLT lysis buffer and stored on ice until RNA extraction.

Fluorescence Activated Cell Sorting

FACS sorting has been used to sort specific fluorescent cell populations commercially for almost 40 years but it was in 2003 when this method was employed to obtain cell-type specific populations in roots. (Birnbaum *et al*., 2003). Protoplasts of GFP fused reporters are now being harvested for FACS on a routine basis to obtain high resolution and cell-type specific expression data. GFP-fusions to cell-type specific markers of the five basic radial zones are available in the lab and are listed in the Figure 13.

RNA Extraction and Microarray Hybridization Preparation

The RNA extraction was consistent for all data sets and was carried out with a RNA easy Micro Kit (Qiagen GmbH). The samples were then amplified, labeled and fragmented using the Affymetrix one- cycle protocol for whole roots and two-cycles for the remaining data sets. These fragmented samples were sent to Expression Analysis Inc. in Durham NC. Here the samples were hybridized to the ATH1 whole-genome gene chip; covering ~22,000 genes (Affymetrix).

Microarray Data Analysis

The RNA extraction was consistent for all data sets and was carried out with a RNA easy Micro Kit (Qiagen GmbH). The samples were then amplified, labeled and fragmented using the Affymetrix one- cycle protocol for whole roots and two-cycles for the remaining data sets. These fragmented samples were sent to Expression Analysis

Inc. in Durham NC. Here the samples were hybridized to the ATH1 whole-genome gene chip; covering ~22,000 genes (Affymetrix).

Gene Ontology Assessment

Automated GO category enrichment of differentially expressed genes is available as a software tool found on the AREX website (www.arexdb.org/index.jsp). This program identifies significantly enriched GO annotations from a list of genes. GO functions were determined cell-type specific genes and genes that were shared among data sets. Gene functions were compiled using the TAIR website (www.arabidopsis.org). The p-value cutoff and the GO cutoff will be set at -4 to represent the significance cutoff used for all of the experiments.

Chapter 3. Characterization of Sulfur Pox: Root Cellular Inclusions formed in Low Sulfur Conditions

At the cellular level abnormal inclusion bodies have been reported as a stress response. Many studies have shown that upon viral infection of plant tissues inclusions begin to appear. Nicotiana *benthamiana* leaves infected with ground nut virus show viral ribonucleic proteins that aggregate into cyptoplasmic inclusions forming interactions with cellular compartments and mobilizing to proliferate throughout the entire plant (Kim et al. 2007). In a separate report to determine if microtubules were necessary for viral movement, Nicotiana *benthamiana* was infected with tobacco mosaic virus (TMV), potato virus X (PVX), tomato bushy stunt virus (TBSV), and turnip vein-clearing virus (TVCV). The GFP fusions of TMV and TVCV both showed accumulation of cellular inclusions in leaf cells (Harries et al. 2009). Plants also contain stress granules and heat stress granules as reported for cells of Arabidopsis and tomato. These may represent the storage site of messenger ribonucleoproteins (mRNPs). These two types of granules are distinct in nature and can be induced during stress conditions such as hypoxia and heat stress (Weber et al. 2008). Heat shock proteins have also been shown to be induced by viral infection as was shown for the heat shock protein 70 genes when viral proteins aggregate in the cytoplasm of Nicotiana *benthamiana* and Arabidopsis *thaliana* (Aparicio et al. 2005). An interesting cellular process that forms inclusions under stress situations such as starvation is autophagy where degradation of cellular components is carried out

by membranous autophagosomes which transport these contents to lysosomes and vacuoles (Oh-ye et al. 2011). In nitrogen starved tobacco BY-2 cells, autophagosomes were found trafficking protein aggregates to the vacuole and in Arabidopsis roots autophagy takes part in response to oxidative stress by sequestering oxidized proteins and transporting them to the vacuole. Other vesicle bound bodies involved in transport such as prevacuolar compartments (PVCs) and multivesicular bodies (MVBs) can also be considered cellular inclusions. Another form of inclusions are crystal structures of inorganic material such as calcium oxalate crystals which form in roots and other plant parts in specialized cells called idioblasts (Webb 1999; Volk et al., 2004). These form cellular inclusions that are very small. Even when they are reported to be large inclusions they must be viewed using fluorescent probes, staining, or electron microscopy and none have an established role in the response to sulfur deprivation. To date no phenotypic response has been shown to occur upon short term sulfur limiting conditions, as well as long term sulfur starvation. Here, we describe a novel phenotype of sulfur starvation in roots of Arabidopsis t*haliana*. These cytoplasmic inclusions are termed 'sulfur pox' (-S pox) because when they were first observed they look like pockmarks or blemishes scattered across sections sulfur starved roots. These sulfur pox are produced under both short term and long term sulfur deprivation conditions in Arabidopsis roots. The phenotype can also be reversed. We discuss metabolic analysis

of roots sections exhibiting this phenotype, and examine microarray data of sulfur-deficient roots subjected to multiple conditions.

Sulfur Pox are a Novel Cellular Inclusion Body and a Unique Phenotype among 28 Abiotic Stresses

We performed a phenotypic analysis on 28 abiotic stresses which include nutrient deficiencies, drought simulation, low pH, and metal toxicities. We analyzed shoots, root hairs, root growth and shape, and performed confocal imaging of the root tip. The seedlings were scored four times over 11 days. During microscopy on day 8, it was observed that there were multiple inclusion spots on the roots and these spots were termed "sulfur pox". Upon inspection at higher magnification it was discovered that these were not spots on the outside of the roots but brightly colored cellular inclusions (Figure 31.) Sulfur deficiency was the only stress during which these inclusions were observed. To see these inclusions very specific plants must be grown under special

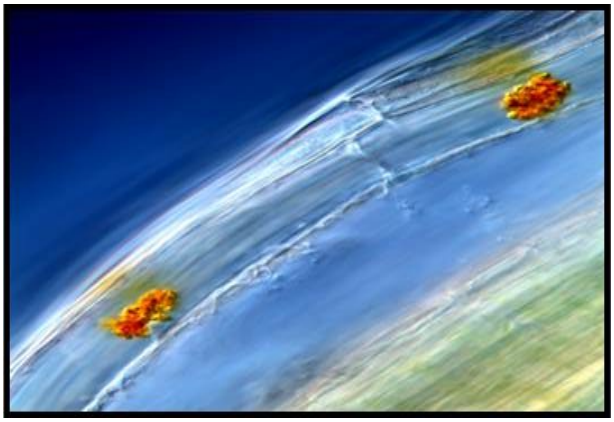

Figure 31: Imaging of cellular inclusions termed "sulfur pox".

conditions. Sulfur pox can be as large as 8nm and occupy the total width of the cell and

have an amber hue easily detectable under a light microscope. This seemingly late but unique phenotypic response led many to assume that the response to low sulfur conditions occurred many days after exposure. I performed a time course of seedlings directly germinated on –S media and observed that the initial appearance of the –S pox actually began 5 days into the experiment (Figure 32). Also, the manner of germination is a factor. An alternate means of producing them in a faster time period is to germinate

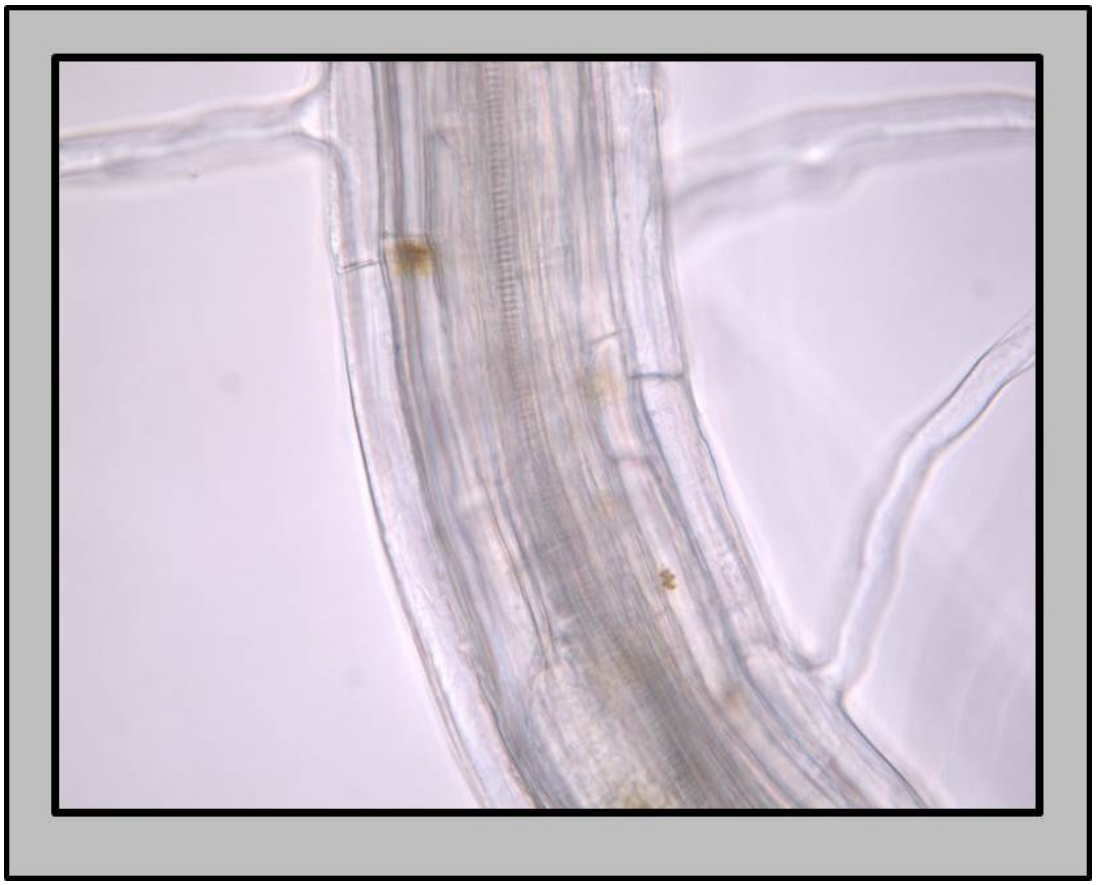

Figure 32: Sulfur pox develop in roots after 5 days in roots grown directly on low sulfur media.

the plants on normal media (MS) and then transfer them to low sulfur media. Under

these conditions the sulfur pox appear within 10.5hrs and this can be achieved prior to 8 days of growth (Figure 33).

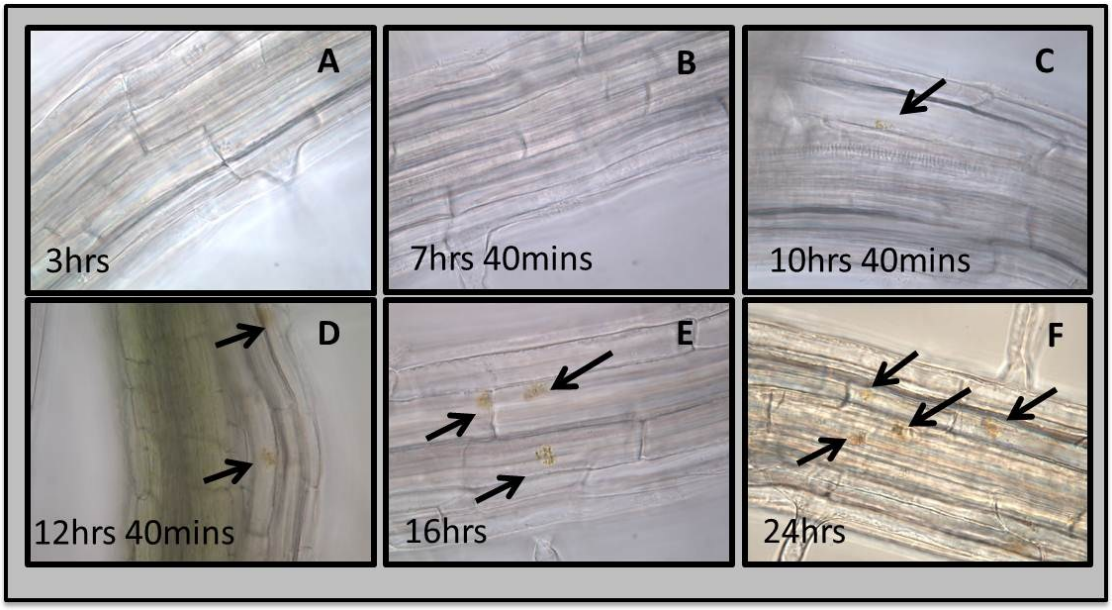

Figure 33: Time course of sulfur pox production in root transferred from enriched media to low sulfur media.

Sulfur pox form in many regions of the root but mainly in differentiated cell-types (Figure 34) between the lower hypocotyl and the middle of the root. They have also been seen in lateral roots, and also, but rarely in root hairs.

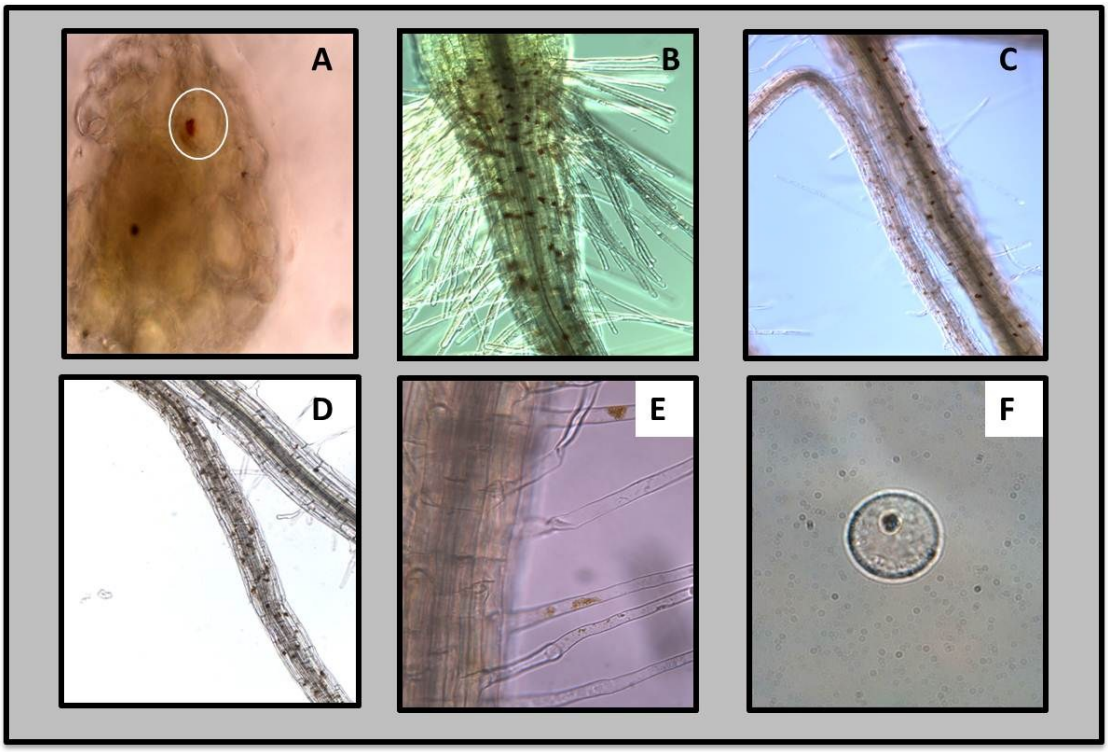

Figure 34: Images of differentiated cells types where sulfur pox have been observed.

Observation of transverse sections and confocal imaging revealed that sulfur pox form mainly in cortex cells and occasionally in epidermal cells. GFP-organelle marker lines show a subcellular localization in the cytoplasm of cells compared to other organelles (Figure 35). Unlike large cellular organelles, such as chloroplasts, which migrate to maximize their position in relation to the sun and then maintain their position, the sulfur

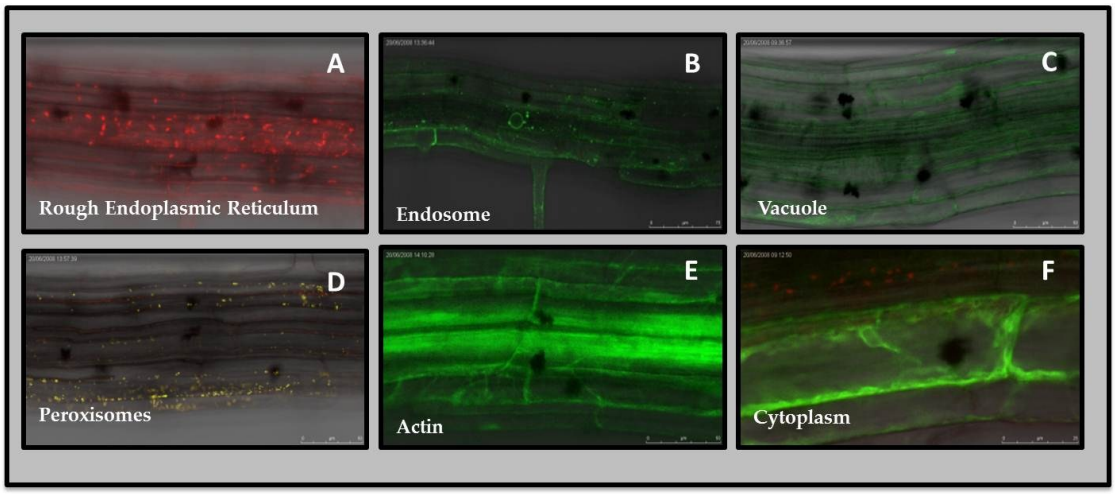

Figure 35: Confocal microscopy of GFP-labeled organelles and sulfur pox localization.

pox move freely within the cytoplasm. This mobility and cytoplasmic localization prompted us to ask what they are made of and how do they actually form these large agglomerations within the cell. A time course was conducted to visualize the process of the -S pox being formed because we knew that they grow larger over time. We have also observed very small particles circulating in the cytoplasm in most cases and generally there is only one per cell. We expected to see the small particles fuse to form larger aggregates but this never occurred. Therefore, it seemed unlikely that active trafficking of some substance to a centralized storage compartment was involved in the formation of sulfur pox. We then considered the fact that we visualize the sulfur pox under the microscope with the roots positioned horizontally. Roots normally grow gravitropically in a vertical direction. It was proposed that the -S pox are very mobile when roots are lying flat because they have plenty of space to roam within the cytoplasm. Therefore we

hypothesized that the –S pox are not buoyant and they form by a steady supply of tiny particles accumulating in the narrow confines of the basal end of the root. We tested this on a microscope where root can be mounted vertically to observe the location of the –S pox (Figure 36). The results show the –S pox resting in the bottom of the cell and remained in the same position over time. The vertical microscope did not have the magnification to observe the actual accumulation of particles but this may be able to be tested in the future.

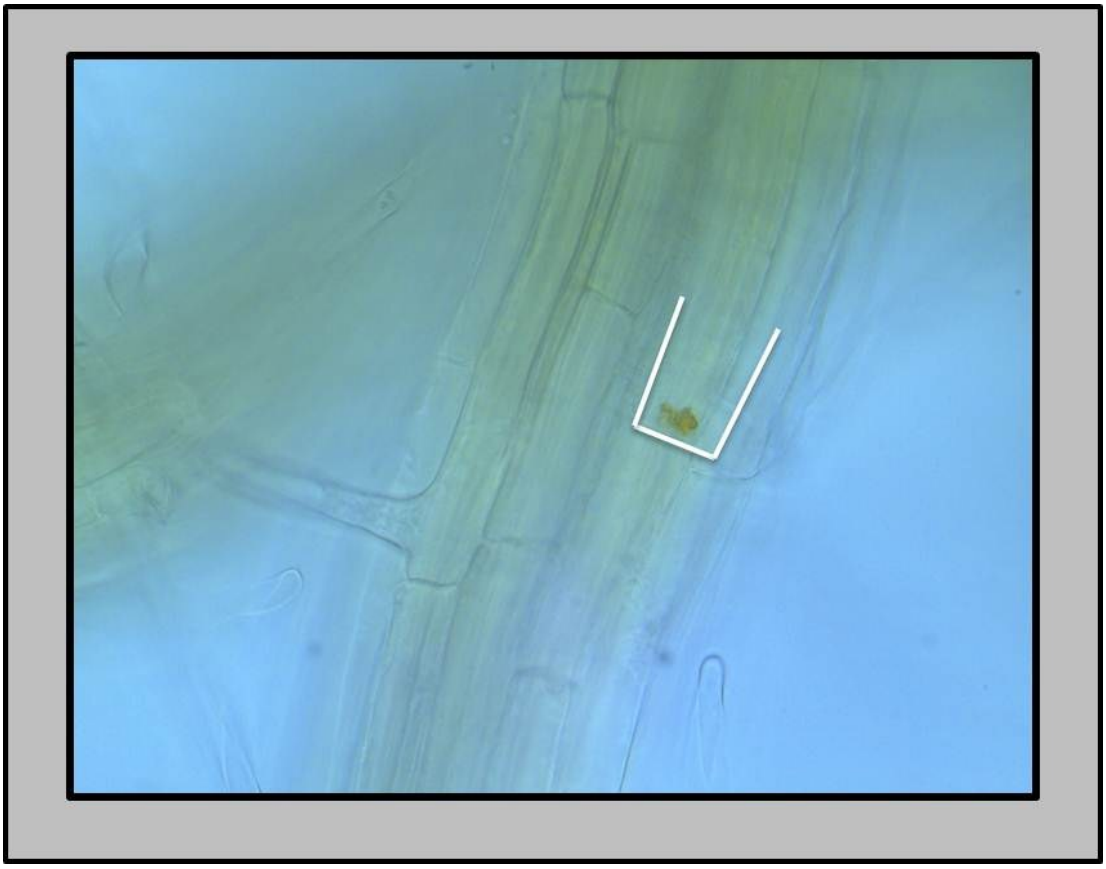

Figure 36: Image of sulfur pox resting in basal cavity of root cells.

This result was only able to partially confirm our hypothesis. The pox could still be

associated with a form of vesicular trafficking of some substance into an ever-growing membrane bound novel structure. Additionally, they could be aggregates of precipitated proteins, or lipid bodies. Thus we stained for association of these molecules with the –S pox (Figure 37). The results show that the –S pox do not stain for vesicles, proteins, or lipids.

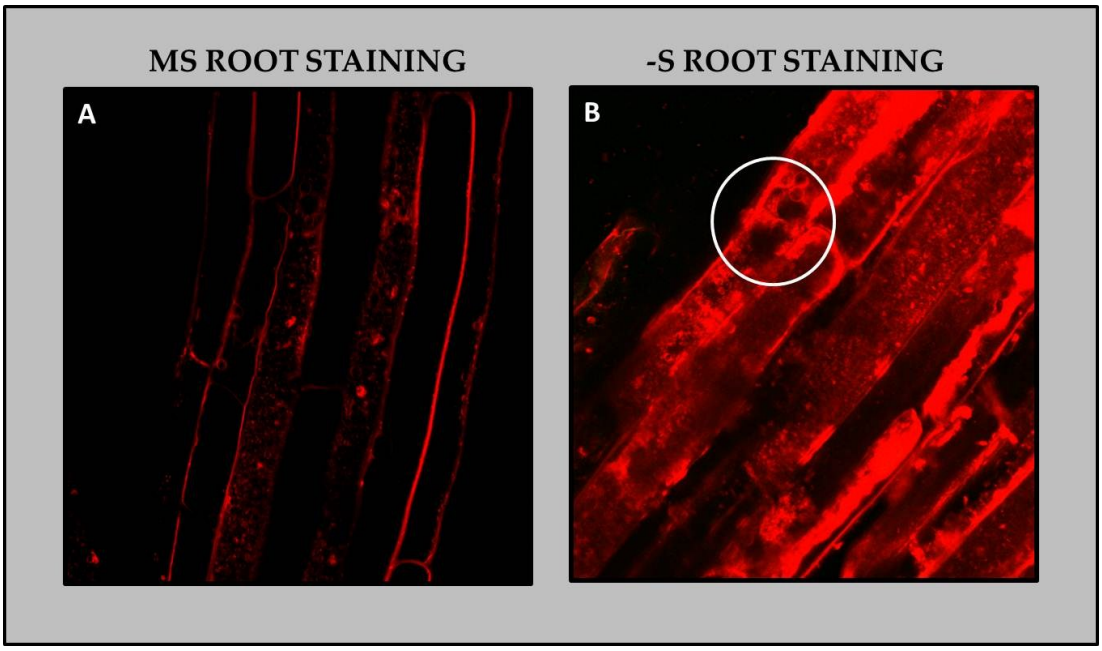

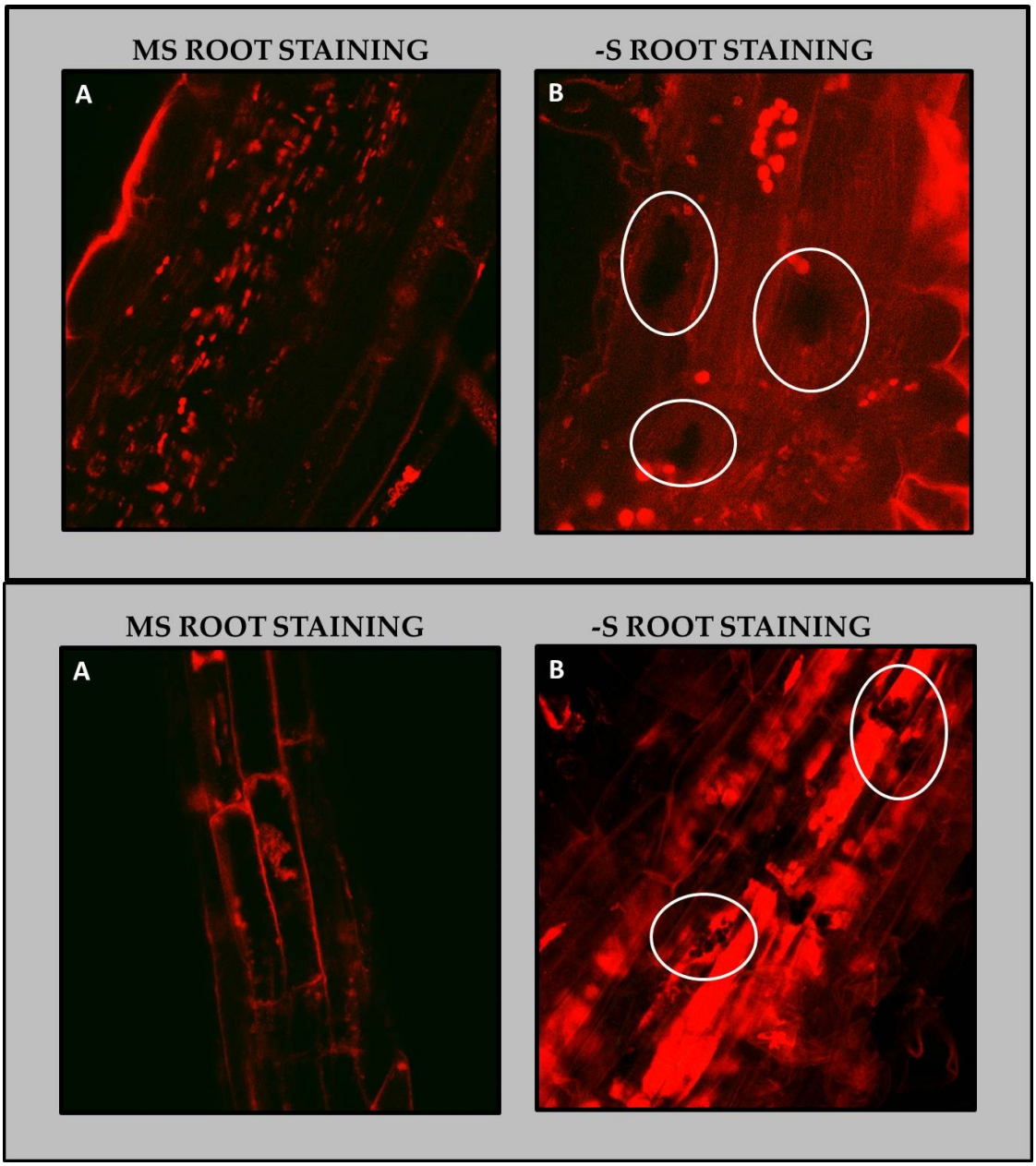

Figure 37: Confocal images of fluorescence staining for vesicles, lipids, and protiens in relation to sulfur pox composition.

Sulfur Pox Microarray Data Sets

To determine if these sulfur pox have a genetic basis, a large data set of whole root and high resolution cell-type specific microarrays was mined to establish a

candidate list of genes that may be involved. Two additional microarrays were also included from whole root sections. One was from seedlings grown on low sulfur for 5 days and 10 days. The second was a time course of 6 day old seedlings that were grown under standard conditions and then transferred to low sulfur media at designated time points. From all of these data sets 259 genes were identified as the cohort (Figure 38). Homozygous Salk T-DNA insertion lines for these genes were selected and tested for the presence or absence of sulfur pox. All of these T-DNA lines have sulfur pox. Next we tested 58 accessions from the Nordborg collection representing natural variants and scored them similarly. All were found to contain –S pox. We next studied a series of

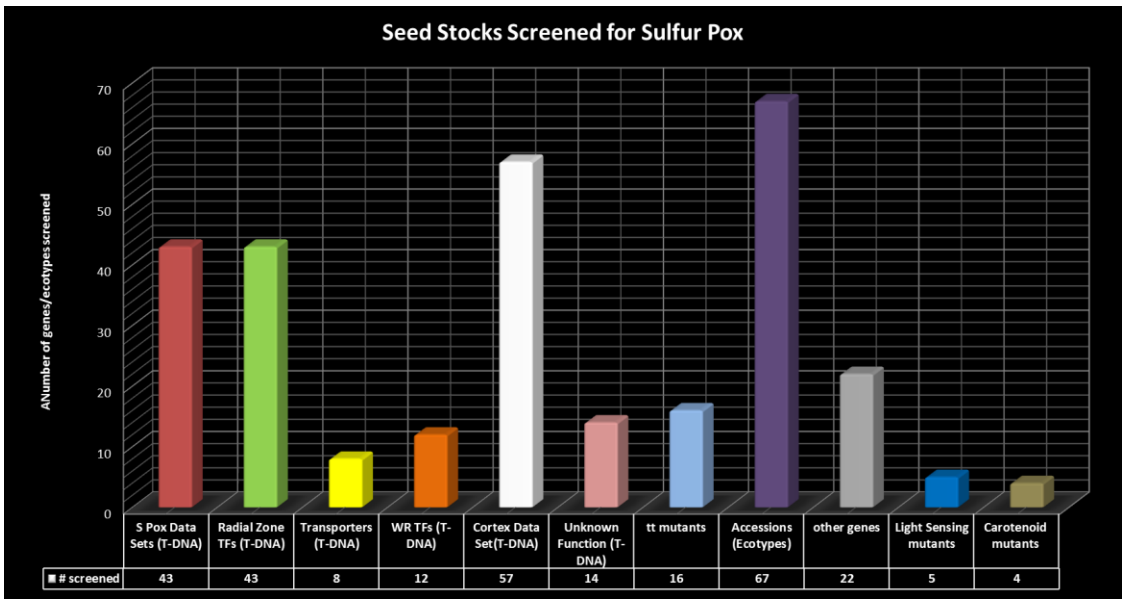

Figure 38: Graph of seeds tested for sulfur pox.

available mutants for genes that showed significance differential expression in the microarray data.

5 and 10 Day Sulfur Pox Microarray Data Analysis

An expression profile was generated on an additional longitudinal section with a goal to determine the genes responsible for the formation and accumulation of these inclusions. Sulfur pox appear just below the hypocotyl/root junction in the oldest cells of the root. Sections of roots ½ inch long were taken from 5 day old and 10 day old plants (Figure 39).

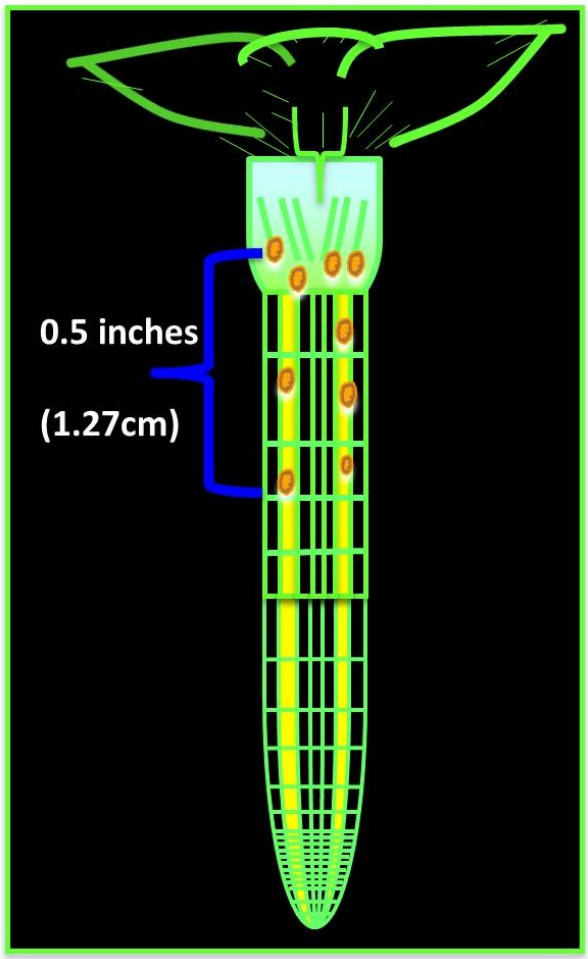

Figure 39: Illustration of root sections containing sulfur pox and length of root excised for microarray experiments.

Compared to the previous data set analyses, we modified the experimental design to for this analysis. First the experimental conditions were modified. The sulfur pox appear at approximately day 5 of in roots of plants grown directly on no sulfur media but only in very small numbers but are plentiful at roughly day 8, thus, we used day 5 and day 10 of constitutive –S growth conditions for the profiling. Next we set multiple levels for genes that meet the significance criteria (Figure 40). The sulfur pox data set had two separate significance and fold change requirements, noted with a star. This would lead us to any genes responsible for the formation and/or maintenance of the sulfur pox.

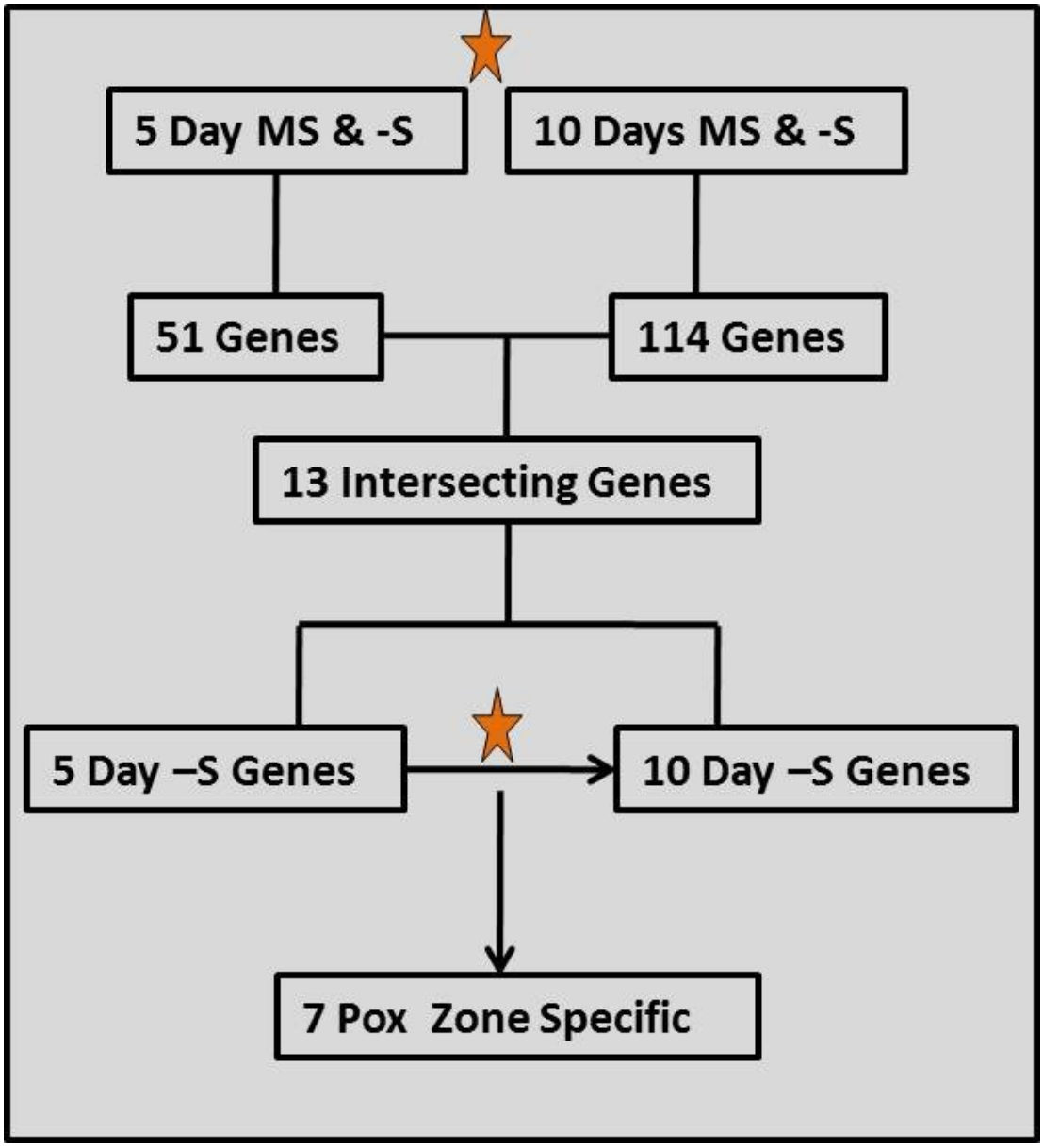

Figure 40: Flow chart of 5 and 10 day sulfur pox microarray data analysis.

The first significance check point is necessary when comparing the 5 and 10 day –S results to their respective controls. There were 51 significant genes for the 5 day analysis and the ratio between up-regulated and down-regulated significant genes was nearly equal with only a slightly higher number of down-regulated genes (Figure 41A).

The 10 day data set yields 114 significant genes with many more down-regulated compared to up-regulated and 114 for the 10 day analysis (Figure 41B). Heatmaps were made to visualize the expression pattern of the data.

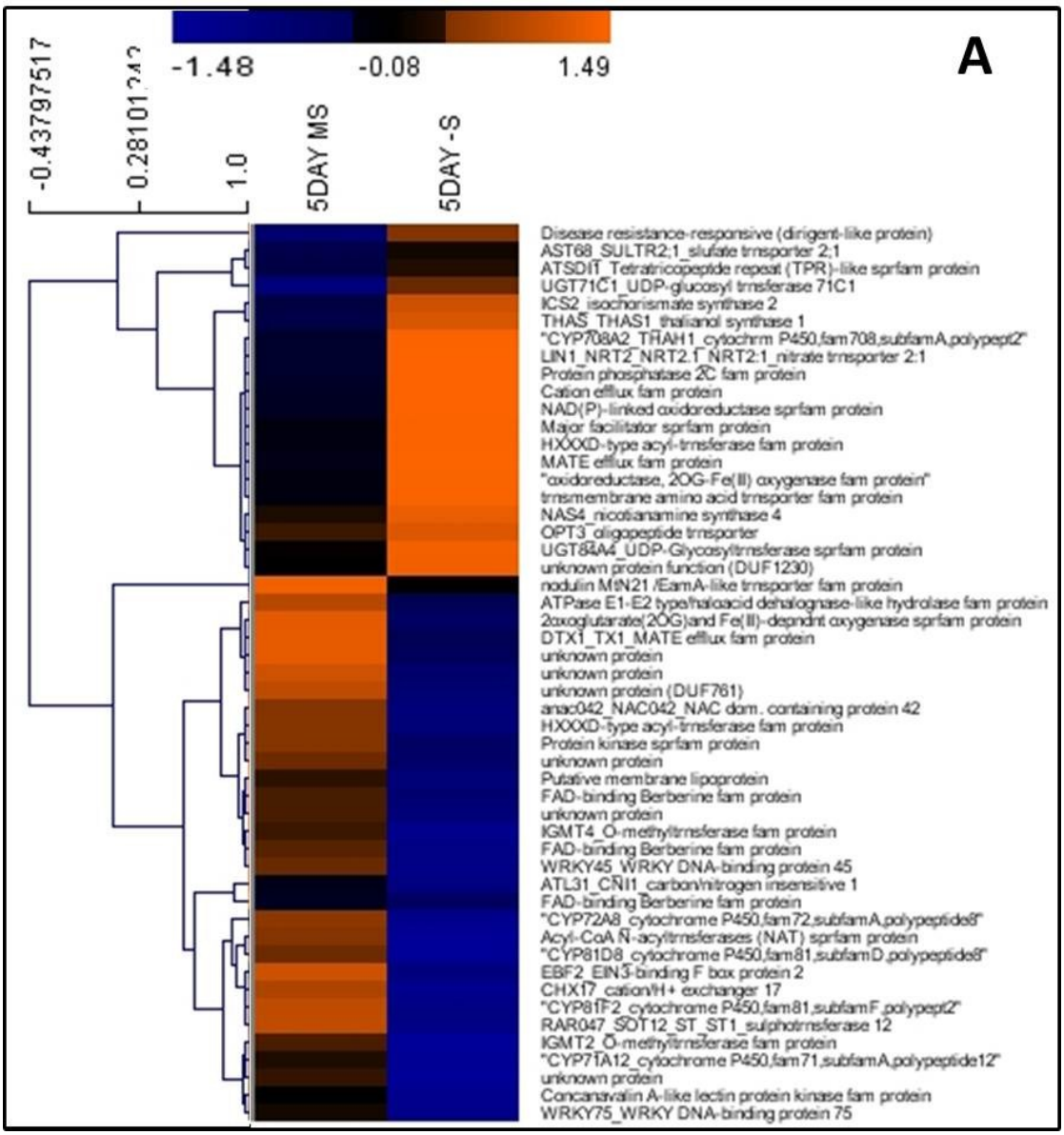

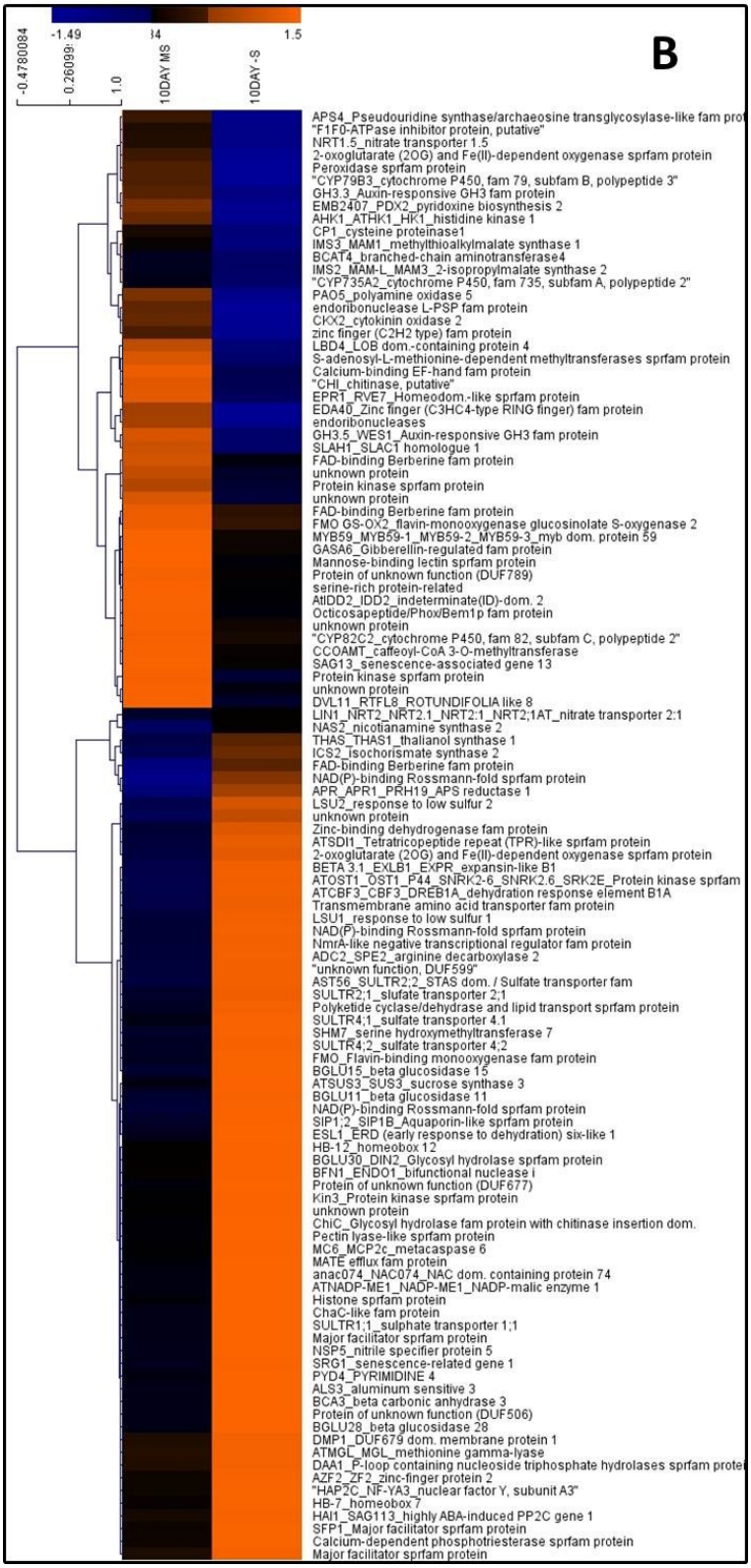
B
-1.49
1.5
-0.4780084
0.26099
1.0
10DAY MS
10DAY -S
APS4_Pseudouridine synthase/archaeosine transglycosylase-like fam prot
"F1F0-ATPase inhibitor protein, putative"
NRT1.5_nitrate transporter 1.5
2-oxoglutarate (2OG) and Fe(II)-dependent oxygenase sprfam protein
Peroxidase sprfam protein
"CYP79B3_cytochrome P450, fam 79, subfam B, polypeptide 3"
GH3.3_Auxin-responsive GH3 fam protein
EMB2407_PDX2_pyridoxine biosynthesis 2
AHK1_ATHK1_HK1_histidine kinase 1
CP1_cysteine proteinase1
IMS3_MAM1_methylthioalkylmalate synthase 1
BCAT4_branched-chain aminotransferase4
IMS2_MAM-L_MAM3_2-isopropylmalate synthase 2
"CYP735A2_cytochrome P450, fam 735, subfam A, polypeptide 2"
PAO5_polyamine oxidase 5
endoribonuclease L-PSP fam protein
CKX2_cytokinin oxidase 2
zinc finger (C2H2 type) fam protein
LBD4_LOB dom.-containing protein 4
S-adenosyl-L-methionine-dependent methyltransferases sprfam protein
Calcium-binding EF-hand fam protein
"CHI_chitinase, putative"
EPR1_RVE7_Homeodom.-like sprfam protein
EDA40_Zinc finger (C3HC4-type RING finger) fam protein
endoribonucleases
GH3.5_WES1_Auxin-responsive GH3 fam protein
SLAH1_SLAC1 homologue 1
FAD-binding Berberine fam protein
unknown protein
Protein kinase sprfam protein
unknown protein
FAD-binding Berberine fam protein
FMO GS-OX2_flavin-monooxygenase glucosinolate S-oxygenase 2
MYB59_MYB59-1_MYB59-2_MYB59-3_myb dom. protein 59
GASA6_Gibberellin-regulated fam protein
Mannose-binding lectin sprfam protein
Protein of unknown function (DUF789)
serine-rich protein-related
AtIDD2_IDD2_indeterminate(ID)-dom. 2
Octicosapeptide/Phox/Bem1p fam protein
unknown protein
"CYP82C2_cytochrome P450, fam 82, subfam C, polypeptide 2"
CCOAMT_caffeoyl-CoA 3-O-methyltransferase
SAG13_senescence-associated gene 13
Protein kinase sprfam protein
unknown protein
DVL11_RTFL8_ROTUNDIFOLIA like 8
LIN1_NRT2_NRT2.1_NRT2:1_NRT2;1AT_nitrate transporter 2:1
NAS2_nicotianamine synthase 2
THAS_THAS1_thalianol synthase 1
ICS2_isochorismate synthase 2
FAD-binding Berberine fam protein
NAD(P)-binding Rossmann-fold sprfam protein
APR_APR1_PRH19_APS reductase 1
LSU2_response to low sulfur 2
unknown protein
Zinc-binding dehydrogenase fam protein
ATSDI1_Tetratricopeptide repeat (TPR)-like sprfam protein
2-oxoglutarate (2OG) and Fe(II)-dependent oxygenase sprfam protein
BETA 3.1_EXLB1_EXPR_expansin-like B1
ATOST1_OST1_P44_SNRK2-6_SNRK2.6_SRK2E_Protein kinase sprfam
ATCBF3_CBF3_DREB1A_dehydration response element B1A
Transmembrane amino acid transporter fam protein
LSU1_response to low sulfur 1
NAD(P)-binding Rossmann-fold sprfam protein
NmrA-like negative transcriptional regulator fam protein
ADC2_SPE2_arginine decarboxylase 2
"unknown function, DUF599"
AST56_SULTR2;2_STAS dom. / Sulfate transporter fam
SULTR2;1_slufate transporter 2;1
Polyketide cyclase/dehydrase and lipid transport sprfam protein
SULTR4;1_sulfate transporter 4.1
SHM7_serine hydroxymethyltransferase 7
SULTR4;2_sulfate transporter 4;2
FMO_Flavin-binding monooxygenase fam protein
BGLU15_beta glucosidase 15
ATSUS3_SUS3_sucrose synthase 3
BGLU11_beta glucosidase 11
NAD(P)-binding Rossmann-fold sprfam protein
SIP1;2_SIP1B_Aquaporin-like sprfam protein
ESL1_ERD (early response to dehydration) six-like 1
HB-12_homeobox 12
BGLU30_DIN2_Glycosyl hydrolase sprfam protein
BFN1_ENDO1_bifunctional nuclease i
Protein of unknown function (DUF677)
Kin3_Protein kinase sprfam protein
unknown protein
ChiC_Glycosyl hydrolase fam protein with chitinase insertion dom.
Pectin lyase-like sprfam protein
MC6_MCP2c_metacaspase 6
MATE efflux fam protein
anac074_NAC074_NAC dom. containing protein 74
ATNADP-ME1_NADP-ME1_NADP-malic enzyme 1
Histone sprfam protein
ChaC-like fam protein
SULTR1;1_sulphate transporter 1;1
Major facilitator sprfam protein
NSP5_nitrile specifier protein 5
SRG1_senescence-related gene 1
PYD4_PYRIMIDINE 4
ALS3_aluminum sensitive 3
BCA3_beta carbonic anhydrase 3
Protein of unknown function (DUF506)
BGLU28_beta glucosidase 28
DMP1_DUF679 dom. membrane protein 1
ATMGL_MGL_methionine gamma-lyase
DAA1_P-loop containing nucleoside triphosphate hydrolases sprfam protei
AZF2_ZF2_zinc-finger protein 2
"HAP2C_NF-YA3_nuclear factor Y, subunit A3"
HB-7_homeobox 7
HAI1_SAG113_highly ABA-induced PP2C gene 1
SFP1_Major facilitator sprfam protein
Calcium-dependent phosphotriesterase sprfam protein
Major facilitator sprfam protein

Figure 41: Heatmap of significant differential gene expression from 5 day and 10 day old roots sections germinated directly on –S media.

The genes from the 5 day –S growth conditions were then compared to those from 10 days also exposed to the –S conditions. The genes that were found in each were considered intersecting or common genes. We found 13 intersecting genes at this step of the process, which eliminated genes that may have been differentially expressed due to other factors such as developmental genes.

Next we evaluated the intersecting genes using the –S treatments to determine significance. The same threshold cut-off of q-value of 10^{-4} and 1.5-fold change applied for the 5 and 10 day –S data of these 13 genes. The genes that pass this screen we interpret as being differentially expressed in the presence of the sulfur pox at 10 days. It should be noted that here we make the assumption that the expression of any genes responsible for -S pox production and accumulation is significantly enhanced at 10 days compared to 5 days. We classified these genes as sulfur pox zone specific genes since the pox have heavily accumulated by 10 days in the root section samples. There were 7 significant differentially expressed genes designated as –S pox zone specific genes. Four of these genes are up-regulated and three are down-regulated (Table 8).

Table 8: Sulfur Pox zone specific genes.

AGI	QVALUE	(-S) 5 DAY MEAN	(-S) 10 DAY MEAN	FOLD CHANGE	ANNOTATION
At3g14770	1.48E-15	0.90801216	2.746543338	3.024786956	SWEET2_Nodulin MtN3 family protein
At1g26410	6.19E-11	0.584424863	1.238900734	2.119863155	FAD-binding Berberine family protein
At5g10180	1.02E-09	3.321399112	6.234130017	1.876959018	AST68_SULTR2;1_slufate transporter 2;1
At3g26460	2.13E-10	2.783620039	5.193111452	1.865596374	Polyketide cyclase/dehydrase and lipid transport superfamily protein
At4g11190	6.95E-06	3.20103953	1.93506846	-1.654225468	Disease resistance-responsive (dirigent-like protein) family protein
At5g23830	2.01E-19	11.28763214	3.607753308	-3.128715068	MD-2-related lipid recognition domain-containing protein
At1g08090	1.41E-18	13.17518428	3.05125907	-4.317950058	LIN1_NRT2_NRT2.1_NRT2:1_NRT2;1AT_nitrate transporter 2:1

The aforementioned results provide information to understand the difference in gene expression at 5 and 10 days of –S growth. These results do not confirm that the genes necessary to produce these sulfur pox are absent from our data set. The data could have been analyzed in many ways and it may also be valid that at 5 days there the gene or genes responsible are elevated and; thus, was excluded during the multilevel significance cut-off. We tested seedlings reported to be homozygous T-DNA insertion lines of three of the –S Pox zone specific genes, as well as, several other genes of interest from this data set as and there was no difference in phenotype compared to wild-type.

Sulfur Pox Time Course Microarray Data Analysis

The next experiment was a 24 hour time course of five day old seedlings transferred from MS media to –S media. Five time points were selected. These were zero hrs, 4 hrs, 8 hrs, 16hrs and 24 hrs post transfer. A total of 58 genes were differentially expressed across this time course. A heatmap was prepared of this data to visualize the expression pattern of these genes (Figure 42). We hoped that induction of the production of the sulfur pox would provide more insight into additional genes that may be involved in the production of these cellular inclusions.

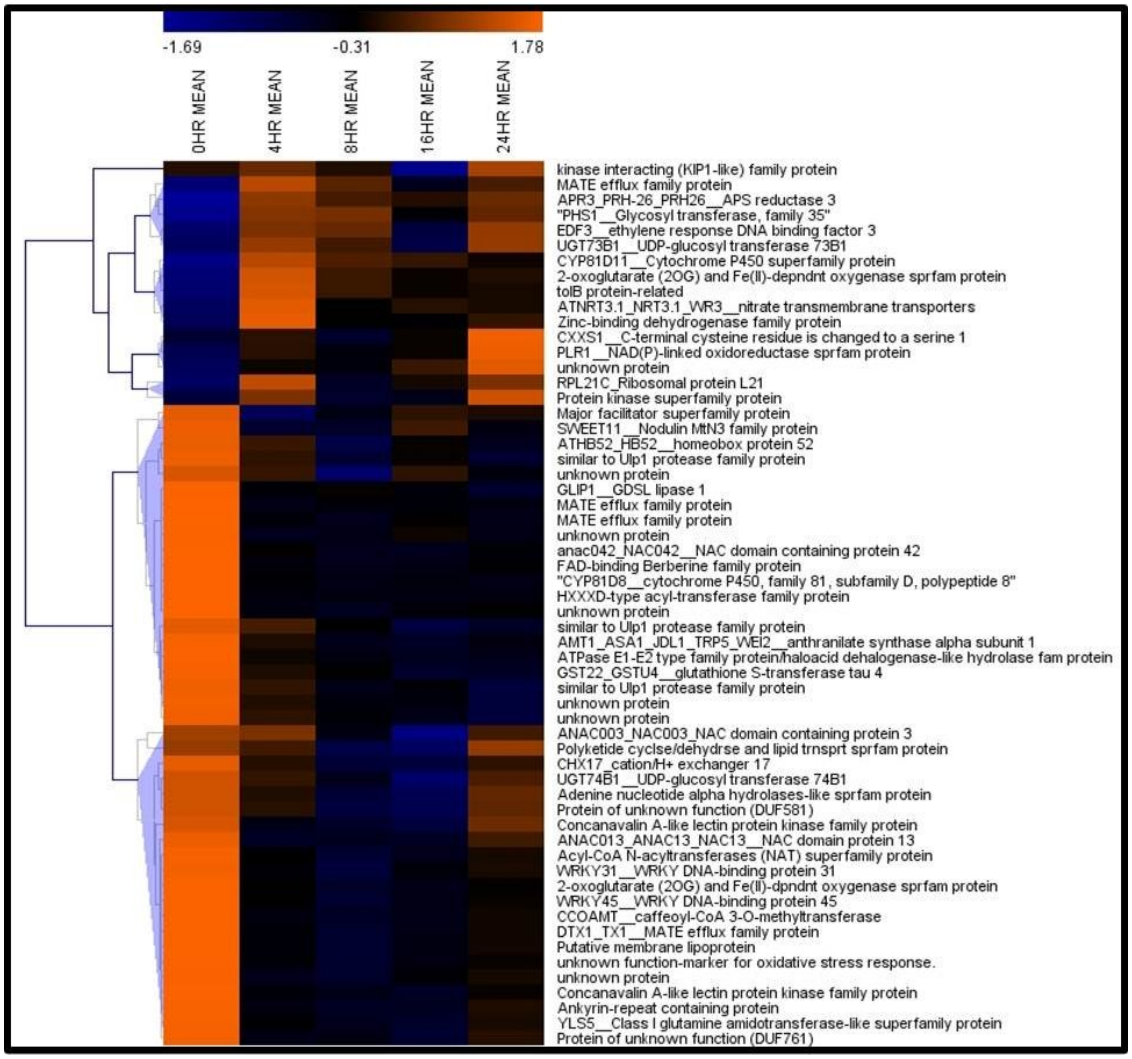

Figure 42: Heatmap of Sulfur Pox time course differential gene expression.

The heatmap expression profile once again illustrates that a large number of genes are down regulated when sulfur limiting conditions are induced. We used this data set as well to select candidate candidates with available homozygous T-DNA insertion seed stocks. Of those tested all retained the ability to produce sulfur pox comparable to wild type seedlings. The T-DNA screen for sulfur pox was a large scale project and we did not validate any seeds for homozygosity unless we noticed a

phenotype, therefore; it is possible that any number of the stocks tested was heterozygous or possessed no transposable elements in the gene of interest. Also, there is a possibility the insertion was in an intron or other regions of the gene where it did not fully disrupt the product function. Furthermore, there was the possibility that production of these inclusions is not actively controlled through gene expression.

This lack of the loss of the sulfur pox phenotype across a large number and wide range of functional categories was still informative. It necessitated heavy scrutiny of the data and critical thing to develop new hypotheses. We possess a wealth of data from a large set of microarray expression profiles from various times, tissues, and developmental zones and observed the behavior of these inclusions in different conditions. Thus, the evidence enables the investigation to focus on more subtle perturbations in the data that has a basis in the general response to sulfur limitation.

Non-targeted Metabolomic Analysis of Sulfur Pox Whole Root Sections

To further our understanding of the composition of the –S pox, we collected whole root sections from 12 day old seedling and shipped them to the UC Davis Metabolomic Core Center for non-targeted analysis. The results were analyzed for significance based on a t-test of $p \leq 0.05$ and the standard deviation of the mean could not overlap. The results reveal many amino acids, a few sugar, and organic compound that are related to phenylpropanoid synthesis. Our results are in line with published

data that shows –S conditions causes plants to store many products and use them sparingly, especially methionine and cysteine (Figure 43).

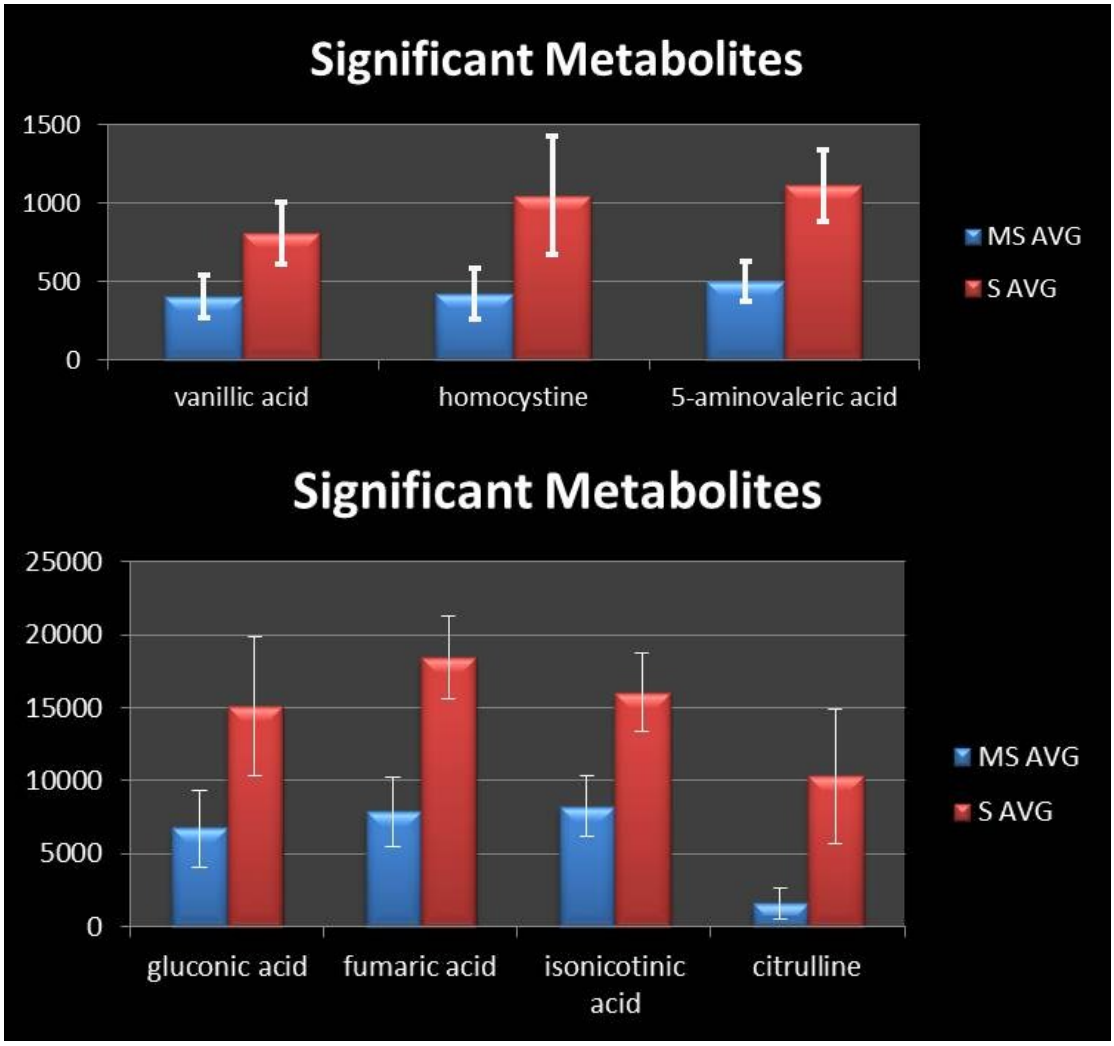

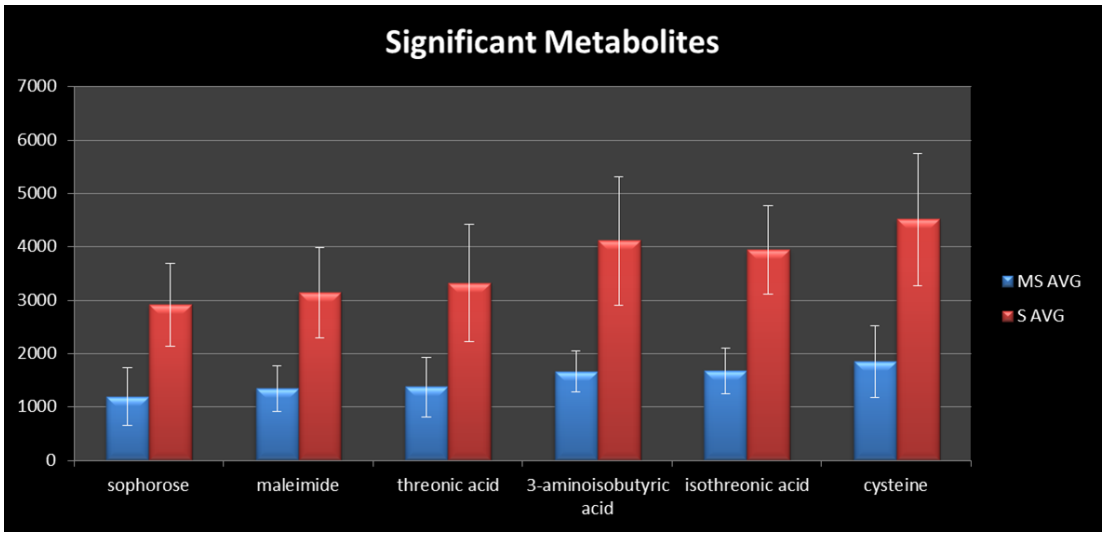
Significant Metabolites
7000
6000
5000
4000
3000
2000
1000
0
sophorose
maleimide
threonic acid
3-aminoisobutyric acid
isothreonic acid
cysteine
MS AVG
S AVG

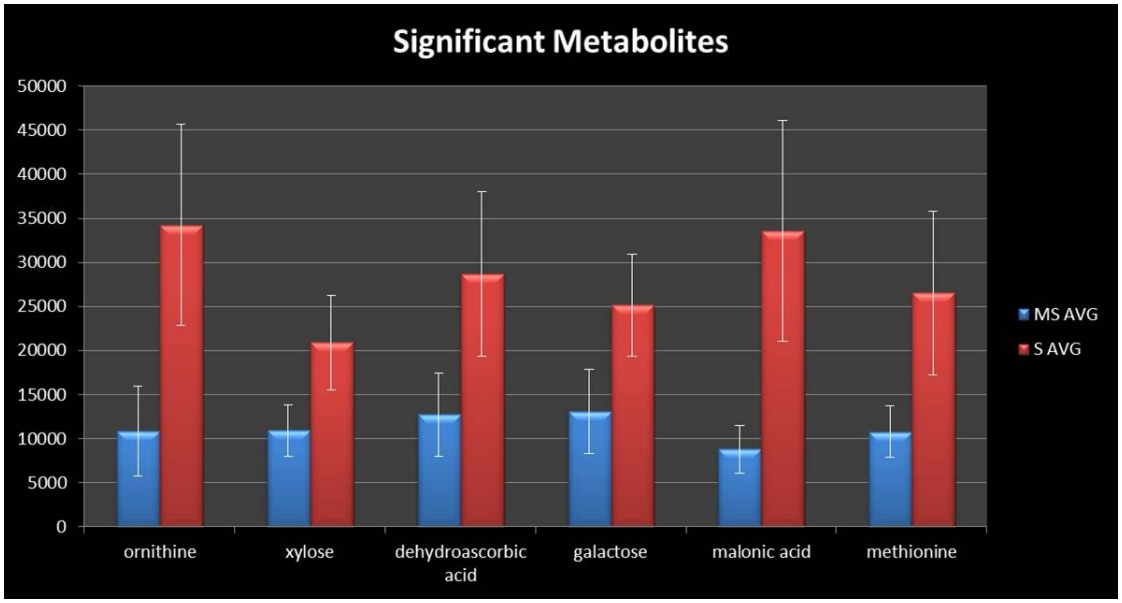
Significant Metabolites
50000
45000
40000
35000
30000
25000
20000
15000
10000
5000
0
ornithine
xylose
dehydroascorbic acid
galactose
malonic acid
methionine
MS AVG
S AVG

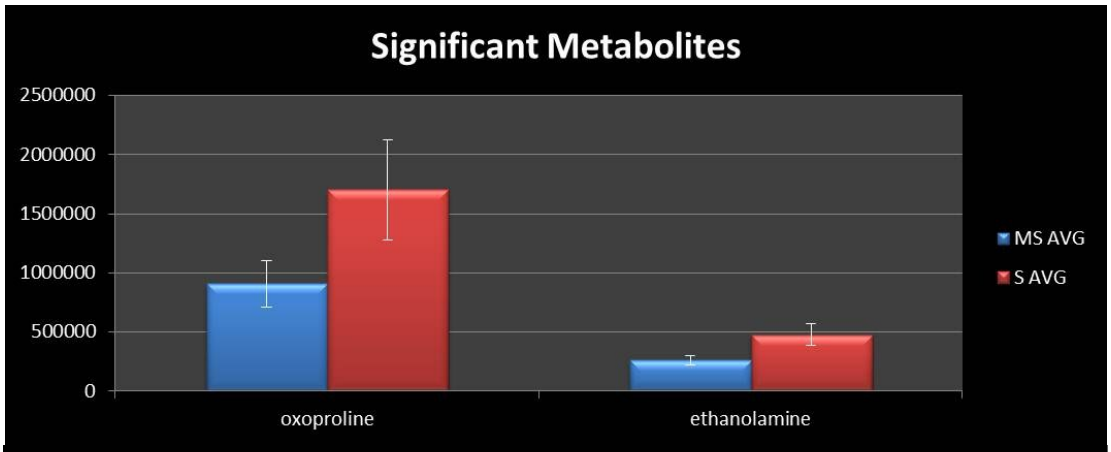
Significant Metabolites
2500000
2000000
1500000
1000000
500000
0
oxoproline
ethanolamine
MS AVG
S AVG

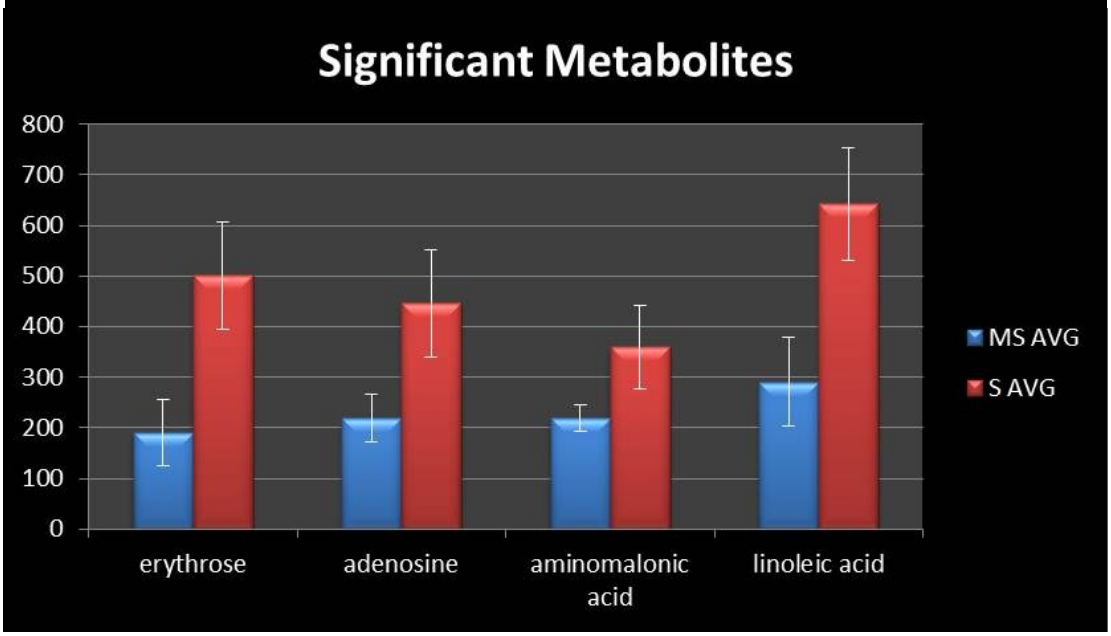
Significant Metabolites
800
700
600
500
400
300
200
100
0
erythrose
adenosine
aminomalonic acid
linoleic acid
MS AVG
S AVG

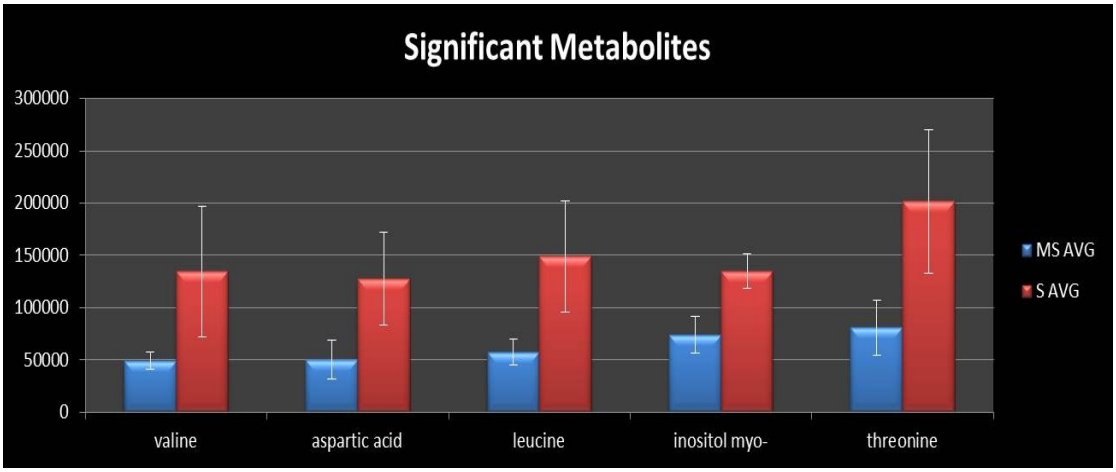
Significant Metabolites
300000
250000
200000
150000
100000
50000
0
valine
aspartic acid
leucine
inositol myo-
threonine
MS AVG
S AVG

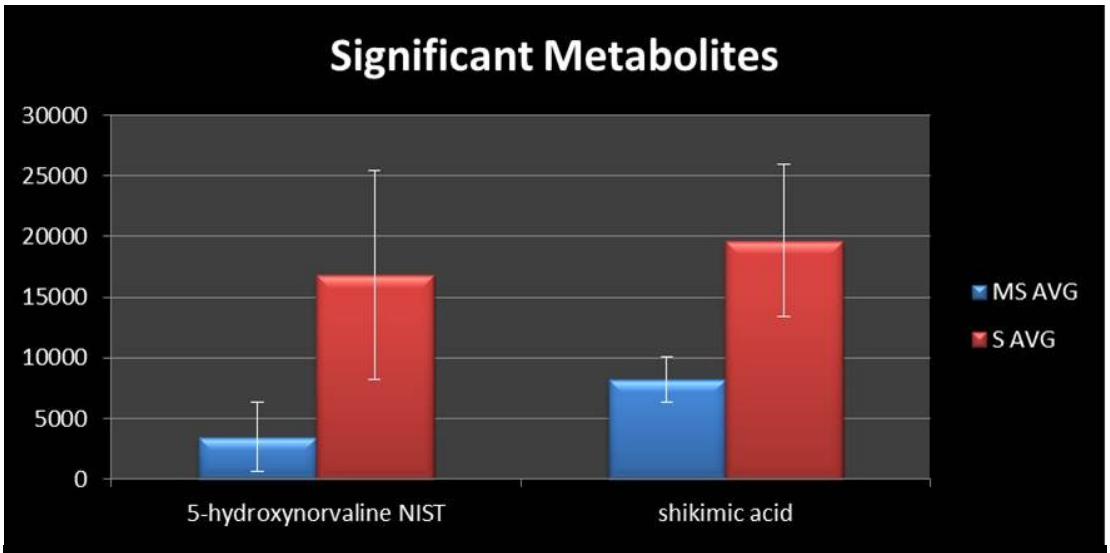
Significant Metabolites
30000
25000
20000
15000
10000
5000
0
5-hydroxynorvaline NIST
shikimic acid
MS AVG
S AVG

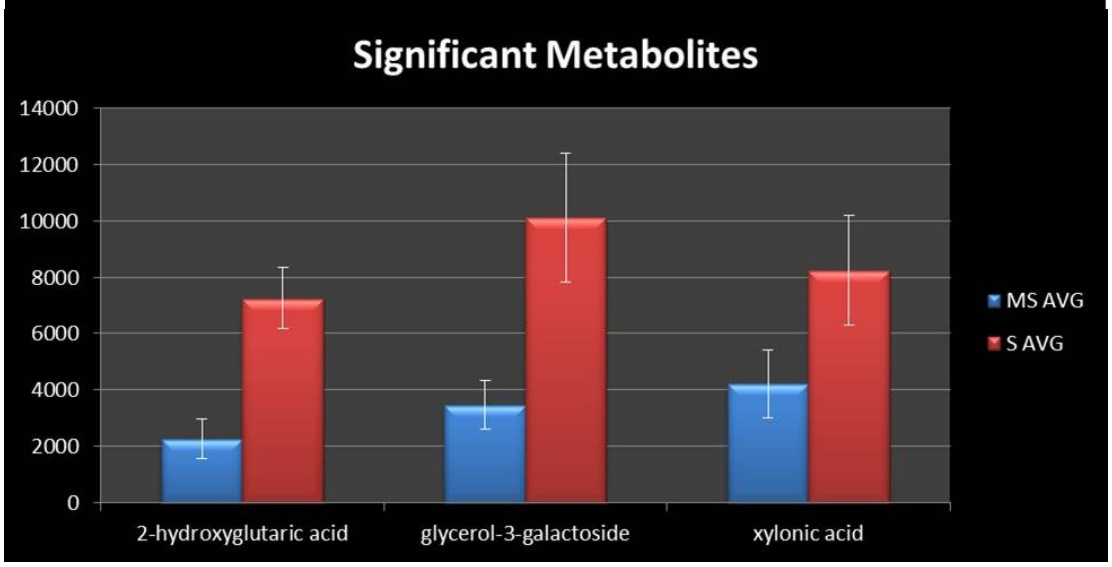
Significant Metabolites
14000
12000
10000
8000
6000
4000
2000
0
2-hydroxyglutaric acid
glycerol-3-galactoside
xylonic acid
MS AVG
S AVG

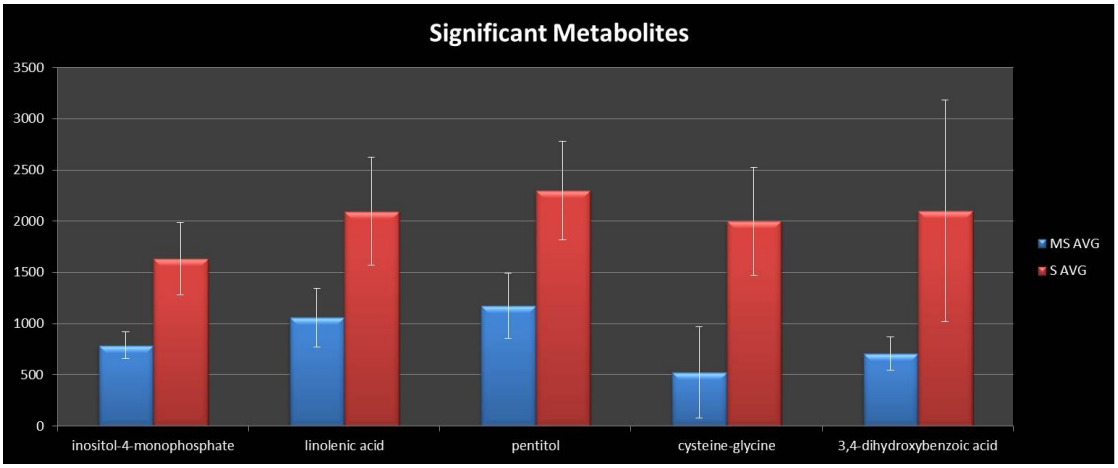
Significant Metabolites
3500
3000
2500
2000
1500
1000
500
0
inositol-4-monophosphate
linolenic acid
pentitol
cysteine-glycine
3,4-dihydroxybenzoic acid
MS AVG
S AVG

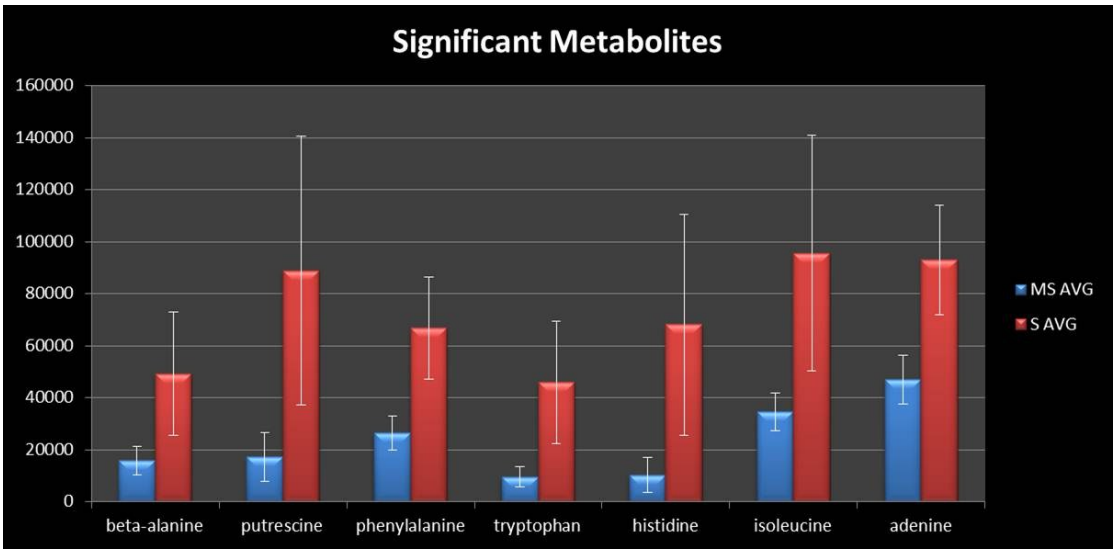

Figure 43: Metabolites of –S root samples that increased.

We also prepare a list of these substances showing the data above with p. values and fold changes (Table 9). There were no compound in our analysis that decreased and significant.

Table 9: List of the Metabolites that increased in abundance in –S root samples.

Metabolite	(MS) AVG	(-S) AVG	(MS) STDEV	(-S) STDEV	ttest ms/ s	Fold Change
erythrose	1.90E+02	5.01E+02	6.61E+01	1.05E+02	1.08E-10	2.63E+00
adenosine	2.19E+02	4.46E+02	4.79E+01	1.05E+02	2.37E-08	2.04E+00
aminomalonic acid	2.19E+02	3.59E+02	2.71E+01	8.29E+01	1.21E-06	1.64E+00
linoleic acid	2.91E+02	6.42E+02	8.73E+01	1.11E+02	8.69E-11	2.21E+00
Metabolite	(MS) AVG	(-S) AVG	(MS) STDEV	(-S) STDEV	ttest ms/ s	Fold Change
vanillic acid	4.03E+02	8.08E+02	1.37E+02	1.99E+02	3.49E-07	2.01E+00
homocystine	4.22E+02	1.05E+03	1.61E+02	3.78E+02	2.65E-06	2.48E+00
5-aminovaleric acid	4.99E+02	1.11E+03	1.30E+02	2.30E+02	6.10E-10	2.23E+00
Metabolite	(MS) AVG	(-S) AVG	(MS) STDEV	(-S) STDEV	ttest ms/ s	Fold Change
inositol-4-monophosphate	7.87E+02	1.64E+03	1.31E+02	3.54E+02	1.76E-09	2.08E+00
linolenic acid	1.06E+03	2.10E+03	2.88E+02	5.28E+02	2.54E-07	1.98E+00
pentitol	1.17E+03	2.30E+03	3.15E+02	4.78E+02	1.78E-08	1.96E+00
cysteine-glycine	5.23E+02	2.00E+03	4.46E+02	5.27E+02	2.36E-09	3.82E+00
3,4-dihydroxybenzoic acid	7.06E+02	2.10E+03	1.61E+02	1.08E+03	4.64E-05	2.98E+00
Metabolite	(MS) AVG	(-S) AVG	(MS) STDEV	(-S) STDEV	ttest ms/ s	Fold Change
sophorose	1.20E+03	2.92E+03	5.41E+02	7.78E+02	7.82E-08	2.44E+00
maleimide	1.35E+03	3.14E+03	4.32E+02	8.41E+02	4.34E-08	2.33E+00
threonic acid	1.37E+03	3.32E+03	5.54E+02	1.10E+03	1.28E-06	2.42E+00
3-aminoisobutyric acid	1.66E+03	4.11E+03	3.78E+02	1.20E+03	3.78E-08	2.47E+00
isothreonic acid	1.68E+03	3.94E+03	4.35E+02	8.27E+02	2.48E-10	2.35E+00
cysteine	1.85E+03	4.51E+03	6.66E+02	1.23E+03	4.25E-08	2.44E+00
Metabolite	(MS) AVG	(-S) AVG	(MS) STDEV	(-S) STDEV	ttest ms/ s	Fold Change
2-hydroxyglutaric acid	2.27E+03	7.25E+03	7.07E+02	1.08E+03	2.27E-15	3.19E+00
glycerol-3-galactoside	3.47E+03	1.01E+04	8.54E+02	2.30E+03	2.54E-11	2.91E+00
xylonic acid	4.21E+03	8.25E+03	1.20E+03	1.94E+03	1.34E-07	1.96E+00
Metabolite	(MS) AVG	(-S) AVG	(MS) STDEV	(-S) STDEV	ttest ms/ s	Fold Change
gluconic acid	6.75E+03	1.51E+04	2.62E+03	4.79E+03	1.97E-06	2.24E+00
fumaric acid	7.87E+03	1.84E+04	2.36E+03	2.82E+03	2.72E-12	2.34E+00
isonicotinic acid	8.25E+03	1.60E+04	2.08E+03	2.69E+03	5.77E-10	1.94E+00
citrulline	1.59E+03	1.03E+04	1.05E+03	4.60E+03	1.12E-07	6.47E+00
Metabolite	(MS) AVG	(-S) AVG	(MS) STDEV	(-S) STDEV	ttest ms/ s	Fold Change
ornithine	1.08E+04	3.42E+04	5.09E+03	1.14E+04	6.52E-08	3.16E+00
xylose	1.09E+04	2.09E+04	2.93E+03	5.34E+03	6.67E-07	1.91E+00
dehydroascorbic acid	1.27E+04	2.87E+04	4.68E+03	9.33E+03	2.17E-06	2.25E+00
galactose	1.31E+04	2.52E+04	4.79E+03	5.81E+03	6.46E-07	1.92E+00
malonic acid	8.79E+03	3.36E+04	2.73E+03	1.25E+04	4.27E-08	3.82E+00
methionine	1.08E+04	2.65E+04	2.91E+03	9.32E+03	1.15E-06	2.46E+00
Metabolite	(MS) AVG	(-S) AVG	(MS) STDEV	(-S) STDEV	ttest ms/ s	Fold Change
valine	4.91E+04	1.34E+05	8.15E+03	6.23E+04	1.88E-05	2.74E+00
aspartic acid	4.98E+04	1.27E+05	1.86E+04	4.45E+04	1.04E-06	2.56E+00
leucine	5.74E+04	1.49E+05	1.21E+04	5.34E+04	6.90E-07	2.59E+00
inositol myo-	7.40E+04	1.35E+05	1.73E+04	1.67E+04	3.90E-11	1.82E+00
threonine	8.06E+04	2.01E+05	2.65E+04	6.88E+04	7.87E-07	2.50E+00
Metabolite	(MS) AVG	(-S) AVG	(MS) STDEV	(-S) STDEV	ttest ms/ s	Fold Change
5-hydroxynorvaline	3.46E+03	1.68E+04	2.86E+03	8.66E+03	5.21E-06	4.86E+00
shikimic acid	8.20E+03	1.97E+04	1.92E+03	6.30E+03	2.88E-07	2.40E+00
Metabolite	(MS) AVG	(-S) AVG	(MS) STDEV	(-S) STDEV	ttest ms/ s	Fold Change
beta-alanine	1.59E+04	4.93E+04	5.58E+03	2.36E+04	1.44E-05	3.10E+00
putrescine	1.73E+04	8.89E+04	9.40E+03	5.17E+04	1.77E-05	5.15E+00
phenylalanine	2.65E+04	6.68E+04	6.67E+03	1.98E+04	3.95E-08	2.52E+00
tryptophan	9.60E+03	4.59E+04	3.84E+03	2.34E+04	3.13E-06	4.78E+00
histidine	1.03E+04	6.80E+04	6.67E+03	4.26E+04	2.33E-05	6.61E+00
isoleucine	3.46E+04	9.56E+04	7.25E+03	4.53E+04	2.55E-05	2.76E+00
adenine	4.70E+04	9.29E+04	9.48E+03	2.10E+04	1.97E-08	1.98E+00
Metabolite	(MS) AVG	(-S) AVG	(MS) STDEV	(-S) STDEV	ttest ms/ s	Fold Change
oxoproline	9.06E+05	1.70E+06	2.00E+05	4.25E+05	4.13E-07	1.88E+00
ethanolamine	2.59E+05	4.75E+05	3.99E+04	9.11E+04	3.15E-09	1.84E+00

Sulfur Starvation Compromises Energy Acquisition and Primary Defense Strategies

The sulfur deficiency response creates a myriad of cellular, metabolic, and developmental complications. Two key mechanisms to maintain homeostasis during stress are energy production and a functional plant defense system. Our data shows enriched down-regulation of genes involved in mitochondrial functioning, protein assembly and transport, and a breakdown of the mechanics from transcription through translation. The maturation zone is the only zone actively utilizing these functions. Meanwhile, the photosynthesis and respiration is inefficient and the plant turn to converting starch to sugars to use for energy and down-regulating its response to glucose. Therefore, although the plant shuts down many vital developmental processes it is still spending more energy than it is acquiring over time.

Depletion of sulfur pools within the plant creates a significant obstacle for plant growth and development. This should be easily understood since sulfur is intimately involved in primary metabolism. As stated in the introduction, sulfur assimilation is localized to chloroplasts where it is incorporated into cysteine and glutathione (GSH), or sulfonated to produce sulfolipids and other organic molecules (Droux, 2004). Within the chloroplast sulfur is vital in the form of GSH to protect the photosynthetic machinery from reactive oxygen species (ROS) and electron transport where it forms a complex with iron to form iron-sulfur clusters (Biswal *et al.*, 2008; Pilon *et al.*, 2006). Energy

acquisition cannot proceed effectively when sulfur resources are depleted. Sulfur assimilation occurs in the chloroplast because it is vital to protect the ability to continue photosynthesis for continued growth and survival.

The other key cost of sulfur deprivation is the inability for the plant to defend itself. In Arabidopsis, the primary defense response against herbivore attack is glucosinolates. Glucosinolates are compartmentalized secondary metabolites that are activated when the vacuole is breached by grazing predators allowing the enzyme myrosinase to trigger their degradation. The by-products of glucosinolates are nitriles and forms of thiocyanates which can repel further predation (Kliebenstein *et al.*, 2001). During the biosynthesis of glucosinolates sulfation must occur to complete the core structure. This process involves 3′-phosphoadenosine 5′-phosphosulfate (PAPS) (See Figure 3, Introduction) and, thus; there is an interconnection between glucosinolate biosynthesis and assimilation of sulfur (Yatusevich *et al.*, 2010). The data sets presented here provide further evidence of the down-regulation of principal components of the glucosinolate biosynthesis pathway. These sulfur rich compounds are likely recycled and the sulfur is redistributed towards primary metabolic functions.

Throughout the life cycle of plants they must carefully distribute precious energy resources between meeting the demands of competition from neighbors to maintain their niche and defending themselves from predators and other environmental challenges (Herms *et al.*, 1992). If the event arrives where the plant is forced to choose

growth or predation it chooses to conserve its resources for growth and leaves itself vulnerable to attack (Izaguirre *et al.*, 2006). Under natural circumstances, other than intensive crop production in poor soil, plants rarely must contend with a completely exhausted sulfur supply equal to these growth conditions. Thus, the stress is compounded and the seedlings must adapt in new ways. These data suggest the plants down-regulate defenses that are sulfur dependent and responds to defend it from other factors. It is proposed that the failure of sulfur starved plants to conjugate sulfolipids compromises membrane production needed to sustain active photosynthetic operations. Additionally, sulfur deficient plants suffer from excess light sensitivity when light levels are normal (Nikiforova *et al.*, 2003). We propose these inclusions are consequences of this specific environmental stress due to the heavy impairment of the primary mechanisms for the plant to adapt and cope with stress situations. Our hypothesis is that these cellular inclusions are products of induction of the phenylpropanoid pathway, namely flavonoids or glycosylated flavonoids, by light sensing mechanisms in response to perceived excess light triggered by the low sulfur conditions. Furthermore, these flavonoids are then oxidized due to cytoplasmic free radical accumulation in the cytoplasm due to down-regulation of glutathione which is derived from assimilated sulphate.

Flavonoids and the Phenypropanoid Pathway

Plants respond to light stress by activating photo-protective compounds derived

from the phenylpropanoid pathway. Phenylpropanoids are a multifunctional class of aromatic compounds involved in pigmentation, disease resistance, protection from abiotic stress (Winkel-Shirley, 2001, 2002; Treutter, 2006). Furthermore, they have structural functions, antioxidant properties, signaling capabilities, and act as a plant sunscreen (Besseau *et al.*, 2007; Agati *et al.,* 2012; Brown *et al.,* 2001; Close *et al.*, 2002). Some of these classes are lignins, condensed tannins, anthocyanidins, and flavonoids.

Characterization of Primary Flavonoids

Flavonoids are a well characterized class of phenylpropanoids in Arabidopsis. All but one product of the pathway are encoded by single genes and the lack of redundancy has made the discovery of null mutants rather straight-forward (Winkel-Shirley, 2001). Mutations in the genes disrupt proper pigmentation of the seed coat, or testa, which stores the embryo. In these mutants the lack compounds required to load the seed coat with phenolic compounds which fortify and protect the embryo from harsh environmental factors and ultraviolet radiation. Synthesis of naringenin chalcone by chalcone synthase (CHS) is the first enzyme of flavonoid biosynthesis (Feinbaum *et al.* 1988). Mutations in the gene produces a flavonoid free plant and designated as *tt4*. Second, chalcone isomerase promotes the synthesis of naringenin which is absent in tt-5 mutants (Shirley et al., 1992). TT6 encodes the enzyme flavanone 3-hydroxylase (F3H) and flavonoid 3′-hydroxylase (F3′H) is the product of TT7 and does not produce cyanidin and quercetin (Schoenbohm *et al.*, 2000). At this point the pathway branches off

synthesizing various dihydroflavonols, flavonols, flavonol glycosides, and anthocyanidins (Figure: 44). Anthocyanidins are darker pigments that give grapes there deep purple color. The TT3 gene encodes dyhydroflavonol 4-reductase (DFR) which is necessary for anthocyanidin accumulation (Shirley *et al.*, (1992). Currently, over two dozen genes have been identified that and their functions determined (Routaboul *et al,* 2006).

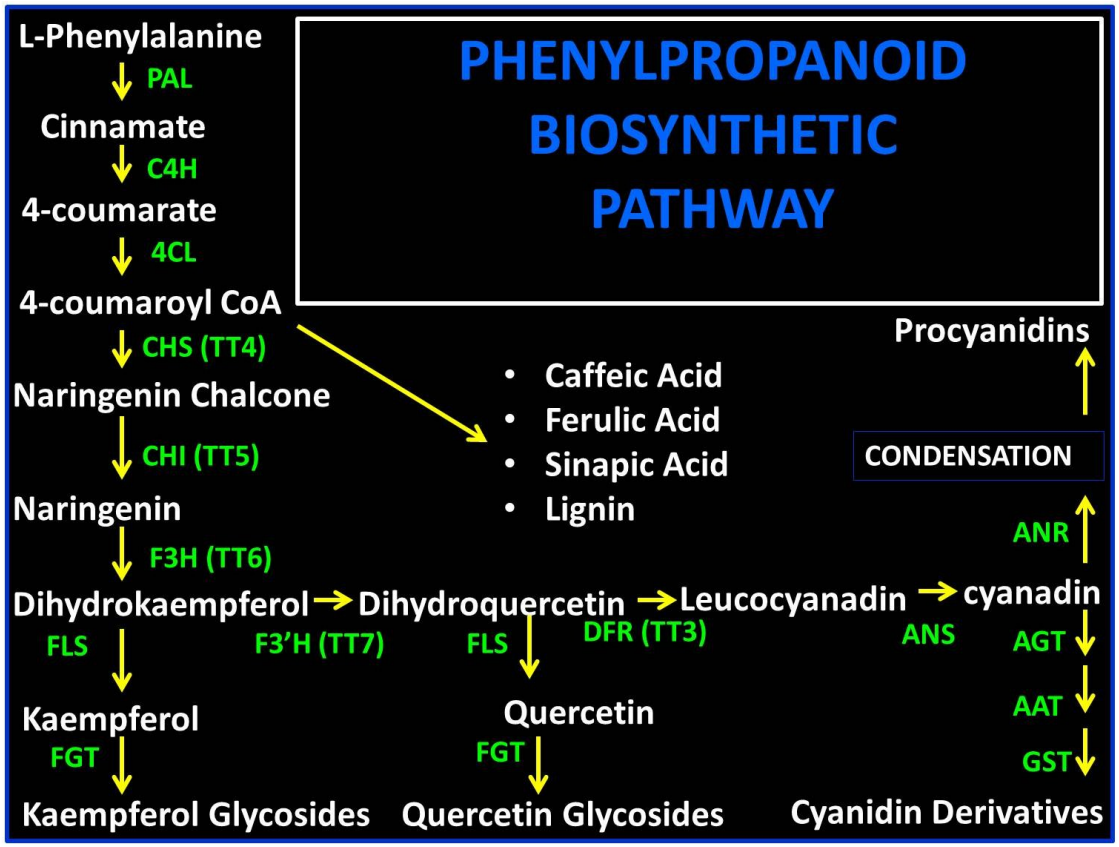

Figure 44: Simplified scheme for phenylpropanoid and flavonoid biosynthesis.

Localization and Transport of Flavonoids

Insight into flavonoid transport, localization, and storage has been the focus of

active research that has made a lot of progress for over a decade. Investigation into the intracellular localization of flavonoid synthesis has not been clearly elucidated but it is thought it occurs on the outer endoplasmic reticulum within the cytoplasm. The case can still be made that it occurs within the vacuole. Furthermore, although transport of flavonoids has been validated the mechanisms involved in transporting them through cells and across membranes are not fully understood (Zhao *et al.* 2010). TT12 is a multidrug and toxic efflux transporter family (MATE) membrane protein that is involved with sequestering proanthocyanidin in the vacuole of Arabidopsis seeds. MATE proteins in Arabidopsis belong to a large family of over 50 proteins, almost all of which have unknown functions (Marinova *et al.*, 2007). Recently, investigators found a MATE protein also promotes vacuolar accumulation of anthocyanins and flavonoid glycosides in Medicago sativa (Zhao *et al.*, 2011). Vacuolar storage of phenylpropanoids and trafficking to and from different cellular processes have also involved glutathione-S-transferases (GST). Maize and Petunia both have GSTs that functions in trafficking of anthocyanidin from the synthesis site at the endoplasmic reticulum to the vacuole for storage where it is protected from oxidation (Alfenito *et al.*,1998; Marrs *et al.*, 1995). The null mutant of the maize GST, *bronze-2* (*bz2*), is unable to import anthocyanidin into the vacuole and it oxidizes in the cytoplasm into a brown substance (Marrs *et al.*, 1995). Arabidopsis also contains a GST that transports anthocyanidin and proanthocyanidins (PAs) which are loaded into the seed coat (Zhao and Dixon, 2009). With the exception of

anthocyanidin and to a lesser extent proanthocyanidins (PAs), very little is known regarding the transport of the flavonoids and other phenylpropanoids which means just as little is known if the transport system fails.

Flavonoid Research in the Arabidopsis Root System

There has been a great deal of interest and investigation into flavonoid expression and activity root systems. The spatial organization and developmental arrangement of the Arabidopsis root has provided researchers with a model organ to expand the body of knowledge of the biological significance of flavonoid compounds and molecular mechanisms. Dark grow plants were absent of flavonoids in the root but when the shoot was exposed to light, and the roots remained in the dark, flavonoids were detected in the root tip. This provided evidence of flavonoid transport from shoots to roots. When they tested light grown *tt4* mutants, flavonoids were not detected in roots unless naringenin was applied to the shoot (Beur *et al*., 2007). It has been reported that flavonoids accumulate in a developmental and tissue specific fashion. Mature plants were found to accumulate flavonoids in leaves and flower parts with the dominant flavonoid being quercetin, while younger seedlings accumulate them in distinct sections of the root. These sections are the upper hypocotyl, the hypocotyl root junction, and the distal portion of the root elongation zone of the root. Quercetin, naringenin chalcone, and kaempferol were detected in different cell types and developmental zones of the root (Peer *et al*., 2001). Furthermore, visualization of the

flavonoids form at 3, 5, and 7 days showed that the flavonoids move through the root in a wave of expression. At the hypocotyl/ root junction the flavonoids formed a ring and kaempferol localized in the epidermis while quercetin was detected in the cortex. A review of detailing of transcriptional profiling at cell-type resolution and the lessons that can be learned for cell-type specific metabolomic profiling highlights flavonoid enrichment is localized to cortex cells across multiple data sets of abiotic stress in Arabidopsis (Rogers *et al*.,2012).

The Relationship between Sulfur, Flavonoids, and Light Sensing

Integration of transcriptomic and metabolomic data, as well as, cross-condition analysis has led researchers to postulate that maintaining lipids for the assembly and maintenance of thykaloid membranes is vital to sustaining photosynthesis even during stress situations. When sulfur is readily available these membranes can be synthesized via sulfolipids. During sulfur-deficient conditions production of these membranes fails and the plant is unable to meet the energy demands to carry out basic biological functions. Chlorophyll content also plummets and the consequence of limited light capture and conversion is a weakened plant that is intolerant to standard light intensity (Nikiforova *et al*., 2003). Plants must respond to the perceived excess light because photo-damage can lead to DNA mutagenesis, destruction of organelles, and organic molecules. The result is induction of the phenylpropanoid pathway to synthesize flavonoids and anthocyanidin. Induction of the pathway doesn't only occur during

stressful situations of excessive light; flavonoid production is a light-dependent under normal light conditions as previously described.

Phytochromes and Photomorphogenesis

Plants normally grow in the environment where they must maximize their exposure to sunlight to successfully grow and develop. Plants have the ability to sense light, and the daily fluctuations in light intensity and availability (Sullivan *et al*., 2003). Not only can plants sense light but they can also react to it or to the lack of light. Plants are able to accomplish this level of sensitivity through expression and regulation of light-sensing molecules that are photoreceptors called phytochrome. Arabidopsis has five phytochrome genes labeled PHYA through PHYE (Frohnmeyer *et al*., 1998). Utilizing these five phytochromes, Arabidopsis seedlings and plants are able to detect the ratio of red to far red light (R-FR) and absorb this spectrum of light (Morelli *et al*., 2002). When plants grown in the dark or shade they become etiolated, where they lack chlorophyll, the hypocotyl stretches, and there is a pronounced hook in the apical meristem where the cotyledons remain closed. The process where plants that exhibit this etiolated phenotype is known as skotomorphogenesis. PHYA is the only phytochrome that is highly expressed in etiolated seedlings and much of the protein is degraded upon exposure to light. The remaining phytochromes are stable in normal light conditions and are expressed during de-etiolation. De-etiolated plants have short hypocotyls and cotyledons are open and ready to capture sunlight and induction of light responsive

genes occurs (Alabadí *et al*., 2008). This process is known as photomorphogenesis.

The *phyA* phenotype displays a wild-type phenotype in red and white light and loss of de-etiolation in far red light. *phyB* mutants are display light sensitivity and has a delayed response to deactivation. The *phyC* phenotype is mainly the elongation of the hypocotyl when grown in photomorphogenic conditions. Excessive lateral root formation is the hallmark phenotype of *phyD,* as well as, and there is a weaker response to red light. *phyE* will have an early flowering response when phyA and phyB are not present (Schepens *et al*., 2004; Salisbury *et al*., 2007, Hudson 2007).

Phytochromes are not in sole control of light sensing. They are actually synthesized in the cytoplasm and remain there in an inactive state known as the Pr state. To enter the nucleus they must be activated to the Pfr state by phytochrome interacting factors (PIF) transcription factors (Ballaré 1999). Four main PIF proteins- PIF1, PIF3, PIF4, and PIF5 preferentially bind phyB although they belong to a 15 or more member family that all bind to phyB exclusively. Once phyB is activated these Pif proteins are degraded (Leivar and Quail 2011). Additional notable components of the light sensing pathway are COP1, DET1, and HY5. COP1 and DET1 play a role in multiple pathways and serve different functions. Both can act independently or form complexes with other genes of the CONSTITUTIVE PHOTOMORPHOGENIC/ DE-ETIOLATED/FUSCA (COP/DET/FUS) group. The phenotype of *cop1* and *det1* is de-etiolation in dark grown conditions; thus, they function as repressors of photomorphogenesis (Lau *et al*., 2012). It

is of interest to mention that *fusca* mutants and strong alleles of one group of *cop/det* mutants all display a phenotype where mature seeds and seedlings are rich in anthocyanidins (Wei *et al.*, 1996). COP1 is at the crossroads of light signaling that actively suppresses photomorphogenesis in the dark by localizing to the nucleus and making transcription factors for degradation.

One target of COP1 is LONG HYPOCOTYL 5 (HY5), which promotes de-etiolation and photomorphogenic programming (Smirnova *et al.*, 2012). HY5 is a transcription factor that is primarily known for activating downstream light responsive genes and promoting photomorphogenesis. Like COP1, HY5 is also considered a central modulator of light signaling. In stark contrast to some *cop/det* mutants, *hy5* mutants lack anthocyanidins. Even more interesting is that a *hy5* mutant was isolated that had a clear root phenotype. This mutant has excessive growth and number of lateral roots, long root hairs, and the primary and lateral roots are agravitropic (Oyama *et al.*, 1997). Further investigation found that HY5 targets repressors of auxin signaling (Cluis *et al.*, 2004). HY5 has been determined to bind chalcone synthase (CHS) *in vivo*, the first committed step in flavonoid biosynthesis. HY5 seedlings accumulate anthocyanidins under normal light conditions. In dark conditions COP1 targets HY5 for degradation but in the presence of ultraviolet-B radiation HY5 expression is revived (Lau *et al.*, 2012). CHS was tested as the primary target of HY5 to induce phenylpropanoid production to protect the plant from the UV-B radiation. Not only was HY5 able to activate CHS, it was also able

to bind and activate the promoters of two flavonol specific MYB regulators, MYB12 and MYB111 in response to UV-B radiation (Stracke *et al.*, 2010). Lastly, HY5 regulates adenosine 5'-phosphosulfate reductase (APR), a primary enzyme of sulfur assimilation by binding directly to the promoters of APR1 and APR2. APR is also regulated by the demand the flux of plant sulfur pools. But HY5 can regulate APR by light and additional factors.

Results from Flavonoid and Light Sensing Mutant Experiments

As described in Chapter 1, differential expression of phenylpropanoids was reflected in the microarray data sets and the literature corroborates the potential for sulfur starvation to induce phenylpropanoid biosynthesis due to a defunct defense system and hypersensitivity to light. Therefore we acquired the following mutants*: tt4-8, tt5-1, tt6-1, tt7-1, tt3-1, myb 11-12-111, myb12, and a myb12* overexpression line. We germinated these seeds on low sulfur media for 10 days and then visualized the roots under a Leica brightfield microscope (Figure 45). The MYB12 knock out did produce sulfur pox but the triple mutant *myb11- 12-111* showed no sign of sulfur pox (Figure 38). We also tested transparent testa (*tt*) mutants; *tt4, tt5, tt6,* and *tt7* showed no sulfur pox when germinated directly on low sulfur media (Figure 46). Since we knew that transfer to –S media from MS media rapidly induces –S pox formation we decided to see if this method would cause pox production in the tt mutants. A small number of pox were observed for *tt4, tt5, tt6,* and *tt7* when transferred from MS media to low sulfur (Figure

47).

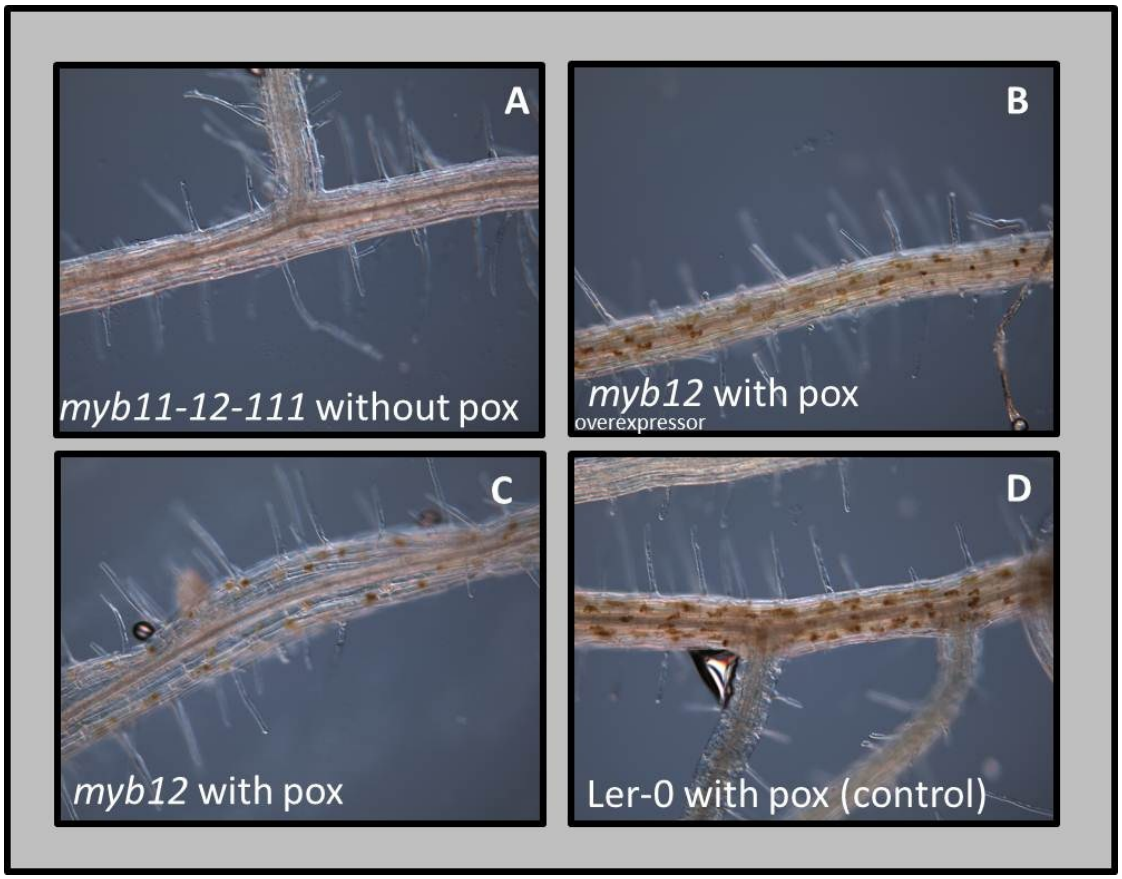

Figure 45: Images of phenylpropanoid pathway regulator mutants.

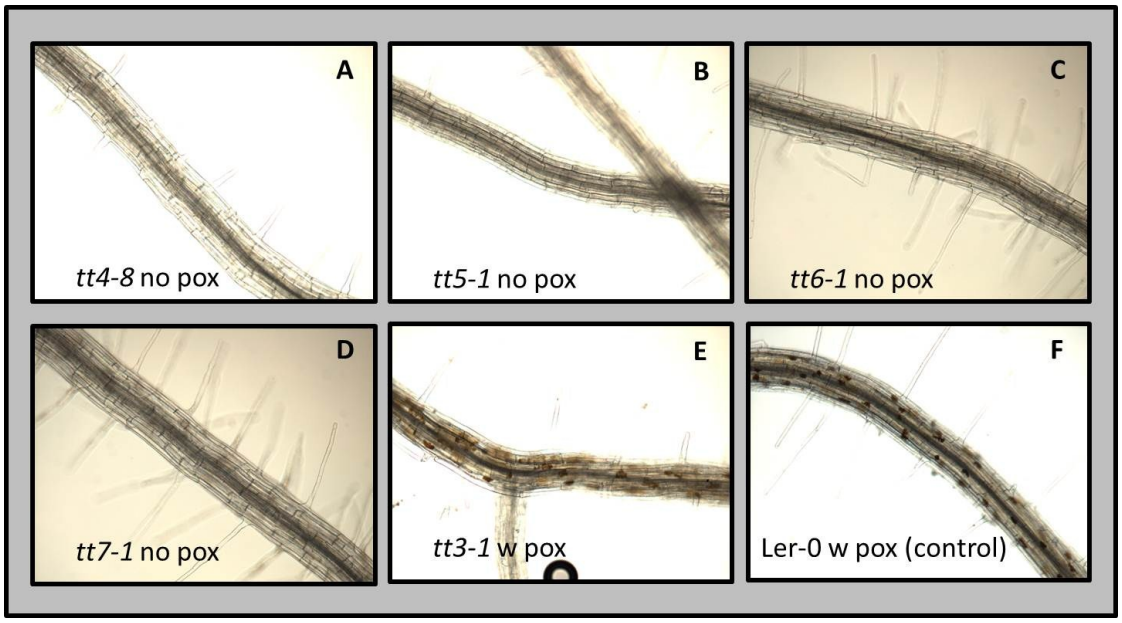

Figure 46: Images of transparent testa mutants germinated directly on low sulfur media.

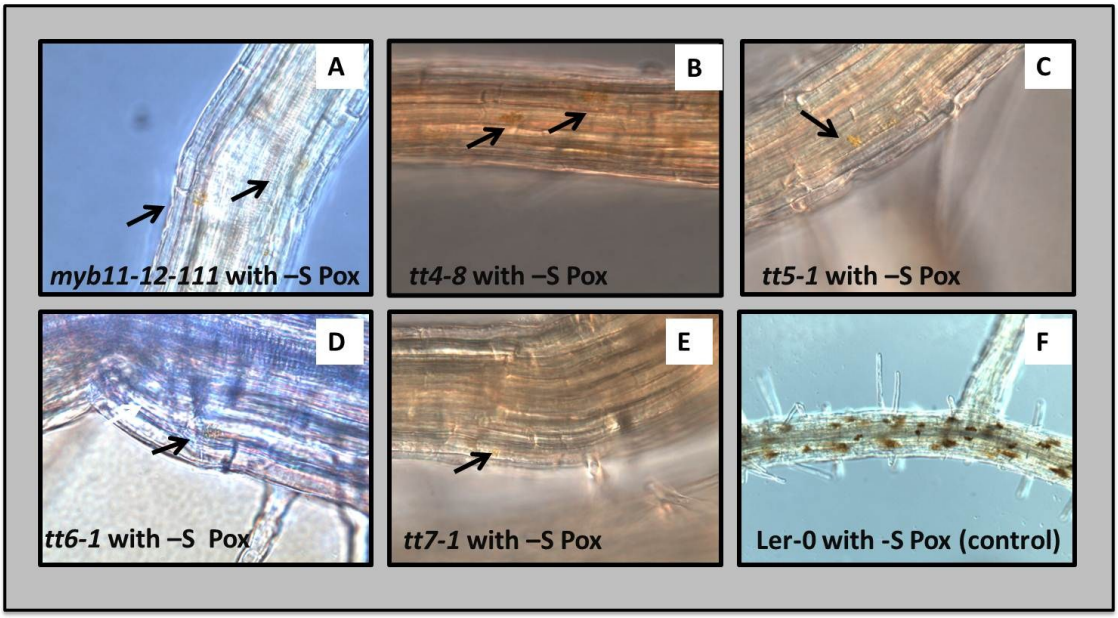

Figure 47: Images of transparent testa mutants transferred from enriched media to low sulfur media.

This led to the theory that these sulfur pox contain the flavonoid quercetin. We

then performed staining for flavonoids with DPBA which binds to flavonoids and will fluorescence using confocal microscopy. We observed no binding of DPBA to the –S pox (Figure 48). The lack of DPBA binding to the –S pox does no rule out that they are flavonoids. It is highly probable that these –S pox are oxidized flavonoids which is what gives them this brown color, much like the maize *bz2* mutant that was unable to sequester anthocyanidins into the vacuole and the anthocyanidins oxidized in the cytoplasm and turned into a brown color. DPBA does not bind to oxidized flavonoids like it binds to de-oxidized flavonoids. It also does not bind to glycosylated flavonoids. Furthermore, the sulfur pox are most likely some type of phenolic compound. They just may not be phenolics that bind DPBA.

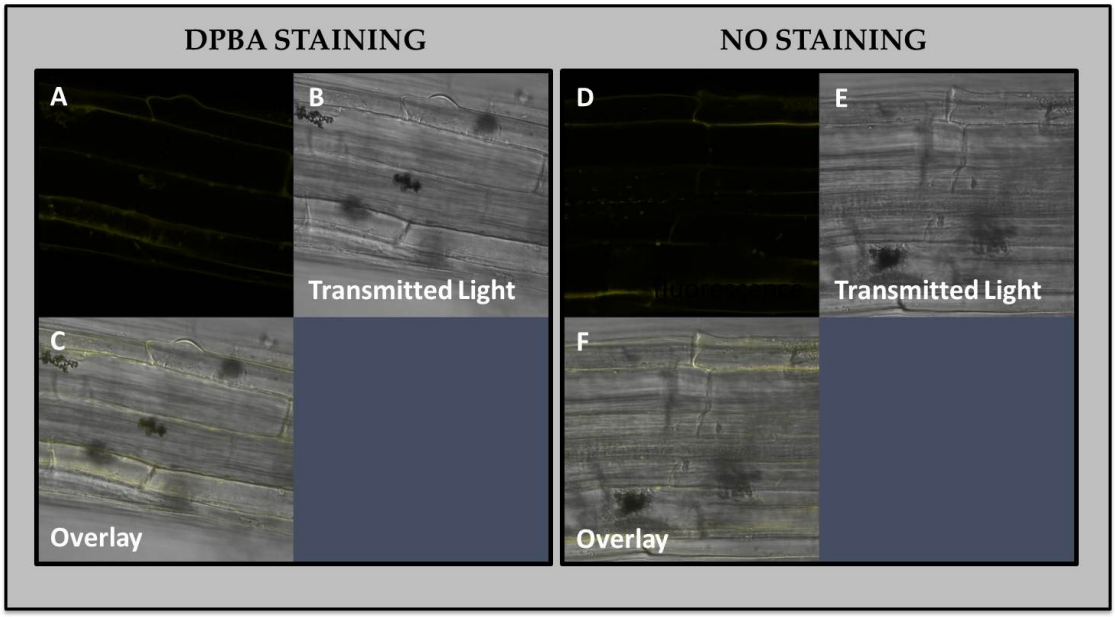

Figure 48: Confocal imaging of DPBA stain for presence of flavonoids.

The absence of –S pox in *tt* and *myb* mutant seedlings roots that were directly

germinated on –S and the decrease of –S pox in *tt* and *myb* mutants transferred from MS media to –S media were promising results that did not disprove this hypothesis. This observation was followed up by a quantification of the –S pox in *myb 11-12-111*, *myb12*, a *myb12* overexpression line (Figure 49A), *tt4-8*, *tt5-1*, *tt6-1*, *tt7-1*, *tt3-1* and the quadruple glucosinolate mutant *myb28/29/cyp79B2/B3* used to rule out the possibility of these inclusions being a result of a disruption of the glucosinolate biosynthetic machinery due to the lack of sulfur reserves (Figure 49B). This experiment was conducted in triplicate of 5 roots of each control and mutant using DIC microscopy with a Leica compound light microscope at 10x magnification. The results are consistent with previous observations confirming the reduction of these inclusions in the mutant, and lack of and/or absence of them in the *tt* mutants and the *myb11-12-111* mutant. Also, the overexpressor line of *myb12* had a significant increase in the number of –S pox. These results are evidence of flavonoid biosynthesis enzymes involvement in the –S pox production or coloration.

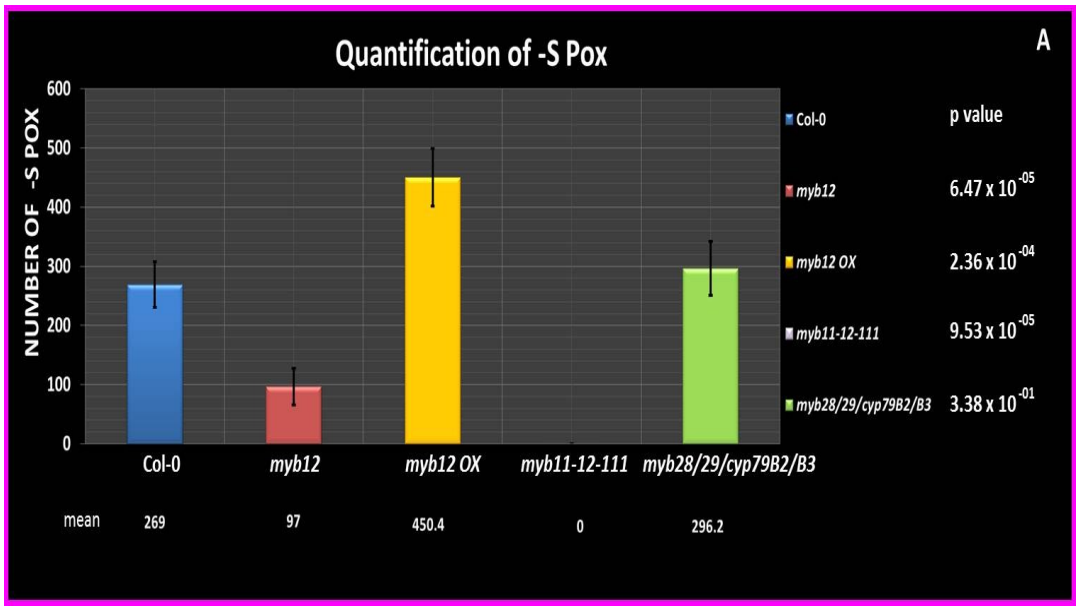

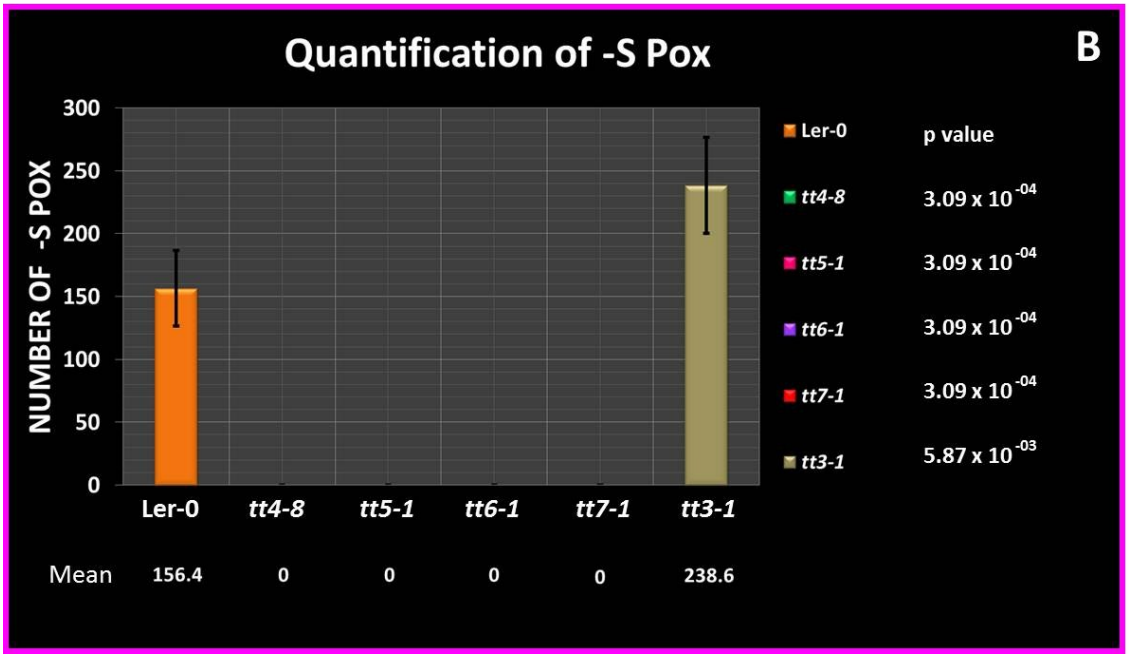

Figure 49: Quantification of –S Pox in phenylpropanoid mutants.

Therefore, next we wanted to take advantage of flavonoids accumulation being light dependent. We place seeds on –S plates and wrapped the plates so that they would be completely germinated in the dark for ten days. The seedlings were fully etiolated

with very short roots and long translucent hypocotyls. There we no – S pox in these seedlings. (Data not shown). These results are in order with the expected results and justification to perform additional experiments.

Now we wanted to acquire light sensing mutants that exhibit the *cop* phenotype when germinated in dark conditions. The dark grown *cop* phenotype is de-etiolated and exhibits attributes of photomorphogenesis. PhyB$^{(Y276H)}$, *cop1-4*, and *det1-1* all have sulfur pox. The *pifq1* quadruple mutant still showed no sign of -S pox (Figure 50).

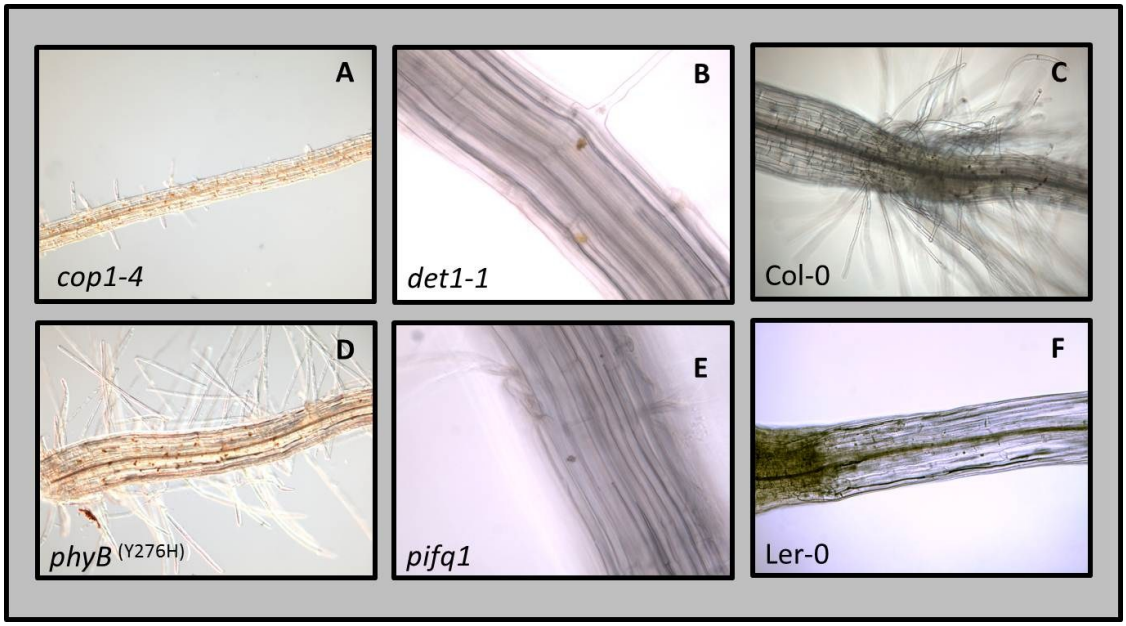

Figure 50: Images of sulfur pox in phytochrome mutants grown on low sulfur media in the dark.

In summary of this Chapter, we have characterized the cellular inclusions that appear in roots grown in the absence of sulfur and determined the length of time that they appear in seedlings germinated on –S media and transferred to –S media. We have stained the roots to determine if they are proteins or lipids, and also to determine if they

are within a vesicle. We found that they are none of these. We tested over 250 mutant seed stocks from multiple microarray results as well as dozens of ecotypes and in all cases we found –S pox until we tested transparent testa mutants. These seeds had zero –S pox when directly germinated and very few that were hard to visualize at 40x magnification when transferred to –S media. Quantification at 10x magnification showed a clear lack of these inclusions in the *tt* mutants and *myb11-12-111* mutant. We did not see DPBA fluorescence localized to the –S pox but this could be due to oxidation and/or glycoslyation. The experiments with the light sensing mutants were also informative as –S pox appeared in the dark grown seedlings in all mutants except *pifq1*, but is has been reported that this mutant does not fully de-etiolate. These results are evidence that phytochromes or downstream targets to promote photomorphogenesis are necessary for –S pox production. Microarray results and metabolomic data confirms that we do have –S conditions but is not very revealing as to what genes or metabolites are involved in their production and composition.

Methods

Growth Conditions and Analysis

Arabidopsis plants were grown on 1% sucrose using prepackaged Murashige & Skoog (MS) media (Caisson), complete MS standard media, or media without sulfate. The MS and complete media each contained 1.5mM of sulfate. The only sulfur in the media was from the MES buffer ($C_6H_{13}NO_4S$) which has a molar mass of 195.2g/mol. In

the media prepared for these experiments only 0.25g of MES was added to every 500L of media solution. Thus, it was concluded that the amount of sulfur in the media was negligible. The solution was raised to a pH of 5.7 using potassium hydroxide KOH and 1% of Agar was added before autoclaving the media. After autoclaving the media was cooled and 50mL was poured onto square plates, allowed, to solidify, and stored at 4°C until plating of seeds. Plants grown on the MS media and the self-made media were compared for consistency and also used for transfer experiments onto no sulfur media. COL-0, wild-type, seeds were placed in single file rows approximately 10-12 seeds, sometimes 20, per plate, wrapped with parafilm, and placed into an incubator at 22C with 16hrs of light and 8hrs of dark.

Microarray Data Set Sample Preparation

The seeds for the 5 and 10 day –S pox analysis were sown directly on –S plate or directly to MS plates (control) with 20 seeds per plate. The 10 Day plates were sown 5days before the 5 Day samples in order to end both experiments simultaneously. Excision of root sections were performed with a standard razor just below the hypocotyl/root junction for 0.5inches. All roots were quickly sectioned in this manner with 3 biological replicates prepared. All sections were immediately placed in RLT lysis buffer and stored on ice until RNA extraction.

Microarray Data Analysis

The RNA extraction was consistent for all data sets and was carried out with a RNA easy Micro Kit (Qiagen GmbH). The samples were then amplified, labeled and fragmented using the Affymetrix one- cycle protocol for whole roots and two-cycles for the remaining data sets. These fragmented samples were sent to Expression Analysis Inc. in Durham NC. Here the samples were hybridized to the ATH1 whole-genome gene chip; covering ~22,000 genes (Affymetrix).

Quantification of –S POX

Seedlings were germinated on MS media for 6 days and then transferred to –S media for 7 days before visualization. Three replicates were made for each seed stock used and 5 roots were cut at the base of the stem. Roots were placed on glass slides in water and visualized at 10x magnification using the DIC setting on a Leica compound light microscope. Sulfur pox were then counted in each root and the results tabulated.

T-DNA Insertion Lines

Candidate genes homozygous for T-DNA insertions were ordered from the SALK Institute. Due to the high volume of T-DNA seed stocks tested for the presence or absence of sulfur pox, we did not validate homozygosity of the insertions.

Point mutation Lines

All point mutation lines were tested for described phenotypes and verified outside of the laboratory. *tt* mutants were received from postdoctoral members of the laboratory. The light sensing mutants were from the lab of Dr. Meng Chen.

Fluorescent Staining

DPBA staining times were for 2 min using saturated (0.25% [w/v]) DPBA and 0.005% (v/v) Triton X-100. Seedlings were then washed for 3min with 100mM sodiumphosphate buffer, pH7.0, plus 0.005% (v/v) Triton X-100. Seedlings were mounted on slides in water. FM4-64, and Biofilm staining was performed by staining for 3 minutes and rinse for one minute and mounting with water onto slides. The Biofilm stain and FM-64 stain were acquired from Molecular Probes.

Chapter 4. Discussion, Future Directions, Conclusion

Discussion

This research has produced a very large data set analyzing the effect of low sulfur on Arabidopsis roots. The results of these experiments have been published and the data is available to the public. It will be useful as investigators continue to describe and understand the effect of low sulfur conditions on the plant as a whole. We have taken a time course across 72 hours and found that the major response occurs early in these controlled conditions. In agriculture, sulfur deprivation does not occur suddenly. It is a gradual process or it is a pre-existing condition. Still, the future goal is to engineer plants that are able to withstand these conditions and still have a high yield. Therefore, these data are valuable since they examine multiple cell-types and developmental stages which respond differently.

These sulfur pox are a unique phenotypic feature, which is first described in this thesis. Their localization primarily to the cortex cell layer in mature root tissue shows that specific tissue types are partitioned to handle tasks under stress induced situations. Mutant analysis suggests that the phenylpropanoid pathway, as well as phytochrome is responsible for their accumulation. Thus, there is a possible signal from the shoot to the root to produce these inclusions when sulfur limitation occurs.

Future Directions

This investigation was originally meant to search for novel transcription factors in the sulfur pathway in order to assemble transcriptional networks. The wealth of transcription factors that have been differentially expressed under low sulfur conditions should be further investigated and tested for a phenotype. There very well may be some associated with the sulfur pox if there is a signal from the shoot to the root.

The composition of these sulfur pox remains unknown. Isolating them completely was not achieved in this research but we were able to detect them in protoplasts after cell sorting. We were unable to produce an enriched population of them but it is still possible that this can be achieved. Methods of cell sorting and using a sucrose gradient may be successful. Further, the biological relevance of these sulfur pox also remains unknown. It was thought they could simply be an artifact of failed processes as the plant can no longer carry out metabolic functions. This is doubtful due to their rapid accumulation after transfer from enriched media to low sulfur conditions. Also, the results of the phytochrome mutant experiments led me to believe they do have a biological role. Determining what they are and why they are produced is worth further exploration.

Conclusion

High resolution data analysis is proving to be a valuable tool to discover novel genes and analyze data in greater detail. Microarray analysis is already becoming

outdated as new tools like RNA-sequencing are expected protocols to use when generating these large scale data sets. Still, our methods have been useful to answer key questions in general stress response, and abiotic stress response at the cell-type and developmental-zone level. The global root response from low sulfur is clarified using these high resolution techniques. We have been able to identify processes that are enriched in specific cell-types and developmental zones, and the tissues that are affected the greatest to the least in transcriptional response by low sulfur.

The characterization of these sulfur pox cellular inclusion is incomplete but this investigation has provided an in-depth analysis of a novel occurrence in Arabidopsis root cells. It is my belief that these are products of the phenylpropanoid pathway and most likely oxidized flavonoids that build up because sulfur is limited and must be conserved. Possibly, this is due to light sensitivity and excessive oxidative cellular conditions. Transport machinery may have made it impossible to sequester these products in proper cellular compartments, as well. The finding that transcription factors affect light sensing, phenylpropanoid biosynthesis, and sulfur assimilation is evidence that there is a common regulatory mechanism involved which makes the potential for these inclusions to occur under these conditions. The results of the dark experiments on mutants that remain de-detiolated produce sulfur pox supports our hypothesis, as well as the flavonoid mutant quantification, but there still needs to be further experimental procedures to validate this proposal.

Bibliography

Agati, G., Azzarello, E., Pollastri, S., & Tattini, M. (2012). Flavonoids as antioxidants in plants: Location and functional significance. *Plant science : an international journal of experimental plant biology*, *196*, 67–76.

Alabadí, D., Gallego-Bartolomé, J., Orlando, L., García-Cárcel, L., Rubio, V., Martínez, C., Frigerio, M., et al. (2008). Gibberellins modulate light signaling pathways to prevent Arabidopsis seedling de-etiolation in darkness. *The Plant journal : for cell and molecular biology*, *53*(2), 324–35.

Alfenito MR, Souer E, Goodman CD, Buell R, Mol J, Koes R, Walbot V (1998) Functional complementation of anthocyanin sequestration in the vacuole by widely divergent glutathione S-transferases. Plant Cell 10: 1135–1149

Amtmann, A., & Armengaud, P. (2009). Effects of N, P, K and S on metabolism: new knowledge gained from multi-level analysis. *Current Opinion in Plant Biology*, *12*(3), 275-283.

Ballaré, C. (1999). *Keeping up with the neighbors: phytochrome sensing and other signalling mechanisms. *Trends in plant science*, *4*(5), 201

Besseau, S., Hoffmann, L., Geoffroy, P., Lapierre, C., Pollet, B., & Legrand, M. (2007). Flavonoid accumulation in Arabidopsis repressed in lignin synthesis affects auxin transport and plant growth. *The Plant cell*, *19*(1), 148–62.

Bick, J. a, & Leustek, T. (1998). Plant sulfur metabolism--the reduction of sulfate to sulfite. *Current opinion in plant biology*, *1*(3), 240–4.

Birnbaum, K. (2003) "A Gene Expression Map of the Arabidopsis Root" Science: 302(5652): 1956-1960.

Birnbaum, K., Jung, J. W., Wang, J. Y., Lambert, G. M., Hirst, J. A., Galbraith, D. W., & Benfey, P. N. (2005). Cell type-specific expression profiling in plants via cell sorting of protoplasts from fluorescent reporter lines. *Nature Methods*,*2*(8), 615-619.

Biswal, B., Raval, M., Biswal, U., & Joshi, P. (2008). Response of Photosynthetic Organelles to Abiotic Stress: Modulation by Sulfur Metabolism. *… Assimilation and Abiotic Stress …*, 167–191.

Bloem, E. (2004). "Significance of Sulfur Compounds in the Protection of Plants Against Pests and Disease." Journal of Plant Nutrition 28: 763-784.

Bogdanova, N., & Hell, R. (1997, February). Cysteine synthesis in plants: protein-protein interactions of serine acetyltransferase from Arabidopsis thaliana. *The Plant journal : for cell and molecular biology*.

Brady, S. M., Orlando, D. A., Lee, J.-Y., Wang, J. Y., Koch, J., Dinneny, J. R., Mace, D., et al. (2007). A high-resolution root spatiotemporal map reveals dominant expression patterns. *Science*, *318*(5851), 801-6.

Brown, D. E., Rashotte, a M., Murphy, a S., Normanly, J., Tague, B. W., Peer, W. a, Taiz, L., et al. (2001). Flavonoids act as negative regulators of auxin transport in vivo in arabidopsis. *Plant physiology*, *126*(2), 524–35.

Buchner, P., Takahashi, H., & Hawkesford, M. J. (2004). Plant sulphate transporters: co-ordination of uptake, intracellular and long-distance transport. *Journal of experimental botany*, *55*(404), 1765–73.

Buer, C. S., Muday, G. K., & Djordjevic, M. a. (2007). Flavonoids are differentially taken up and transported long distances in Arabidopsis. *Plant physiology*, *145*(2), 478–90.

Cao, M.-J., Wang, Z., Wirtz, M., Hell, R., Oliver, D. J., & Xiang, C.-B. (2012). SULTR3;1 is a chloroplast-localized sulfate transporter in Arabidopsis thaliana. *The Plant journal : for cell and molecular biology*.

Chang, C. J., Li, Y.-H., Chen, L.-T., Chen, W.-C., Hsieh, W.-P., Shin, J., Jane, W.-N., et al. (2008). LZF1, a HY5-regulated transcriptional factor, functions in Arabidopsis de-etiolation. *The Plant journal : for cell and molecular biology*, *54*(2), 205–19.

Chaudhuri, B. (2008) Protonophore- and pH-insensitive glucose and sucrose detected by FRET nanosensors in Arabidopsis root." The Plant Journal [Epub ahead of print]

Chen, J. and Zho, T. (2004) "Networks of Transcription Factors with Roles in Environmental Stress Response" Trends in Plant Science: 9(12):591-596.

Close, D., & McArthur, C. (2002). Rethinking the role of many plant phenolics–protection from photodamage not herbivores? *Oikos*, *99*(1), 166–172.

Cluis, C. P., Mouchel, C. F., & Hardtke, C. S. (2004). The Arabidopsis transcription factor HY5 integrates light and hormone signaling pathways. *The Plant journal : for cell and molecular biology*, *38*(2), 332–47.

Dinneny, J. R., Long, T. A., Wang, J. Y., Jung, J. W., Mace, D., Pointer, S., Barron, C., et al. (2008). Cell identity mediates the response of Arabidopsis roots to abiotic stress. *Science*, *320*(5878), 942-5.

Dolan, L., Janmaat, K., Willemsen, V., Linstead, P., Poethig, S., Roberts, K., & Scheres, B. (1993). Cellular organisation of the Arabidopsis thaliana root. *Development (Cambridge, England)*, *119*(1), 71–84.

Droux, M. (2004). Sulfur assimilation and the role of sulfur in plant metabolism: a survey. *Photosynthesis research*, *79*(3), 331–48.

Feinbaum, R., & Ausubel, F. (1988). Transcriptional regulation of the Arabidopsis thaliana chalcone synthase gene. *Molecular and Cellular Biology*, *8*(5).

Frohnmeyer, H., Bowler, C., & Zhu, J. (1998). Different roles for calcium and calmodulin in phytochrome◎and UV-regulated expression of chalcone synthase. *The Plant Journal : for cell and molecular biology*, 13(6), 763-772

Gifford, M. L., Dean, A., Gutierrez, R. a, Coruzzi, G. M., & Birnbaum, K. D. (2008). Cell-specific nitrogen responses mediate developmental plasticity. *Proceedings of the National Academy of Sciences of the United States of America*, *105*(2), 803–8.

Haneklaus, S., Bloem, E., & Schnug, E. (2007). Sulfur interactions in crop ecosystems. (pp. 17-58). Dordrecht: Springer Netherlands.

Hawkesford, M. J. (2000). Plant responses to sulphur deficiency and the genetic manipulation of sulphate transporters to improve S-utilization efficiency. *Journal of experimental botany*, *51*(342), 131–8.

Heafield, M. T., Fearn, S., Steventon, G. B., Waring, R. H., Williams, A. C., & Sturman, S. G. (1990). Plasma cysteine and sulphate levels in patients with motor neurone, Parkinson's and Alzheimer's disease. *Neuroscience Letters*,*110*(1-2), 216-220.

Hell, R., & Wirtz, M. (2011). Molecular Biology, Biochemistry and Cellular Physiology of Cysteine Metabolism in Arabidopsis thaliana. *The Arabidopsis book / American Society of Plant Biologists*, *9*(2008), e0154.

Hemm, M. R., Rider, S. D., Ogas, J., Murry, D. J., & Chapple, C. (2004). Light induces phenylpropanoid metabolism in Arabidopsis roots. *The Plant journal : for cell and molecular biology*, *38*(5), 765–78

Herms, D. a., & Mattson, W. J. (1992). The Dilemma of Plants: To Grow or Defend. *The Quarterly Review of Biology*, *67*(3), 283. doi:10.1086/417659

Hesse, H., Nikiforova, V., Gakière, B., & Hoefgen, R. (2004). Molecular analysis and control of cysteine biosynthesis: integration of nitrogen and sulphur metabolism. *Journal of Experimental Botany*, *55*(401), 1283-1292.

Hesse, R. H. a. H., Ed. (2007). Sulfur in Plants as Part of a Metabolic Network, Springer

Hirai, M. (2003). "Global expression profiling of sulfur-starved Arabidopsis by DNA macroarray reveals the role of O-acetyl-L-serine as a general regulator of gene expression in response to sulfur nutrition." The Plant Journal 33: 651-663.

Hirai, M. Y., & Saito, K. (2004). Post-genomics approaches for the elucidation of plant adaptive mechanisms to sulphur deficiency. *Journal of Experimental Botany*, *55*(404), 1871-1879. OXFORD UNIV PRESS.

Hirai, M. Y., Klein, M., Fujikawa, Y., Yano, M., Goodenowe, D. B., Yamazaki, Y., Kanaya, S., et al. (2005). Elucidation of gene-to-gene and metabolite-to-gene networks in Arabidopsis by integration of metabolomics and transcriptomics. *The Journal of Biological Chemistry*, *280*(27), 25590-25595.

Hirayama, T., & Shinozaki, K. (2010). Research on plant abiotic stress responses in the post-genome era: past, present and future. *The Plant Journal*, *61*(6), 1041-1052. Wiley Online Library.

Hoefgen, R., & Nikiforova, V. J. (2008). Metabolomics integrated with transcriptomics: assessing systems response to sulfur-deficiency stress. *Physiologia Plantarum*, *132*(2), 190-198.

Hudson, M. E. (2000). The genetics of phytochrome signalling in Arabidopsis. *Seminars in cell & developmental biology*, *11*(6), 475–83.

Hung, C.-J., Huang, P.-C., Lu, S.-C., Li, Y.-H., Huang, H.-B., Lin, B.-F., Chang, S.-J., et al. (2002). Plasma homocysteine levels in Taiwanese vegetarians are higher than those of omnivores. *The Journal of nutrition*, *132*(2), 152-158.

Ingenbleek, Y. (2010). Hyperhomocysteinemia is a biomarker of sulfur-deficiency in human morbidities~2009-10-03~2009-11-18~2009-12-22. *The Open Clinical Chemistry Journal,2*(1), 49-60.

Ingenbleek, Y., & McCully, K. S. (2012). Vegetarianism produces subclinical malnutrition, hyperhomocysteinemia and atherogenesis. *Nutrition Burbank Los Angeles County Calif*, *28*(2), 148-153.

Iyer-Pascuzzi, A. S., Jackson, T., Cui, H., Petricka, J. J., Busch, W., Tsukagoshi, H., & Benfey, P. N. (2011). Cell Identity Regulators Link Development and Stress Responses in the Arabidopsis Root. *Developmental Cell*, *21*(4), 770-782.

Izaguirre, M. M., Mazza, C. a, Biondini, M., Baldwin, I. T., & Ballaré, C. L. (2006). Remote sensing of future competitors: impacts on plant defenses. *Proceedings of the National Academy of Sciences of the United States of America*, *103*(18), 7170–4.

Jost, R., Altschmied, L., Bloem, E., Bogs, J., Gershenzon, J., Hähnel, U., Hänsch, R., et al. (2005). Expression profiling of metabolic genes in response to methyl jasmonate reveals regulation of genes of primary and secondary sulfur-related pathways in Arabidopsis thaliana. *Photosynthesis Research*,*86*(3), 491-508.

Kataoka, T., & Hayashi, N. (2004). Root-to-shoot transport of sulfate in Arabidopsis. Evidence for the role of SULTR3; 5 as a component of low-affinity sulfate transport system in the root vasculature. *Plant physiology*, *136*(December), 4198–4204.

Kawashima CG, Yoshimoto N, Maruyama-Nakashita A, Tsuchiya YN, Saito K, Takahashi H, Dalmay T (2009) Sulphur starvation induces the expression of microRNA-395 and one of its target genes but in different cell types. Plant J 57:313–321

Kliebenstein, D. J., Kroymann, J., Brown, P., Figuth, a, Pedersen, D., Gershenzon, J., & Mitchell-Olds, T. (2001). Genetic control of natural variation in Arabidopsis glucosinolate accumulation. *Plant physiology*, *126*(2), 811–25.

Kost, D., Chen, L., & Dick, W. A. (2008). Predicting plant sulfur deficiency in soils: Results from Ohio. *Biology and Fertility of Soils, 44*(8), 1091-1098.

Kutz, A., Müller, A., Hennig, P., Kaiser, W. M., Piotrowski, M., & Weiler, E. W. (2002). A role for nitrilase 3 in the regulation of root morphology in sulphur-starving Arabidopsis thaliana. *The Plant Journal*, *30*(1), 95-106.

Lau, O. S., & Deng, X. W. (2012). The photomorphogenic repressors COP1 and DET1: 20 years later. *Trends in plant science*, *17*(10), 584–93.

Lee, J. (2006) “Transcriptional and posttranscriptional regulation of transcription factor expression in Arabidopsis roots” *Proc* Natl Acad Sci U S A: 103(15): 6055-60.

Leivar, P., & Quail, P. H. (2011). PIFs: pivotal components in a cellular signaling hub. *Trends in plant science*, *16*(1), 19–28.

Leustek, T., & Martin, M. (2000). "Pathways and Regulation of Sulfur Metabolism Revealed Through Molecular and Genetic Studies." Annu. Rev. Plant Physiol. Plant Mol Biol. 51: 141-165.

Levesque, M. (2003) “Trait-to-Gene: A computational method for inferring the function of uncharacterized genes” Current Biology: 13:129-133.

Ma, S., & Bohnert, H. J. (2007). Integration of Arabidopsis thaliana stress-related transcript profiles, promoter structures, and cell-specific expression. *Genome Biology*, *8*(4), R49. BioMed Central.

Marinova, K., Pourcel, L., Weder, B., Schwarz, M., Barron, D., Routaboul, J.-M., Debeaujon, I., et al. (2007). The Arabidopsis MATE transporter TT12 acts as a vacuolar flavonoid/H+ -antiporter active in proanthocyanidin-accumulating cells of the seed coat. *The Plant cell*, *19*(6), 2023–38.

Marrs KA, Alfenito MR, Lloyd AM, Walbot V (1995) A glutathione S-transferase involved in vacuolar transfer encoded by the maize gene bronze-2. Nature 375: 397–400

Maruyama-Nakashita, A. (2003). "Transcriptome Profiling of Sulfur-Responsive Genes in Arabidopsis Reveals Global Effects on Sulfur Nutrition on Multiple Metabolic Pathways." Plant Physiology 132: 597-605.

Maruyama-Nakashita, A., Nakamura, Y., Watanabe-Takahashi, A., Yamaya, T., & Takahashi, H. (2004). Induction of SULTR1;1 sulfate transporter in Arabidopsis roots involves protein phosphorylation/dephosphorylation circuit for transcriptional regulation. *Plant & cell physiology*, *45*(3), 340–5

Maruyama-Nakashita, A., Nakamura, Y., Tohge, T., Saito, K., & Takahashi, H. (2006). Arabidopsis SLIM1 is a central transcriptional regulator of plant sulfur response and metabolism. *The Plant Cell*, *18*(11), 3235-51.

.Morelli, G., & Ruberti, I. (2002). Light and shade in the photocontrol of Arabidopsis growth. *Trends in plant science*, *7*(9), 399–404.

Mugford, S. G., Yoshimoto, N., Reichelt, M., Wirtz, M., Hill, L., Mugford, S. T., Nakazato, Y., et al. (2009, March). Disruption of adenosine-5′-phosphosulfate kinase in Arabidopsis reduces levels of sulfated secondary metabolites. *The Plant cell*.

Nakajima, K., Sena, G., Nawy, T., & Benfey, P. (2001). Intercellular movement of the putative transcription factor SHR in root patterning. *Nature*, *413*(September), 307–311

Nikiforova, V. (2003). "Transcriptome analysis of sulfur depletion in Arabidopsis thaliana: interlacing of biosynthetic pathways provides response specificity." The Plant Journal 33: 633-650.

Nikiforova, V. (2005). "Systems Rebalancing of Metabolism in Response to Sulfur Deprivation, as Revealed by Metabolome Analysis of Arabidopsis Plants." Plant Physiology 138: 304-318.

Oyama, T., Shimura, Y., & Okada, K. (1997). The Arabidopsis HY5 gene encodes a bZIP protein that regulates stimulus-induced development of root and hypocotyl. *Genes & Development*.

Peer, W. a, Brown, D. E., Tague, B. W., Muday, G. K., Taiz, L., & Murphy, a S. (2001). Flavonoid accumulation patterns of transparent testa mutants of arabidopsis. *Plant physiology*, *126*(2), 536–48.

Pilon, M., Abdel-Ghany, S. E., Van Hoewyk, D., Ye, H., & Pilon-Smits, E. a H. (2006). Biogenesis of iron-sulfur cluster proteins in plastids. *Genetic engineering*, *27*, 101–17.

Potters, G., Pasternak, T. P., Guisez, Y., Palme, K. J., & Jansen, M. A. K. (2007). Stress-induced morphogenic responses: growing out of trouble? *Trends in Plant Science*, *12*(3), 98-105.

Routaboul, J.-M., Kerhoas, L., Debeaujon, I., Pourcel, L., Caboche, M., Einhorn, J., & Lepiniec, L. (2006). Flavonoid diversity and biosynthesis in seed of Arabidopsis thaliana. *Planta*, *224*(1), 96–107.

Saito, K. (2004). "Sulfur Assimilatory Metabolism. The Long and Smelling Road." Plant Physiology 136: 2443-2450.

Salisbury, F. J., Hall, A., Grierson, C. S., & Halliday, K. J. (2007). Phytochrome coordinates Arabidopsis shoot and root development. *The Plant journal : for cell and molecular biology*, *50*(3), 429–38.

Schepens, I., Duek, P., & Fankhauser, C. (2004). Phytochrome-mediated light signalling in Arabidopsis. *Current opinion in plant biology*, *7*(5), 564–9.

Scheres, B., Benfey, P., & Dolan, L. (2000). Root development. *The Arabidopsis book / American Society of Plant Biologists*.

Schoenbohm, C., Martens, S., Eder, C., Forkmann, G., & Weisshaar, B. (2000). Identification of the Arabidopsis thaliana flavonoid 3′-hydroxylase gene and functional expression of the encoded P450 enzyme. *Biological chemistry*, *381*(8), 749–53.

Shirley, B.W., Hanley, S. and Goodman, H.M. (1992) Effects of ionizing radiation on a plant genome: analysis of two Arabidopsis transparent testa mutations. Plant Cell, 4, 333- 347.

Shibagaki, N., Rose, A., McDermott, J. P., Fujiwara, T., Hayashi, H., Yoneyama, T., & Davies, J. P. (2002). Selenate-resistant mutants of Arabidopsis thaliana identify Sultr1;2, a sulfate transporter required for efficient transport of sulfate into roots. *The Plant journal : for cell and molecular biology*, *29*(4), 475–86.

Singh, K. B. (1998). Transcriptional regulation in plants: The importance of combinatorial control. *Plant Physiology, 118*(4), 1111-1120.

Si-wei Yuan, Xue-long WU, Zhi-hong Liu, Hong-bing Luo, Rui-zhi Huang, Abiotic Stresses and Phytohormones Regulate Expression of FAD2 Gene in Arabidopsis thaliana, Journal of Integrative Agriculture, Volume 11, Issue 1, January 2012, Pages 62-72, ISSN 2095-3119, 10.1016/S1671-2927(12)60783-4.

Smirnova, O. G., Stepanenko, I. L., & Shumny, V. K. (2012). Mechanism of action and activity regulation of COP1, a constitutive repressor of photomorphogenesis. *Russian Journal of Plant Physiology*, *59*(2), 155–166.

Sullivan, J. a, & Deng, X. W. (2003). From seed to seed: the role of photoreceptors in Arabidopsis development. *Developmental Biology*, *260*(2), 289–297.

Takahashi, H. (1997). "Regulation of sulfur assimilation in higher plants: A sulfate transporter induced in sulfate-starved roots plays a central role in Arabidopsis thaliana." Proc. Natl. Acad. Sci. 94: 11102-11107.

Takahashi, H., Watanabe-Takahashi, A., Smith, F. W., Blake-Kalff, M., Hawkesford, M. J., & Saito, K. (2000). The roles of three functional sulphate transporters involved in

uptake and translocation of sulphate in Arabidopsis thaliana. *The Plant Journal*, *23*(2), 171-182.

Treutter, D. (2006). Significance of flavonoids in plant resistance: a review. *Environmental Chemistry Letters*, *4*(3), 147–157.

Van den Bulcke, T. (2006) "Inferring Transcriptional Networks by Mining 'Omics' Data" Current Bioinformatics: 1(3): 1-13.

Volk, Gayle. (2004). "Calcium Channels are Involved in Calcium Oxalate Crystal Formation in Specialized Cells of Pistia *stratiotes L*" Annals of Botany: 93:741-753.

Wang, D. (2006). "A Genomic Approach to Identify Regulatory Nodes in the Transcriptional Network of Systematic Acquired Resistance in Plants" PLoS Pathogens: 2(11): 1042-1050.

Webb, M. (1999) "Cell-Mediated Crystallization of Calcium Oxalate in Plants" The Plant Cell: 11: 751-761.

Wei, N., Deng, X., Det, C. O. P., & Nts, M. U. T. A. (1996). The Role of the COP / DET / FUS Genes in Light Control of Arabidopsis Seedling Development ', *04*, 871–878.

Winkel-Shirley, B. (2001). Flavonoid biosynthesis. A colorful model for genetics, biochemistry, cell biology, and biotechnology. *Plant physiology*, *126*(2), 485–93

Winkel-Shirley, B. (2002). Biosynthesis of flavonoids and effects of stress. *Current opinion in plant biology*, *5*(3), 218–23.

Yatusevich, R., Mugford, S. G., Matthewman, C., Gigolashvili, T., Frerigmann, H., Delaney, S., Koprivova, A., et al. (2010). Genes of primary sulfate assimilation are part of the glucosinolate biosynthetic network in Arabidopsis thaliana. *The Plant journal : for cell and molecular biology*, *62*(1), 1–11

Yoshimoto, N., Takahashi, H., Smith, F. W., Yamaya, T., & Saito, K. (2002). Two distinct high-affinity sulfate transporters with different inducibilities mediate uptake of sulfate in Arabidopsis roots. *The Plant journal : for cell and molecular biology*, *29*(4), 465–73

Yoshimoto, N., Inoue, E., Saito, K., Yamaya, T., & Takahashi, H. (2003). Phloem-Localizing Sulfate Transporter, Sultr1;3, Mediates Re-Distribution of Sulfur from Source to Sink Organs in Arabidopsis1. *Plant Physiology*, *131*(4), 1511-1517.

Yoshimoto, N., Inoue, E., Watanabe-Takahashi, A., Saito, K., & Takahashi, H. (2007). Posttranscriptional regulation of high-affinity sulfate transporters in Arabidopsis by sulfur nutrition. *Plant physiology*, *145*(2), 378–88.

Zhao, F., & McGrath, S. P. (1994). Extractable sulfate and organic sulfur in soils and their availability to plants. *Plant and Soil*, *164*(2), 243-250

Zhao, J., & Dixon, R. a. (2010). The "ins" and "outs" of flavonoid transport. *Trends in plant science*, *15*(2), 72–80.

Zhao, J., Huhman, D., Shadle, G., He, X.-Z., Sumner, L. W., Tang, Y., & Dixon, R. a. (2011). MATE2 mediates vacuolar sequestration of flavonoid glycosides and glycoside malonates in Medicago truncatula. *The Plant cell*, *23*(4), 1536–55.

Biography

Terry Jackson was born at Kenner Army Hospital on July 28, 1973 in Fort Lee, Virginia. He lived right outside of the army base in Prince George, Virginia until his graduation from the local high school. He graduated with a bachelor's degree in Biology from Virginia State University in the spring of 2003. He then received a Post-baccalaureate award from the National Institutes of Health to conduct biomedical research. He worked in the laboratory of the Head of Hematology at Duke University Medical Center, Marilyn Telen, MD on modifiers of sickle cell disease. Through this work he co-authored the manuscript entitled, "β2 Adrenergic Receptor and Adenylate Cyclase Gene Polymorphisms Affect Sickle Red Cell Adhesion" which was published in the *British Journal of Haematology*, Aril 2008.

Terry was admitted to the Ph.D. University Program in Genetics and Genomics at Duke University in the fall semester of 2005. He joined the lab of Dr. Philip Benfey in 2006 and has completed his dissertation and defense in the spring of 2013. While in the lab he received the Dean's Award for Excellence in Mentoring in 2010. He has been second author of two manuscripts while a doctoral candidate in Dr. Benfey's lab. The first manuscript entitled, "Cell Identity Regulators Link Developmental and Stress Responses in the Arabidopsis Root.", which was published in *Developmental Cell*, October 2011. The second is entitled, "Cell type-specific transcriptional profiling:

implications for metabolite profiling", published in *The Plant Journal*, December 2011. He is currently preparing a first author paper to complete his Doctoral work.